THE IMPACT OF TEMPERATURE, ELEVATION, AND ASPECT ON THE POTENTIAL DISTRIBUTION OF PERMAFROST IN SAN JUAN MOUNTAINS, COLORADO

A Dissertation

by

MUHAMMAD IRHAM

Submitted to the Office of Graduate and Professional Studies of
Texas A&M University
in partial fulfillment of the requirements for the degree of

DOCTOR OF PHILOSOPHY

Chair of Committee,	John R. Giardino
Committee Members,	John D. Vitek
	Hongbin Zhan
	Chris Houser
Head of Department,	Michael Pope

May 2016

Major Subject: Geology

ABSTRACT

A portions of San Juan Mountains are located in the alpine critical zone, which extends from the boundary layer between the atmosphere and the surface of Earth. In this zone, atmospheric and geomorphic processes drive all interactions. The focus of this research is on changes associated with the location of potential permafrost in the San Juan Mountains of Colorado. Study of potential permafrost can provide important information regarding the distribution and stability of permafrost under warming climatic conditions. Understanding patterns of temperature and aspect are vital steps in understanding the distribution of potential permafrost in alpine environments, its current stability, and such changes that might occur in the future. To study this question, three objectives were assessed. First, historical climate records, standard adiabatic rate, and ArcGIS methods were applied to analyze the impact of temperature on the climate change. Second, aerial photographs and field investigations were applied to classify the spatial extent of permafrost in a selected region of the San Juan Mountains. Digital Elevation Models (DEM) in ArcGIS were created to evaluate elevation, slope, and aspect relative to the elevations of permafrost. Finally, the traditional temperature models and tracing the toe of rock glaciers were applied and compared to approximate the potential spatial increase or decrease in permafrost.

Temperature observations from 1895 to 2013 in the study area indicate that mean annual temperatures (MAAT) have increased by ~2.7^0C. The temperature changes in this location are much greater in the winter than other seasons and these changes are

unprecedently higher and faster changes when compare to global average. A frost-number study shows that one-third of the soil may be frozen in a year. Additionally, high frost numbers tend to occur in the higher elevations and along the northeastern part of study area. The temperature at top of permafrost (TTOP) analysis reveals that local variation in aspect accounts for most of the changes in the extent of potential permafrost. Permafrost distribution models and topoclimatic information from rock glaciers, however, show almost no difference in the extent of permafrost for the objective methods. Permafrost locations display a strong correlation with rock glaciers except in the northeastern part of the study area where no rock glaciers are found, but the potentail permafrost may still exist.

This study indicates that the San Juan Mountains have experienced climate change. Global temperature changes have influenced alpine permafrost in the San Juan Mountains. Higher summer and winter temperatures since 1980, along with more precipitation, can contribute to the decreasing extent of potential permafrost in this region.

DEDICATION

I dedicate my dissertation work to my family and many friends. A special feeling of gratitude to my loving wife, Irawati Arsyad whose words of encouragement and push for tenacity ring in my ears. My daughters Shirra, Izzy, and Meurah have never left my side and are very special for being there for me throughout the entire doctorate program.

I also dedicate this dissertation to my many friends who have supported me throughout the process. I will always appreciate all they have done, especially Scott Van Winkle for helping me develop my skills and for the many hours of proofreading.

I dedicate this work and give special thanks to my best friends Buyung and Anis who were more generous with their precious time, both of you have been my best supporters.

ACKNOWLEDGEMENTS

I would like to thank my committee chair, Dr. John R. Giardino, and my committee members, Dr. John Vitek, Dr. Hongbin Zhan, and Dr. Christ Houser, for their guidance and support throughout the course of this research.

Thanks also go to my friends and colleagues and the department faculty and staff for making my time at Texas A&M University a great experience.

Finally, thanks to my wife and my daughters for their encouragement, patience and love.

TABLE OF CONTENTS

Page

LIST OF FIGURES

LIST OF TABLES

CHAPTER I

INTRODUCTION

Introduction

The San Juan Mountains, which are located in southwestern Colorado (Figure 1.1), were extensively glaciated during the Pleistocene (Atwood, 1915; Blair, 1996; and Carrara, 2011). Areas that were not covered with glacial ice experienced periglacial conditions. Then, around 18,000 BP, the climate in the area began to warm and the main glaciers in the region began to melt (Blair, 1996). From 18,000 BP to 10,000 BP, the climate transitioned from full glacial conditions to an alpine-type climate. Although the region covered by glacial ice declined dramatically, frozen ground remained in the area (i.e., permafrost) (Baars, 1992; Carrara, 2011).

From 10,000 BP to the present, a warming trend with slight perturbations continued in the San Juan Mountains (Baars, 2000). One of the perturbations was the Little Ice Age, which resulted in lower temperatures, increased snow cover and growth of small glaciers that remained in the area until the end of the 19th century (Blair, 1996). Along with this decrease in temperature, one can assume that the spatial extent of permafrost in the area also increased. Following the Little Ice Age, the area once again began experiencing an increase in temperature, and it is assumed that the extent of potential permafrost decreased.

Today, much attention is focused on the impact of changing climate conditions on various mountain regions around the world (Anisimove and Nelson, 1995; Smith and

Riseborough, 1996; Gruber and Haeberli, 2007; Liu et al., 2010; Johnson et al., 2011; Jogenson et al., 2010; Stoffel and Huggel, 2012; Stoffel et al., 2014; Whiting et al. (2014); Bronniman et al., 2014; and Park et al., 2016). This is true for the San Juans, also, and Blair (1996) suggested that knowledge about climate change in the San Juans is, unfortunately, lacking. A major need exists to have more understanding about the trend of increased temperature and precipitation in this area, as well as potential impacts. Brenning et al. (2008) and Hipp et al. (2014) pointed out that during the last ten years, the extent of permafrost in alpine region has diminished rapidly. They argued that this magnitude of change has been the subject of much speculation.

Changing climatic conditions have a variety of impacts on alpine environments. For example, Leopold et al. (2010) and Magnin et al. (2015) have demonstrated a high sensitivity of permafrost in mountain regions related to increasing air temperature. Smith et al. (2010); Desyatkin et al. (2015) and Chadburn et al. (2015) suggested that the increase in Mean Annual Air Temperature (MMAT) impacts the depth of thaw, timing, and rate of refreezing. Studies of changing permafrost conditions in other parts of the Rocky Mountains by Hoffman et al. (2007) and Janke et al. (2012) have been used to suggest that the increase in air temperature was the cause of the decline in the extent of glaciers in the Rocky Mountains of Colorado.

An increase in temperature can result in continued thawing of the permafrost in the San Juan Mountains. The thawing of the permafrost in high-elevation catchments (i.e., horizontal down-slope movement and vertical-settling movement) might result in unanticipated changes in various processes (i.e., hydrological, geomorphological and

ecological) operating in the alpine ecosystem (Stoffel and Huggel, 2012; Etzelmüller, 2013; and Chin, 2016). These changes in the various processes might lead to loss of vegetation cover, lack of plant and animal diversity, increase in the rate of erosion, early melting of snow cover, and loss of ice stored in rock glaciers and ground ice (Pauli et al., 2003; Ernakovich et al., 2014). The melting of the ice along with earlier melting time of snow cover can lead to increased peak flow in streams, as well as flushing of sediments to lower areas of the drainage basin (Quinton and Baltzer, 2013 and Gamache, 2014).

Changes in climatic conditions and the extent of permafrost have been reported to result in subsidence and slope instability (Stoffel and Huggel, 2012; Fischer et al., 2013; and Burn, 2013). For example, Burke et al. (2012) reported that thawing of permafrost was responsible for shifting of the bases of ski lifts. Giardino (per communication, 2014) reported the thawing permafrost resulted in the tilting of the Monarch Ski Lodge, which resulted in it eventually being demolished. All of these warming conditions appear to have direct impact on an increased melting of permafrost, ice cores and ice matrices stored in rock glaciers and talus (William et al., 2006; Caine, 2010; Janke et al., 2012). Thus, all this research highlights the need to understand the extent of permafrost, as well as the potential impact of increased temperature on the spatial extent of permafrost.

Problem Statement

The impact of warming temperatures on reducing the spatial extent of permafrost has been demonstrated in other areas (Janke, 2005). Unfortunately, in the San Juan

Mountains, most work on permafrost has been speculative at best (Janke, 2012; Leopold et al., 2014 and Giardino, per communication 2014). The spatial extent of permafrost in the San Juan Mountains has not been mapped and the nature of change is unknown. No one has asked the question as to how warming temperatures in the San Juan Mountains are impacting the spatial extent of permafrost in these mountains? Additionally, how will these warming temperatures impact the spatial extent of permafrost in the future? Therefore, the purpose of this dissertation is to answer these research questions.

Objectives

From the problem statement, three objectives have been established for this dissertation.

Objective 1)

Analyze the temperature trend and rate of temperature change in the San Juan Mountains and examine relevant feedback and mechanisms from high-elevation responses regarding climate change.

Objective 2)

Model the current extent of potential permafrost in the San Juan Mountains using three separate models.

Objective 3)

Model the future potential change in the spatial extent of permafrost in the San Juan Mountains related to increasing temperatures.

Research Hypotheses

This research has three multiple-working hypotheses because the occurrence of periglacial landforms are influenced by temperature variation, topographical slope, location, and aspect. I hypothesize that:

1. Changing temperature, along with elevation, slope and aspect have a combined influence on the rate of change in the distribution of permafrost.
2. Thawing of permafrost will result in potential unstable slopes.
3. Risk associated with potential slope instability is related to the rate of change in temperature, slope, elevation, and aspect.

Study Area Location

The area of study for this research is a portion of the San Juan Mountains in southwestern Colorado (Figure 1.1). The San Juan Mountains are a rugged mountainous region of ~20,000 km^2. Of this 20,000 km^2, ~2,000 km^2 are above tree line. The study area is located in the northwestern part of the San Juan Mountains ($37^0$35' N to $38^0$6' N and -$108^0$0'W to $107^0$30'W) and has an area of ~1,480 km^2. The position of the study area is located south of Ridgeway, north of Silverton, east of Placerville, and west of Eureka (Figure 1.1). The study area is drained by two tributaries of the Colorado River, including the San Miguel, and Uncompahgre Rivers.

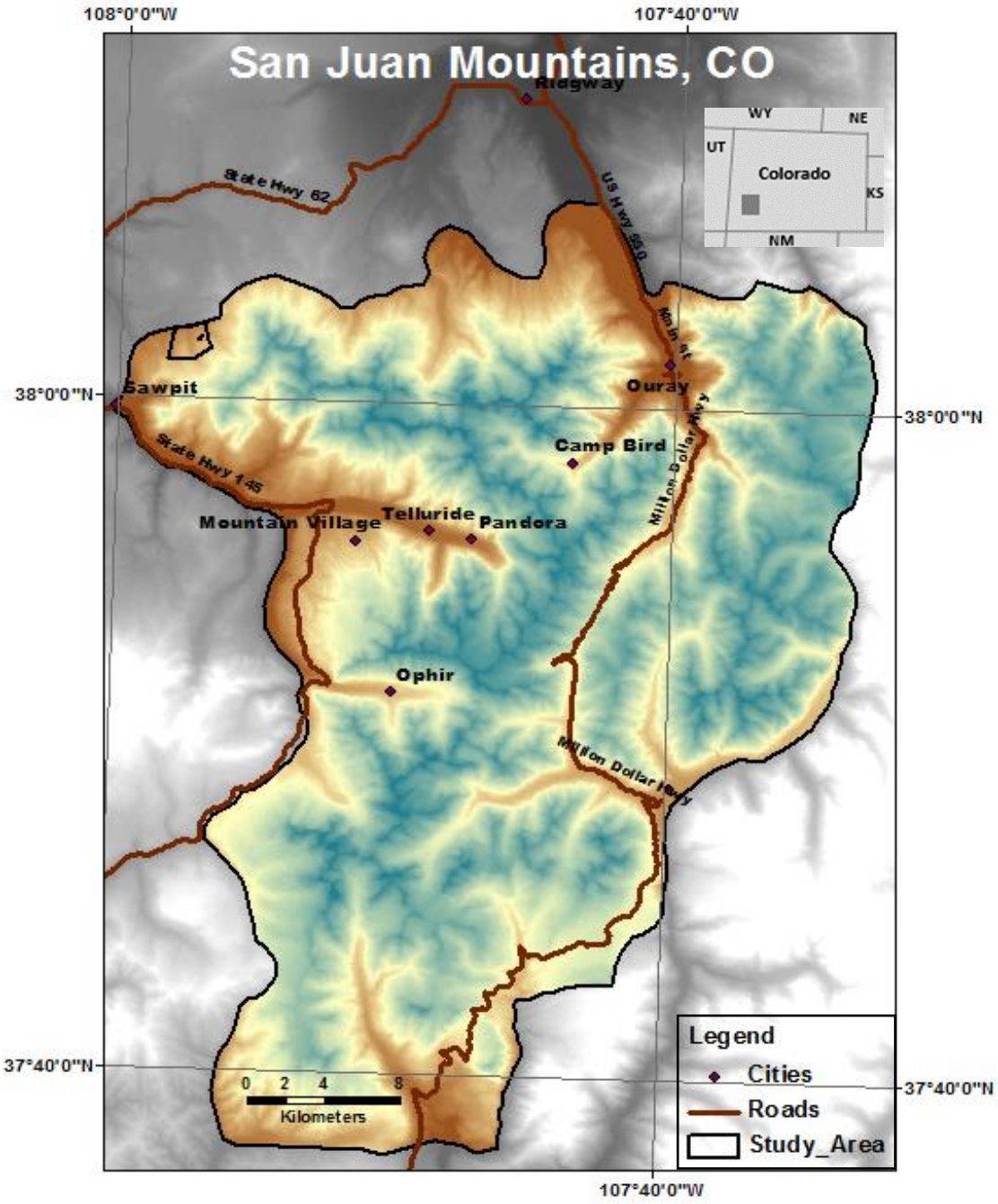

Figure 1.1. Map of the study area in the San Juan Mountains of southwestern Colorado.

The San Juans are characterized by numerous mountain peaks exceeding 4,200 m in elevation (Carrara, 2011). The study area also contains numerous lakes and bogs at and above the tree line.

Regionally, the mountain range consists of anticlinal arches, intervening basins, and glaciated mountains found at alpine and subalpine elevations (Pirkle and Yoho, 1985). According to Blair (1996), geologic processes of this mountain range can be classified as those either generated underground (mountain building and volcanic activity) or having occurred on the surface of Earth and are represented by general erosion processes. The region displays a complex landscape shaped by the dynamic forces of running water, glaciers, and tectonic uplift (Blair, 1996).

Justification

Studies of permafrost and climate change will continue to be a topic of interest as human development increases in the Colorado alpine environment. The main focus of this research will be to contribute new knowledge on the distribution of potential permafrost in the San Juan Mountains using various techniques. This research will provide an understanding of the impact of changing temperature, as well as elevation, and aspect on the occurrence and present condition of permafrost in the San Juan Mountains. Hence, this research can be used as a guideline to predict detailed changes in permafrost and evaluate risks to protect people and infrastructure from the impact of a changing environment in the alpine zone.

CHAPTER II

LITERATURE REVIEW

Alpine Environment

In an alpine environment, within the critical zone, the surface layer acts as an open system that is subject to elemental gains and losses of energy. Studying this central component of the critical zone is imperative, because knowledge of an alpine system is still limited despite its fundamental importance (Anderson et al., 2007; Anderson et al., 2008). Rates of energy production and loss, bedrock weathering, erosion and mass movement have been estimated in the literature, but a comparison among sites is often challenging (Brantley et al., 2007). Earth-surface processes in this environment are unique because they involve an integrated area of studies that forms the core of a network that advances interdisciplinary understanding of the environment that sustains life.

Alpine environments have landscapes dominated by high relief, steep slopes, tectonic activities, and extreme micro-climates (Giardino, 1979; Blair, 1996). This patchwork of landforms is shaped by various geologic and geomorphic processes influenced by the various subsystems of Earth and are composed of various assemblages, which can serve as pathways (the debris transport system) to move energy and material (Barsch, 1977; and Giardino, 1979) from higher to lower elevations. The energy input into this alpine system consists of potential, kinetic, radiation, thermal and chemical as expressed through gravity, climate, hydrology, and geochemistry. Meanwhile, the material inputs include snow, ice, rain, melt water, rock, soil, dust, and vegetative debris

(Giardino, 1983; Pauli et al., 2003; William et al., 2006; Baroni et al., 2007). Because energy and material have a tendency to follow similar pathways, various input interactions occur in the debris transport system.

Interactions of energy and material inputs, along with geomorphic processes associated with erosion, transportation, and deposition in alpine environments create a debris cascade system (Giardino, 1979; Haeberli, 1985; Barsch, 1996; Haeberli, 2013). The resulting landforms function as sources, sinks, and conduits for energy and rock debris. The individual landforms, which make up the alpine debris system, include glaciers, and subsequent erosional and depositional remnants. Examples of these include cirques, arêtes, roche mountanees, and various types of moraines. In addition, mass movement and periglacial features are present, including debris flows, protalus ramparts, talus, and rock glaciers.

As a critical zone, an alpine system sculptured by glaciers and modified by periglacial processes remains a focus of many geoscientists (Degenhardt, 2009). Changes in mean annual air temperature, net radiation patterns, distribution of snow cover, and other variables will alter the processes modifying alpine systems (Caine, 2010). Humans, through anthropogenic climate change, mining, recreational use, and other activities, threaten the nature and stability of alpine systems (Konrad and Humphrey, 2000). Development, in the form of project property, contraction transportation, mining and energy projects continue to occur in this region (Giardino and Vitek, 1988; Barsc 1996; Bürki, 2003; Guvorushko, 2011). As a result, alpine areas, as a critical zone, and humans have become delicately interconnected.

Alpine Climate

In the alpine environment, a warming climate is widely expected over the next century (Harris et al., 2003; Gruber and Haeberli, 2007; and Jorgenson et al., 2010). An enhanced greenhouse effect has significant implications for permafrost in this environment. For this reason, systematic monitoring of the climate and ground thermal conditions in the permafrost regions have been discussed as a means of detecting climate change (Anisimov and Nelson, 1996; Smith and Riseborough 2002; Gruber and Haeberli, 2007; and Escobedo, 2008). Whereas measurements can reveal if change has occurred, identifying a change and detecting an effect have to be distinguished because other factors also influence ground temperatures.

Long-term continuous temperature observations in soils and at the ground surface are essential in investigations of the response of permafrost to climate changes. Smith and Riseborough (2002) suggested that research should be directed toward understanding the physical relationship between the temperature of permafrost and the air temperature (IPCC, 1990). Analyzing the responses of permafrost to climate change, however, requires an adequate functional description of the permafrost-climate system. Air surface and permafrost temperatures will change differentially, depending on the interplay of these climatic, local and lithologic effects. Keeping track of these separate influences is a key requirement for detection.

In the permafrost-climate relationship, Smith and Riseborough (2002) categorized four levels of temperature regimes to be considered. They are: (1) the temperature at standard screen height; (2) the temperature at the snow surface; (3) the

temperature at the ground surface; (4) the temperature at the top of permafrost. Temperatures at each of these levels differ on a mean annual basis. Differences in mean values arise because heat transfer coefficients through the layers of the system have correlations with temperature through time (Anisimov and Nelson, 1996). In the lower atmosphere, turbulent transfer varies diurnally and seasonally between stable and unstable conditions. Heat conduction in the ground varies between frozen and thawed states. The presence or absence of the snow cover determines whether heat transfer immediately above the ground surface is predominantly conductive or convective (van Everdingen, 2005; Bales et al., 2011).

Geographical locations and different landscape conditions also need to be considered. In a recent study of time series of observations in different geographical locations and landscape conditions, Smith and Riseborough (2002) showed that different locations and conditions display different trends in temperature regimes. In another study, Gruber and Haeberli (2007) showed that general trends in the ground-surface temperatures are closely related to the air temperature trend.

Climate and Permafrost

Permafrost is land that remains frozen (at or below 32°F or 0°C) for two or more consecutive years (Briggs et al., 2014). Permafrost covers about one-fifth of the total land surface of Earth (Janke et al., 2012). Permafrost generally occurs in areas where moisture seeps through the soil but because of cold temperatures, it freezes and over time, a layer of frozen soil or subsoil develops 1 m to 1,000 m below the surface

(Wellman et al., 2013). Permafrost is not determined by the moisture content in the soil; it is instead defined by its temperature. Because permafrost is determined by temperature, certain areas of permafrost can have different types of ice beneath the soil, as well as variability in ice content from 0% to 50% (Jorgenson et al., 2010). This ice is typically called ground ice, and it can occur in three forms: solid piece of relatively pure ice, veined pattern, or sometimes as ice wedges.

Permafrost can occur in high mountains and is fundamental to geomorphic processes and ecologic development in tundra and boreal forests. Because permafrost impedes drainage and ice-rich permafrost settles upon thawing, the degradation of the permafrost in response to climate change will have consequences for boreal ecosystems (Jorgenson et al. 2001; Kanevskiy et al., 2008). Thawing permafrost affects surface hydrology by impounding water in subsiding areas and enhances drainage of upland areas (Woo et al., 1993). Consequently, changes in soil drainage alter the degradation and accumulation of soil carbon (Schur et al. 2008), habitats for vegetation and wildlife (Jorgenson et al., 2010), and emissions of greenhouse gases (Christensen, 2004; Burke, 2012; Johnson et al., 2011). The consequences will range from microsite changes in hydrology and vegetation to possible global contribution of greenhouse gases (Lin, 2009; Caine, 2010).

Permafrost responds to climatic change (Osterkamp, 2007). The ~20 ^{0}C increase in air temperature at the Pleistocene–Holocene transition led to a large reduction in the area of permafrost (Arctic Climate Impact Assessment, 2005). The degradation of permafrost during this transition period resulted in the formation of a contemporary

discontinuous zones where permafrost previously was continuous as well as, the reduction of permafrost thickness by thawing of permafrost from its base (Jorgenson et al,. 2001). Therefore, the stability of permafrost depends on climate changes over differing periods and magnitudes, which can cause permafrost to persist over hundreds to thousands of years or to be newly formed during cold, snow-poor winters and persist only for years to decades.

Jorgenson et al. (2010) stated that permafrost is not connected directly to the atmosphere because its thermal regime is mediated by topography, surface water, groundwater, soil properties, vegetation, and snow, and numerous interactions occur among these ecological components that can lead to positive and negative feedbacks to the stability of the permafrost. Topography affects the amount of solar radiation received at the soil surface, causing permafrost in the discontinuous zone to occur generally on north-facing slopes in the northern hemisphere that receive less direct radiation, in flat low-lying areas where vegetation has a greater insulating effect and where air temperatures tend to be colder during winter inversions (Viereck et al., 1986). Even though the permafrost is not connected directly to the atmosphere, according to (Janke et al., 2012), annual mean permafrost temperatures are very closely related to the annual mean ground surface temperatures, which is related to the Mean Annual Air Temperature (MAAT). The difference between these two is known as thermal balance (Smith et al., 2010). The value of the thermal balance can be easily derived from the annual mean-soil temperature profiles. Thermal balance can vary from year to year, however, at the same location the range of variations usually do not exceed 0.5°C (Janke

et al., 2012). The stability of permafrost depends on air temperatures and ecological factors and both greatly complicate the prediction of the consequences of climate change (Ernakovich et al., 2014).

The active layer of permafrost, therefore, is a complicated system that reflects various natural and anthropogenic factors (Guvorushko, 2011). The most important of these factors are the air temperature, hydrologic regime and physical properties of soils, the occurence of related geocryogenic processes (e.g., cryoturbation, differential heaving etc.), vegetation transitions, and different types of natural and human-imposed disturbances. Nevertheless, the long-term measurements of the thickness of the active layer can identify trends in permafrost evolution.

Permafrost and Rock Glaciers

Rock glaciers are an important component of high-mountain systems; they are common in Arctic and alpine permafrost regions and play an important role in alpine mass balances and aspects of morphologic stability (Jansen and Herganten, 2006). In addition, rock glaciers can serve as a visible indicator of the occurrence of mountain permafrost (Barsch, 1977; and Haeberli, 1985). Permafrost phenomena in mountain areas are a function of: Mean Annual Air Temperature (MAAT), elevation, direct solar radiation, (i.e., aspect) local relief and topography, snow cover thickness and duration, and avalanche activity (Haeberli, 2013).

According to Giardino (1979) rock glaciers are a deposit of poorly sorted, angular to tabular debris that is held together by a matrix of ice-cemented clasts. This

original definition has been expanded to include flow rate, size, location, micro-relief, and distribution (Washburn, 1980; Haeberli, 1985; Martin and Whalley, 1987). Giardino and Vitek (1988) argued that rock glaciers should be thought of in the context of a space-time continuum (Figure 2.1). They agreed that rock glaciers occupy a transitional position on the landscape continuum. In the alpine debris cascade, rock glaciers are the transitional form in the transportation system. Thus, most movement of energy and debris through the alpine debris cascade passes through a rock glacier, if one is present.

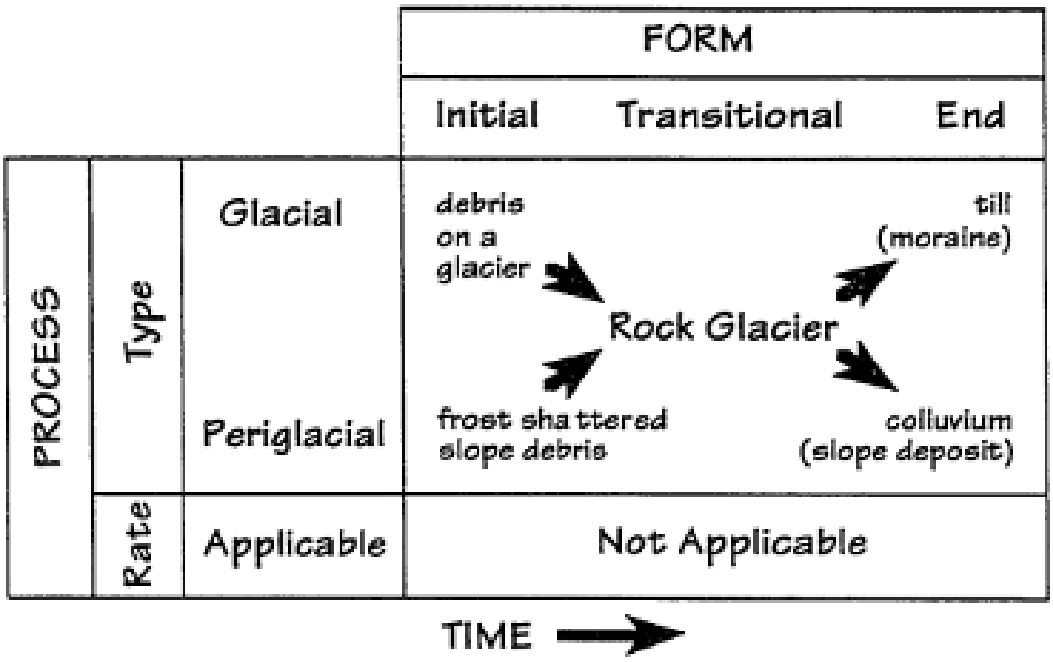

Figure 2.1. Conceptual diagram of an alpine landscape continuum involves space, time, and processes (Giardino and Vitek, 1988).

In addition to the terrestrial feature, rock glaciers are found on Martian landscapes (Degenhardt at al., 2003) and serve as a transport mechanism for debris from alpine areas (Burger et al., 1999).

Barsch (1977) calculated that rock glaciers transport approximately twenty percent of rock debris in the eastern Swiss Alps. Giardino (1979) estimated that rock glaciers transport ten percent of the debris in the Mounts Mestas area of southern Colorado. Both studies showed that rock glaciers transport significant volumes of material.

Early studies defined rock glaciers as a dead glacier (Streenstrup, 1883), a peculiar form of talus (Spencer, 1900) and as chrystocrenes (Tyrrell, 1910). The first major research regarding rock glaciers was carried out by Howe (1909) and Capps (1910). They defined rock glaciers as a movement of mass in a glacier-like way, like rock streams (Howe, 1909) that create a wrinkled pattern on the surface (Capps, 1910). Capps highlighted five major characteristics of rock glaciers, which are composition, size, form and shape, margin, and movement. Wahrhaftig and Cox (1959) redescribed the morphology of rock glaciers by classifying them based on the geometry of the length to breadth ratio, and topographic position. A combination of the original morphological criteria observed by Capps (1910) and classification by Wahrhaftig and Cox (1956) remain the basic means for identification of rock glaciers.

Other studies have included variables describing the rock glacier as a special form of an ice-cored moraine (0strem, 1964; Barsch, 1996; and Haeberli, 1985). Wahrhaftig and Cox (1956) hypothesized that the internal ice of rock glaciers forms as

interstitial ice within the debris because rock glaciers form only via periglacial processes (Barsch, 1996; Haebarli, 1985). Potter (1972) argued that rock glaciers may also develop by a continuum of processes from glacial to periglacial, by the transformation from a debris-covered ice glacier into a rock glacier, similar to Giardino and Vitek (1988). Potter (1972) presented several lines of evidence that supported a glacial origin for at least some rock glaciers, expanding on a concept proposed by Outcalt and Benedict (1965).

In his detailed study of the Galena Creek rock glacier in the Absaroka Mountains, Wyoming, Potter (1972) observed an ice-core in the rock glacier and documented multiple exposures of clear, layered ice beneath the thin, but continuous surface rubble; crystallography and fabrics of the ice conformed to those of true glaciers. In a more generalized study, development and expansion concepts of rock glaciers that are similar to those of Potter were proposed by Whalley (1974) stating that most rock glaciers are glacigenic. Whalley argued that accumulation of interstitial ice within talus or till could not effectively explain the internal structure and observed flow of rock glaciers. Whalley's study produced a large distraction in rock glacier research as cited by Haeberli (1985). This idea began a protracted argument on the subject of the original rock glaciers to be only ice-cored versus ice-cemented (Whalley, 1974) or produced by permafrost (Barsch, 1977; Haeberli et al., 2006).

Rock glaciers can be described as an interconnected, cascading system of debris, ice, and water, which is comprised of four interrelated subsystems: talus, surface, subsurface, and outflow (Giardino, 1979; Humlum, 2000). Surrounding cliffs provide

coarse to fine-talus input, depending upon the pattern and density of headwall fractures, as well as chemical and physical weathering of surrounding bedrock cliffs (Giardino, 1983; Haeberli, 1985). Therefore, Giardino and Vitek (1988) proposed that rock glaciers are best defined by morphology rather than origin or thermal conditions. More specially, a rock glacier may be characterized according to a combination of the following variables: ice content, debris input (talus or moraine), flow rate, size, location on the hillslope, microrelief (ridge and furrow), and distribution, which is influenced by lithology, geographic location, topographic, micro-cilmate, and other local environment variables (Capp, 1910; Wahrhaftig and Cox, 1959; Haeberli, 1985; Giardino and Vitek, 1988; Whaley and Martin, 1992; Clark et al. 1998).

Rock glaciers can vary in elevational distribution in glacial or periglacial environments. Rock glaciers were thought to exist in low precipitation, continental climates where frost weathering is dominant and temperature is sufficiently cool to maintain ice. In an alpine environment, however, rock glaciers are restricted to dry, continental climates at elevation below the equilibrium line of glaciers and above the lower permafrost limit, and driven by topoclimates (Barrsch, 1977; and Haeberli, 1985).

Rock glaciers provide important topoclimatic information. According to Janke (2005), the distribution of rock glaciers may include active or inactive forms and can be used to model the distribution of permafrost. Topographic variables such as elevation, slope, and aspect influence snow accumulation with low radiation budgets where rock glaciers are produced, also provide historical information about where permafrost once existed (Janke et al., 2012). Some rock glaciers have shown an indication that Mean

Annual Air Temperature (MAAT) over ten thousand years ago was cooler ~3.0 – 4.0^{0}C with permafrost extending 600 – 700 m lower than today. This situation indicates that a significant change of temperature occurred to degrade permafrost. As the temperature continues to rise, the area of permafrost will continue to shrink.

Degrading permafrost can lead to a variety of hazards, such as debris flow or outburst floods from breeching of proglacial lakes (Haeberli et al., 2006). Because rock glaciers have a debris cover, act as an insulator, and protect internal ice from melting, the climatic responses of rock glaciers are unique. The debris on rock glaciers will filter short-term climate anomalies. Consequently, rock glaciers do not respond to yearly fluctuations in temperatures. Therefore, geomorphic and environmental variables must be evaluated as rock glaciers respond to climatic fluctuations (Janke, 2005).

CHAPTER III

DESCRIPTION OF THE STUDY AREA

Location and Ecoregion

The San Juan Mountains, a segment of the southern Rockies, extend southeastward for ~240 km from Ouray, in southwestern Colorado, U.S., along the course of the Rio Grande to the Chama River, in northern New Mexico. Many peaks in the northern section of this area exceed 4,300 m (Figure 3.1 and Table 1). The mountains, composed mainly of volcanic rocks, serve as a source for headstreams of the Rio Grande and San Juan River and are part of the Uncompahgre, San Juan, Rio Grande, and Carson national forests.

Table 1. List of San Juan Mountain peaks in northern section that exceed 4,000 m

No	Mountain	elevation (m)
2	Teakettle Mountain	4,212
3	Dallas Peak	4,209
4	Potosi Peak	4,202
5	Gilpin Peak	4,174
6	Ulysses S. Grant Peak	4,196
7	Pilot Knob	4,187
8	Golden Horn	4,197
9	Fuller Peak	4,194
10	Rolling Mountain	4,174
11	Grizzly Peak	4,187

The Continental Divide occurs along the San Juan Mountains. Approximately 2,000 km^2 of the San Juan Mountains are in the alpine zone above the timberline with on elevation of 4,200 m (Carrara, 2011). The study area encompasses high, rugged areas

and contains numerous lakes and bogs at and above the treeline. Regionally, the mountain range is associated with anticlinal arches, intervening basins, and glaciated mountains, located at alpine and subalpine elevations (Pirkle and Yoho 1985). According to Blair (1996), geologic processes of this mountain range can be classified as those either generated underground (mountain building and volcanic activity) or having occurred on the surface of Earth and are represented by general erosional processes. The region displays a complex landscape shaped by the dynamic forces of running water, glaciers, and tectonic uplift (Blair, 1996).

The San Juan Mountains are typically high energy environments, subject to strong winds, frequent freeze-thaw cycles at higher elevations, accumulation and melting of snow masses in some parts and heavy rainfall in others. Collectively, these agents speed up the process of weathering, whereas elevation and slope hasten the transport of erosional debris. Slope, thin soils, and the general absence of a permanently frozen subsoil, means that water is lost rapidly downslope, and mountain plants are often well adapted to drought conditions.

As a result of variation in elevation and relief, the San Juan Mountains contain a number of vegetation zones. These zones are designated as the transition and Upper Sonoran zones found below 2,285 m, the montane zone between 2,285 to 2,900 m, the subalpine forest zone extending from 2,900 to 3,660 m, and the alpine zone above 3,660 m.

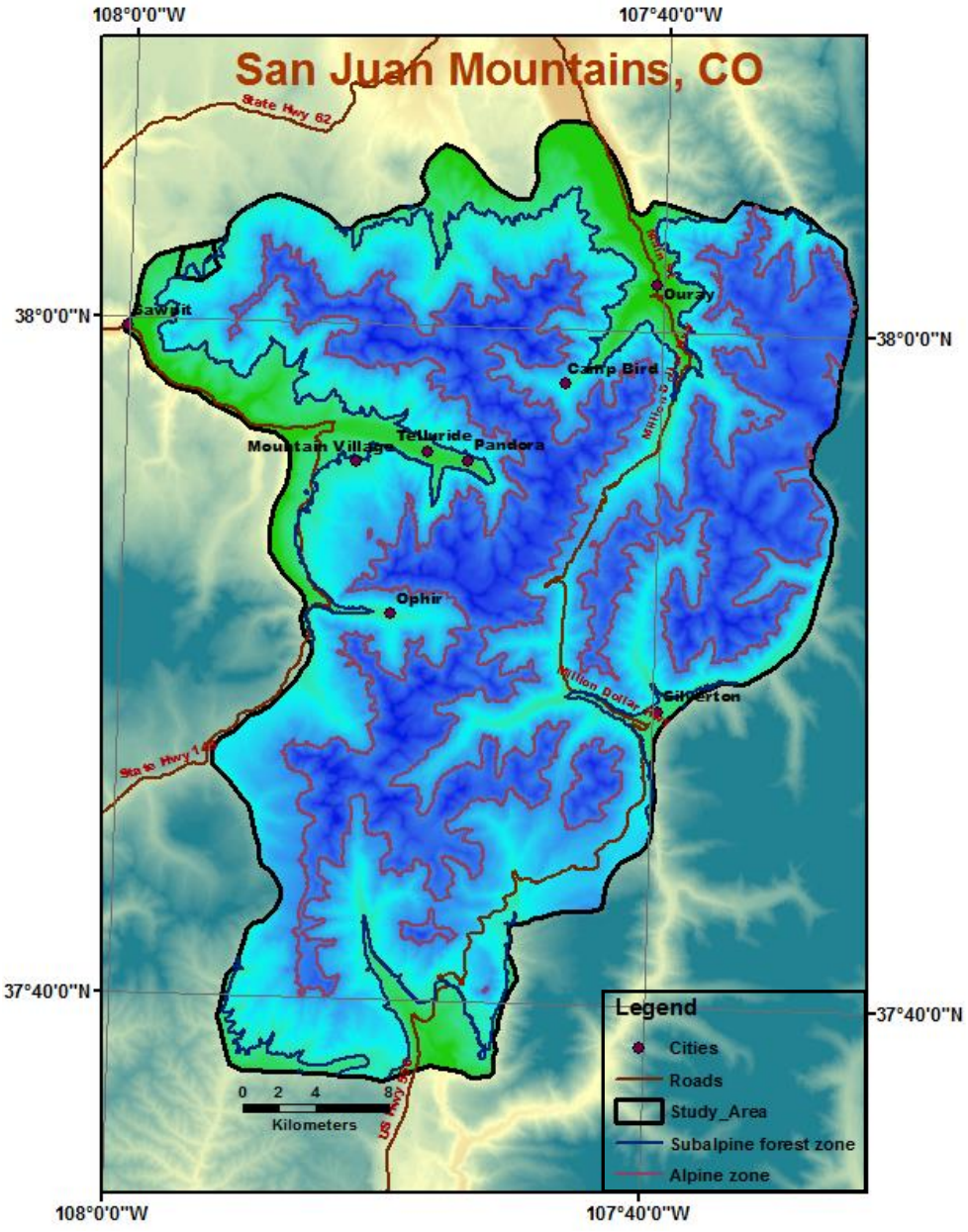

Figure 3.1. The alpine zone (blue shade), subalpine zone (light blue shade), montane zone (green shade), and northern part of San Juan Mountains (dark blue) in the study area of the San Juan Mountain.

Geology

The San Juan Mountains are geologically young, cover ~20,000 km^2 and are among the highest and most rugged mountains in North America. The mountains are part of the extensive Southern Rocky Mountains. The San Juan Mountains reveal a creation and demise of the many mountain ranges in this region during the past 1.8 billion years (Gonzales and Kalstrom, 2011). The geological formations in this area range from Precambrian rocks through Paleozoic sediments to a thick sequence of Tertiary volcanic rock.

Approximately ~65 million years ago, during the Laramide Orogeny, volcanic activities and the uplift of Uncompagria (i.e., Ancestral Rockies) occurred in this area (Baars, 2000). The Laramide orogeny created a series of mountain ranges and related structural sedimentary basins. In many areas, the mountain units are bound by upturned sedimentary rocks and bordered by steep reverse and thrust faults (Gonzales and Kalstrom, 2011).

Over time, the Ancestral Rockies were eroded away and, essentially, disappeared. Extended periods of volcanic activity occurred ~30 million years ago where pyroclastic debris and lava filled in the valleys and fissures in the rugged surface areas (Lipman et al., 1970). After the volcanic activities ended, the pools of magma under the surface of Earth in this area shrank, creating spaces into which portions of the surface sank and formed bowls or calderas.

In the past several million years, the San Juan Mountains have been worn and sculpted by the active erosive forces of glaciers and rivers. Removal of crustal mass may

be facilitating minor uplift (Blair, 1996). This erosion has also exposed windows into the crust showing formation of the rock structure and mountain building processes.

The San Juan Mountains consist of a sequence of middle to late Tertiary igneous and pyroclastic rocks two km thick that were erupted from at least 15 calderas (Steven and Lipman, 1976). These volcanic rocks unconformably overlie metamorphosed sedimentary, volcanic and intrusive rocks of Precambrian age, as well as sedimentary rocks of Paleozoic, Mesozoic, and early Cenozoic age (Carrara 2011).

According to Carrara (2011), the San Juan Mountains were extensively glaciated during the Pleistocene as indicated by numerous cirques, broad U-shaped valleys, and moraines that emerge from canyons at the base of the mountains. Atwood (1915) recognized tills of three different ages in the San Juan Mountains. These tills were termed the Cerro, Durango, and Wisconsin. Atwood and Mather (1932) also suggested that the San Juan Mountains were covered by ~5,000 km^2 of glacial ice in the form of valley glaciers, regional ice field, and transection glaciers.

Initially formed from volcanic activity, the complex landscape of the San Juan Mountains, with the present valley and canyons, displays the effect of the dynamic force of flowing water, glacial processes, and tectonic uplift upon the variety of rocks in the study area. The San Juan Mountains will continue to depend on the cycle of mountain building and beveling as the force of plate tectonics and erosion work in opposition to transform layers of crust into the future form of mountains.

Soil

The volcanic nature of much of the San Juan Mountains provide rich soils for healthy wildflowers, grasses and bushes, aided by how wet they are compared to many other parts of Colorado.

Soil orders occur in zones corresponding to vegetation. Soils in the spruce-fir zone are acidic, often shallow and infertile as a result of recent origin, leaching and the acidic foliage. Little bacterial activity occurs at the low temperatures of this zone, and much of the carbon in the ecosystem is locked up in humus (Blair 1996). Alpine soils tend to be shallow, poorly developed mineral soils with very limited organic matter. An exception is the accumulation of peat in fens, found in low areas where soils are not washed away. Soils derived from volcanic tuff are highly erodible and may provide habitat for some of the rare plants by continually opening up bare areas that are free from competition of other plants.

In the San Juan Mountains, the present or absent of permafrost involves major variations in the physical structure of the soil, which is a key in determining vegetation coverage, plant community structure and productivity, and the ecosystem carbon balance (Genxu et al., 2008). Permafrost in soil in this area is greatly affected by cold temperature and by the present of perennially frozen ground beneath the seasonally thawed layer. Seasonal freezing and thawing force the development of isolated and massive ice resulting in variety of patterned-ground features (Ping et al., 2015). Because the underlying permafrost impedes subsurface drainage, soils are often wet as well as cold, which greatly affects oxidation/reduction, decomposition, and other biochemical

processes. Degradation of permafrost, however, can alter soil properties which rapidly modified sediment load, hydrology path flow, potential release of organic carbon, and geochemistry of water (Chin et al., 2016).

Hydrology

The surface water in the San Juan Mountains comes from snow, ice melt and precipitation. In the alpine environment, meltwater supply is continuous during the summer months, especially from rock glaciers (Burger et al., 1999). Water movement through soil and rock is controlled by local weather, the seasons, thermal properties of the rock-debris layer, and physical mechanisms that control meltwater. The average mean-annual discharge, however, is significantly lower than glacier supply, although the general discharge patterns are the same (Millar and Westfall, 2010). In the southern Sierra Nevada Range of California, for example, snowpack has affected the timing and rate of water discharge, rate of atmospheric exchange, and rates of biogeochemical processes (Bales et al., 2011). In a warming climate, snowfall amounts and timing of melt change will shift toward rain rather than snow, as the primary form of precipitation and runoff.

Rock glaciers in this region also supply meltwater. Water in rock glaciers can flow near the surface, above the active permafrost layer, or can flow in the deep surface beneath permafrost. The permafrost layer acts as an impermeable boundary to water from rock debris or melting ice. During the late summer and early fall, lowering temperatures create freezing fronts that move upward from the perennial permafrost and

downward from the rock-glacier surface, squeezing together the remaining water in the central portion of the active layer (Burger et al., 1999).

In addition to the inputs previously mention, discharged water can also come from permafrost or an internal ice structure. Water that comes from these sources usually has a pH greater than 6 and is below 1^0C (Baltensperger et al., 1990). Electrical conductivity is low during high discharge and high during cold weather (Krainer and Mostler, 2002).

Discharge from rock glaciers can alter the geochemistry of an alpine stream, river, and lake system. Higher nitrate concentrations have been emitted from most rock glaciers in alpine environments, especially in the San Juan Mountains and increase seasonally (William et al., 2006). Nitrate, calcium, and sulfate are also higher in rock glaciers that are linear to the thickness of rock glaciers. Chemical weathering in the San Juan Mountains can alter minerals to form weathering products of new minerals (Admunson et al., 2007). This process impacts water composition (Gaillardet et al., 2004), but until recently, it has been viewed primarily as a set of inorganic reactions.

Climate

The San Juan Mountains are considered arid or semi-arid with annual precipitation amounts in most areas of less than 25 cm. In this area, the high plateaus and small mountain ranges, however, receive considerably more precipitation than the more widespread middle and lower elevations because of orographic lifting and cooler temperatures. Most areas above 2,450 m receive 50 – 70 cm annually, whereas

mountains above 3,300 m often receive about ~1.0 m per year. Therefore, the climatic pattern in the San Juan Mountains varies from south to north. The northern region generally lies outside the typical major pathways of winter and summer moisture-bearing air masses. Winter moisture comes infrequently from Pacific air masses, and summers are generally hot, with infrequent convective rainfall (Carara, 2011).

The San Juan Mountains are affected by air masses originating in several regions. Between October and May, air masses travel from the Pacific Ocean to reach the San Juan Mountains. These air masses can originate in the Gulf of Alaska or off the coast of Baja California. These air masses bring large amounts of snow for which the San Juan Mountains are known (Carrara, 2011).

Between July and September the San Juan Mountains are affected by the North American monsoon that brings frequent afternoon thunderstorms. At this time, the San Juan Mountains receive approximately 30–35 percent of the annual precipitation compared to other seasons. During the monsoon, low-level moisture is drawn from the eastern tropical Pacific and Gulf of California by a thermal low in the desert southwest (Hales, 1972). In addition, air masses from the Gulf of Mexico, may at times, flow west across the highlands of Mexico and north along the Gulf of California, thereby, contributing upper-level moisture and reinforcing the monsoonal circulation. Precipitation from the monsoon may continue into the late fall, usually through much of October (Carrara, 2011).

Mean January and July temperatures were estimated for tree-line, and the Lake Emma site by extrapolation from the Red Mountain Pass station (Table 2) and by using a

winter lapse rate of 4.1^{0}C/km and a summer lapse rate of 6.2°C/km used in the Colorado Front Range (Barry and Chorley, 1976). Regardless of the accuracy of these temperature estimates, harsh periglacial conditions in the higher regions of the San Juan Mountains are indicated by numerous active rock glaciers (Howe, 1909; Atwood and Mather, 1932; Carrara and Andrews, 1975; White, 1979; Degenhardt, 2009).

The San Juan Mountains are known to have the most amount of snow in almost every winter in Colorado (Lemke et al., 2007). The first snows usually fall in mid-September and remain on north-facing slopes late in the summer. By late October, much of the high mountains are covered by snow and winter is in full force in this region.

Table 2. Climate data from stations in San Juan Mountains, Colorado

Station Location	**Elevation (m)**	**Mean**		
		Annual precipitation (cm)	**January temperature (^{0}C)**	**July temperature (^{0}C)**
Ouray	2,390	58.5	-3.4	18.2
Telluride	2,680	58.6	-6.0	15.1
Silverton	2,825	62.4	-8.9	13.1
Red Mountain Pass	3,415	109.2	-8.6	10.8
Timberline	3,570	121.5	-9.2	9.8
Treeline	3,660	128.6	-9.6	9.3
Lake Emma	3,740	134.9	-9.9	8.8

The climate in the San Juan is linked to patterns of land-cover and land-use, particularly in a semi-arid region of variable topography. The biotic communities in this area are the products of species evolution and migration over time on a constantly shifting landscape driven by changes in climate at a variety of temporal and spatial

scales (Carrara, 2011). Variability in temperature, humidity and precipitation affects biotic productivity and diversity regionally and locally. Shifts from one climatic regime to a new pattern can be abrupt.

CHAPTER IV

METHODOLOGY

The methodology of this study was developed to determine the past, present and future potentail spatial pattern of permafrost in the San Juan Mountains. Specially, the methods focuses on the impact of changes in temperature by using National Oceanic and Atmospheric Administration (NOAA) and Snow Telemetry (SNOTEL) sites in Colorado. Second, a frost number was calculated as a transfer function to serve as a surrogate for permafrost occurrence. Third, the occurrence of rock glaciers were used again as surrogates to map the spatial extent of permafrost during the Pleistocene and into Holocene. Because rock glaciers contain either an ice-core or an ice matrix, the ground underneath would be permanently frozen. Thus, to map the extent of potential permafrost 98 rock glaciers were mapped in the study area, and the toe of each rock glacier was used to map the lower elevation of permafrost. It should be realized that permafrost more than likely extended beyond the toe of rock glaciers, however, for this study the extent of permafrost is assumed to be a toe of the rock glacier.

The methods used in this study are described in the following section.

Temperature Trend Analysis

The impact of temperature was evaluated using two data sets. The data sets included: data collected from SNOTEL and National Climatic Data Center of the National Oceanic and Atmospheric Administration (NCDC-NOAA) climate stations

(Figure 4.1). The standard adiabatic rates for mountains ware used to establish local temperature for this research through the use of ArcGIS® data layers. Climate records were analyzed using linear regression. By applying this method, temperature related to climate change was categorized and interpreted. Digital Elevation Model (DEM) was obtained for the study area. Climate distribution was produced by the overlay method in ArcGIS®, which was processed using elevation data.

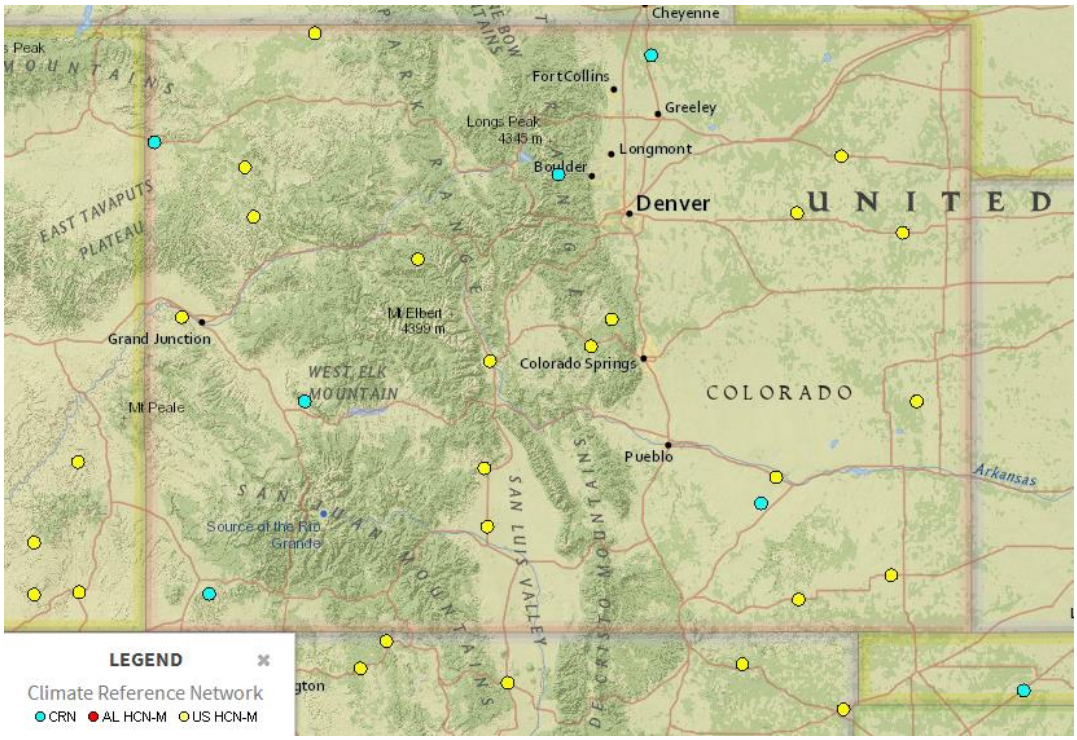

Figure 4.1. National Climatic Data Center of the National Oceanic and Atmospheric Administration (NCDC-NOAA) climate stations (blue dot).

To predict long-term change of temperatures in the San Juan Mountains study area, data were collected from 24 field stations (figure 4.2). The data are readily

available at NCDC-NOAA for large area coverage and the SNOTEL network for smaller coverage areas in the State of Colorado. From these data, the temperature trend was examined and analyzed.

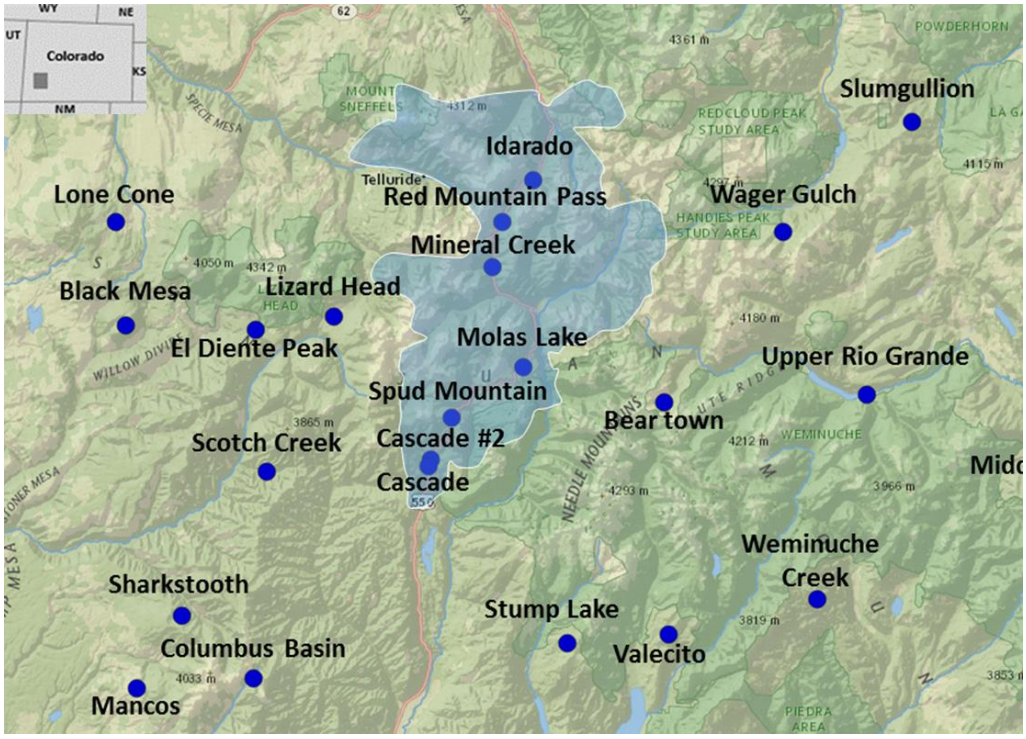

Figure 4.2. Snow Telemetry (SNOTEL) climate stations.

Frost Number and Temperature at the Top of Permafrost Layer Model

Researchers have developed various methods to map the extent of permafrost. These various approaches include hydrology, physical processes, and geomorphic indicators (Damm and Langer, 2006; Etzelmuller et al., 2007). The extend of potential permafrost has been mapped in other areas by Grosse et al. (2005), Janke (2005), and

Nyenhuis et al. (2005) using proxy indicators, such as rock glaciers, pattern ground, solifluction lobes, vegetation pattern, and other characteristic types of land-cover.

Most studies regarding permafrost require a minimum amount of direct measurement data. Nelson and Outcult (1987) developed a unique way to calculate the frost number, which is a dimensionless ratio that is the sum of either freezing or thawing degree days of frost and thaw penetration depths. Thus, they were able to differentiate a latitudinal zone of permafrost. To obtain these data, one has to monitor temperatures in the field. Fortunately, the San Juan Mountains have nine SNOTEL sites that collect temperature data.

Janke et al. (2012) developed a quick way to calculate the frost number (F). The equation (1) below was used to calculate frost numbers.

$$F = \frac{DDF^{0.5}}{DDF^{0.5} + DDT^{0.5}} \quad (1)$$

Where, F is the frost number, DDF is the sum of degree-days (i.e. a positive number) for frozen states, and DDT is the sum of degree-days for thawed states.

Another approach to determine the temperature at the top of permafrost was developed by Smith and Riseborough (2002), who integrated air and surface temperature to create a seasonal surface-transfer function. This transfer function can be shown as:

$$TTOP = \frac{(nt * It) - (nf * \frac{kf}{kt} * If)}{P} \quad (2)$$

Where:
TTOP is the temperature at top of permafrost;
kt is thermal conductivity of ground (thawed);
kf is thermal conductivity of ground (frozen);
nt is thawing n-factor;
nf is freezing n-factor

It is air annual thawing index;
If is the annual freezing index;
P is the period of one year record (number of day's record).

This transfer function is based on snow cover and the thermal conductivity of the soil to produce a temperature at the top of the permafrost (TOPM). From their research, two important factors stand out. The ratio between thermal conductivity of the ground and thawed and frozen states appears to be a critical factor in identifying the equatorial edge of discontinuous permafrost. On the other hand, snow cover appears to be the important factor for determining the polar edge of discontinuous permafrost in Arctic regions. I attempted to use this technique in the San Juan Mountains, also.

Janke et al. (2012) modified Smith and Riseborough's (2002) work to develop a more accurate way to estimate the temperature at the top of a permafrost layer. The temperature at the top of the permafrost layer (TTOPL) is given as:

$$TTOPL = \frac{(rk * nt * It) - (nf * If)}{P} \quad (3)$$

Where:

TTOPL is the temperature at top of permafrost;
rk is thermal conductivity ratio (kt/kf);
kt is thermal conductivity of ground (thawed);
kf is thermal conductivity of ground (frozen);
nt is thawing n-factor, for temperature between air and ground surface during summer;
nf is freezing n-factor, for temperature between air and ground temperature that takes into effect of snow cover;
It is degree days for thawed conditions;
If is degree days for frozen conditions;
P is the period of one year record (number of day's record).

The third method of mapping the extent of potential permafrost is based on the location of rock glaciers. Because rock glaciers in San Juan Mountains either contained an ice-core or an ice matrix, the assumption was made that the ice-core or ice matrix of the rock glacier had to be resting on slopes underlain with the permafrost. Research by Haeberli et al. (2006), Janke et al. (2012), and Hasler et al. (2014) support this assumption.

Ninety-eight rock glaciers were mapped in the study area using Google® imagery. The rock glaciers were then overlaid onto topographic map and DEMs to determine the elevation of the location of the toe of each rock glaciers. This step was accomplished by entering the data as layer in ArcGIS®.

Model of the Spatial Extent of Potential Permafrost

To evaluate the distribution of potential permafrost in the past and future, the impact of temperature, elevation, and aspect on mountain permafrost was assessed using topographic maps, DEMs on ArcGIS®, and the standard adiabatic rate for mountains. The standard adiabatic lapse rate of mountain temperature was used to correct temperature for elevation. Both NOAA and SNOTEL temperature data were used. Because NOAA and SNOTEL sites were at lower elevations than much of the study area, the temperatures at the various station elevations were corrected for elevation. This correction provided a first-approximation of air temperature within the study area.

Potential permafrost areas that were identified using the GIS were then evaluated using temperature and permafrost number model. By applying this method, an additional method to assess the extent of permafrost were used.

In ArcGIS®, the Digital Elevation Model (DEM) was used for the study area. Slopes were calculated by the overlay method and were processed using elevation and distance from location of toe of rock glacier to the highest location of the rock glacier. Orientation measurements for the rock glaciers were converted to vector space for the tracing of each rock glacier in GIS. To create a model showing the spatial increase and decrease in potential permafrost, a multinomial logistic regression was applied, which is based on the aforementioned topo-climatic information.

To evaluate the change in the spatial distribution of potential permafrost in the study are aover a temporal scale of 100 years, a multinomial logistic-regretion model was developed and processed via ArcGIS®. An incremental change of 0.5^0C was used to establish various spatial-temporal scenarios to forecast the future changes in the distribution of potential permafrost in the study area. The model was calibrated for temperatures from 4^0C cooler to 4^0C warmer following Janke, (2005). In this method, mean scores of permafrost probability were used to evaluate permafrost sensitivity under different temperature regimes.

CHAPTER V

DATA, ANALYSIS, AND DISCUSSION

The San Juan Temperature Change

Once all the data were collected, the location and toe elevations of rock glaciers establish and climatic data for the respective NOAA and SNOTEL sites compiled, the data was used to create a model to forecast future distribution of potential permafrost for the study area.

The San Juan Mountains appear to have a common roughness element characteristic of mountainous region; however, the roughness element in important in the climate system in this region. Through perturbations of large-scale atmospheric flow patterns, these elements are one of the trigger mechanisms of cyclogenesis in mid-latitudes (Carrara, 2011). It should be understood that precise picture of the climatic characteristics of this regions is complicated either by a lack of observational data at the spatial and temporal resolutions for complex topography, or by the considerable difficulty in representing a complex terrain in current general-circulation climate models (GCMs) (Humlum, 2000; Rangwala and Miller, 2011). Thus, the result of the model regarding the distribution of potential permafrost should be viewed as a first approximation.

The weather data used in this study are readily available from the National Climatic Data Center of National Oceanic and Atmospheric Administration (NCDC-NOAA) for large-area coverages and from the Snow Telemetry (SNOTEL) system for

smaller areas in the State of Colorado. From these data, temperature trends were examined and analyzed.

Temperature trends in the study area are highly variable in time and space. During a single day, temperatures in the high mountains can vary from below freezing (below 0^0C) to above 15^0C. Large extremes can also occur in lower elevations, as well as the semi-arid regions in the southwestern part of the study area. Additionally, large seasonal changes exist from over 40^0C in the summer to -40^0C in the winter (see Appendix I). Because the San Juan Mountains have a complex terrain (Figure 5.1 and Table 3), according to Rangwala and Miller (2011) most temperature and precipitation observations are biased because they are commonly measured in the valleys. It is often difficult to effectively examine the climate in the mountains.

Table 3. SNOTEL weather stations used for analysis

No	Station	Latitude (N)	Longitude (W)	Elevation (meter)	Avg. Temperature (^{0}C)
1	Lone Cone	37.89	-108.20	2926.08	2,65
2	El Diente Peak	37.79	-108.02	3048.00	2,06
3	Lizard Head Pass	37.80	-107.92	3108.96	1,50
4	Scotch Creek	37.65	-108.01	2773.68	2,84
5	Idarado Mine	37.93	-107.68	2987.04	2,12
6	Red Moutain Pass	37.89	-107.71	3413.76	0,43
7	Mineral Creek	37.85	-107.73	3060.19	1,36
8	Molas Lake	37.75	-107.69	3200.40	1,31
9	Spud Mountain	37.70	-107.78	3249.40	2,33
10	Cascade #2	37.66	-107.80	2718.82	4,84
11	Slumgullion	37.99	-107.20	3486.91	0,40
12	Beartown	37.71	-107.51	3535.68	0,34
13	Upper Rio Grande	37.72	-107.26	2865.12	2,39
14	Cascade	37.66	-107.85	2718.82	4,84

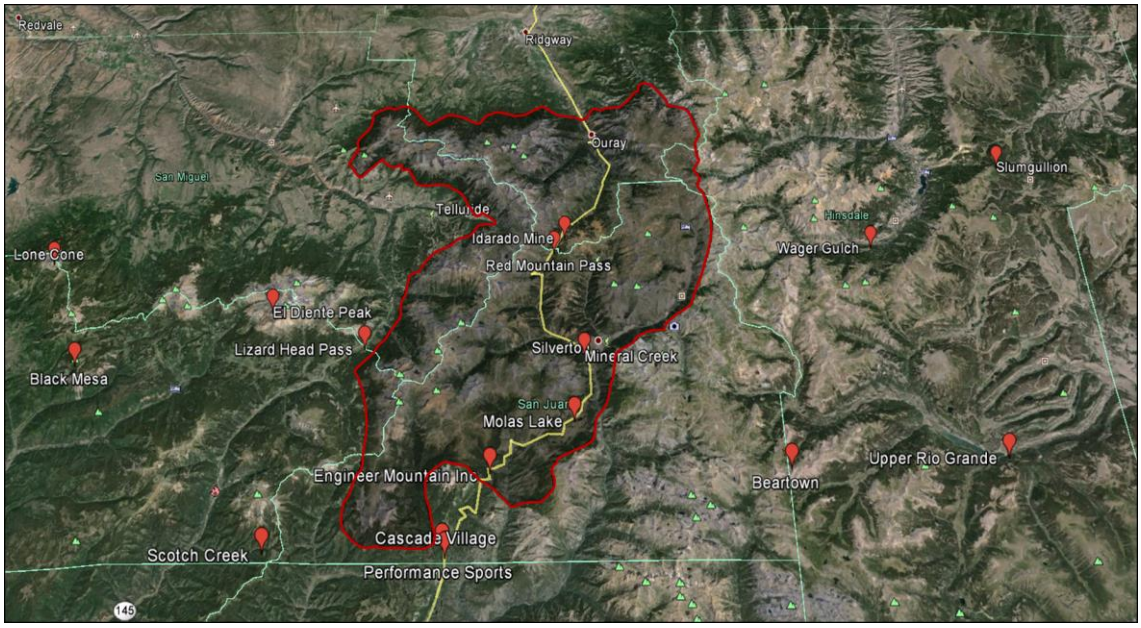

Figure 5.1. The complex terrain of the San Juan Mountains study area (polygon) and SNOTEL weather location (plotted on a Google Earth image).

In this study, mean annual trends of temperature (MAAT) were examined from 1895 to 2013 (Figure 5.2). Three NOAA division sites in Southwestern Colorado were used for the analysis of temperature. The average mean-annual temperatures (MAAT) for each NOAA station for the last 100 year are sown in Figure 5.3. The average mean-annual temperature for each station is: 5.3^0C for Colorado drainage, 3.9^0C for Rio Grande drainage, and 5.23^0C for Alamosa basin, respectively. At the same time, global temperatures have risen by ~0.7^0C (Lemke, et al., 2007; Rangwala and Miller, 2011). Temperature in the San Juan Mountains show unprecedented changes that are higher and have occurred faster than the global average. This increasing temperature change in the

San Juan Mountains is similar to the warming trend shown in global climate data (Solomon et al, 2007).

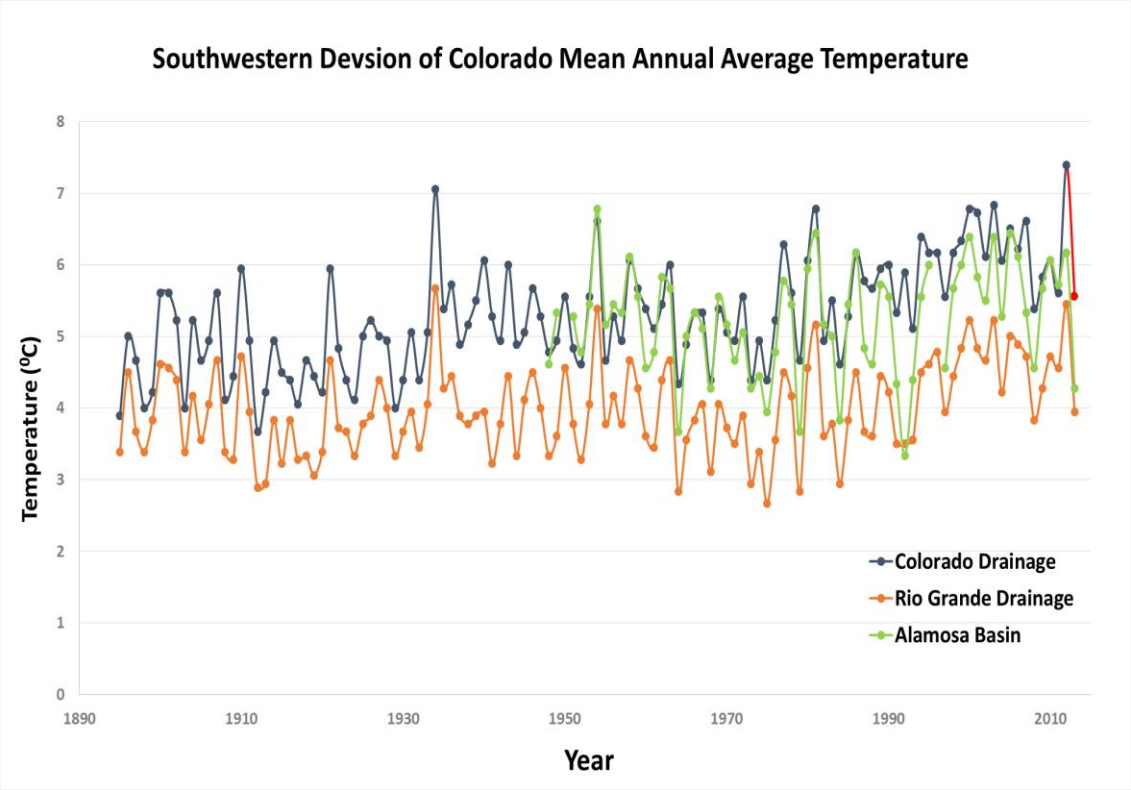

Figure 5.2. Climatological data from NOAA Climate Division showing Colorado State mean-annual air temperature (MAAT). National Climate Data Center of National Oceanic and Atmospheric Administration (NCDC - NOAA). The data show how mean annual air temperatures increase over a 100 period.

Temperature data from SNOTEL in the study area for the period 1994 to 2013 is shown in Figure 5.4. The average mean-annual air temperature for the SNOWTEL sites (Figure 5.5) is likely to exceed the Colorado mean warming in the last 18 years by

1.22^{0}C (Figure 5.3) with significant relationship between number of year and the temperature. The results show that the average annual air temperatures have increased by ~0.11^{0}C every year for the last 18 years (Figure 5.5). This indication is largest in the winter (Figure 5.6), where the lowest winter temperatures are likely to increase more than the average winter temperatures.

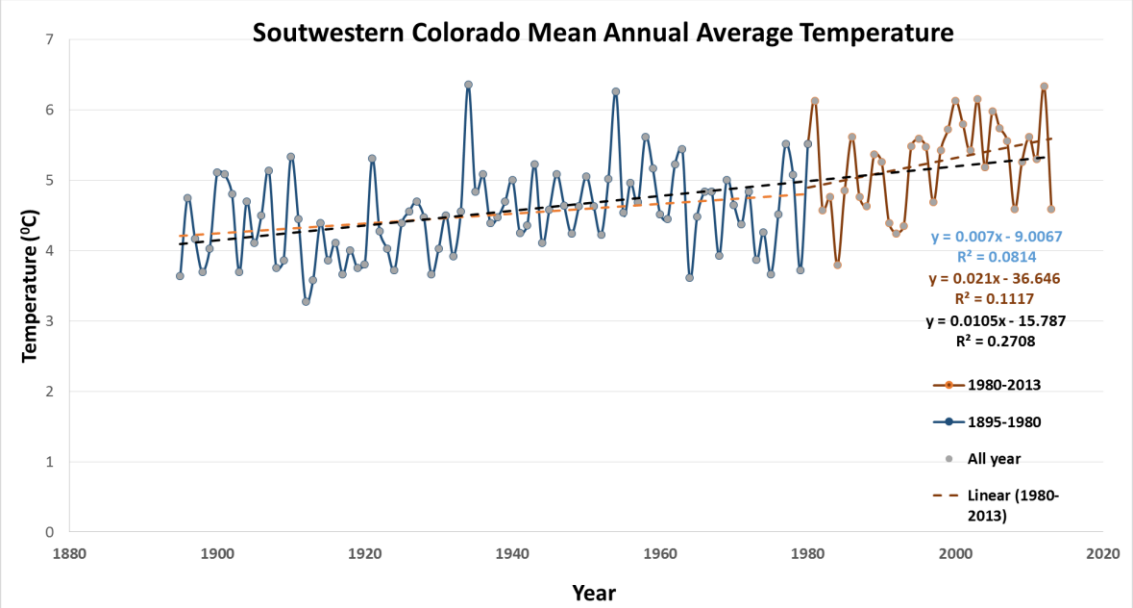

Figure 5.3. Climatological data from NOAA Climate of Colorado State mean-annual air temperature (MAAT). National Climate Data Center of the National Oceanic and Atmospheric Administration (NCDC - NOAA). The profile shows the increase in MAAT is significant for the last thirty years starting from 1980 compare to the years before 1980.

When exploring the seasonal differences in average annual temperature, the temperature differences are much greater in the winter than during any other season. The

trends show the warming gradually increases in all seasons, especially during the last decade (Figure 5.4, 5.5 and 5.6). Figure 5.4 and 5.6 also show that inter-annual variability in the MAAT is much greater in the winter than in the summer. This large variability could result in part from variations in winter precipitation and snow cover (Rangwala and Miller, 2011).

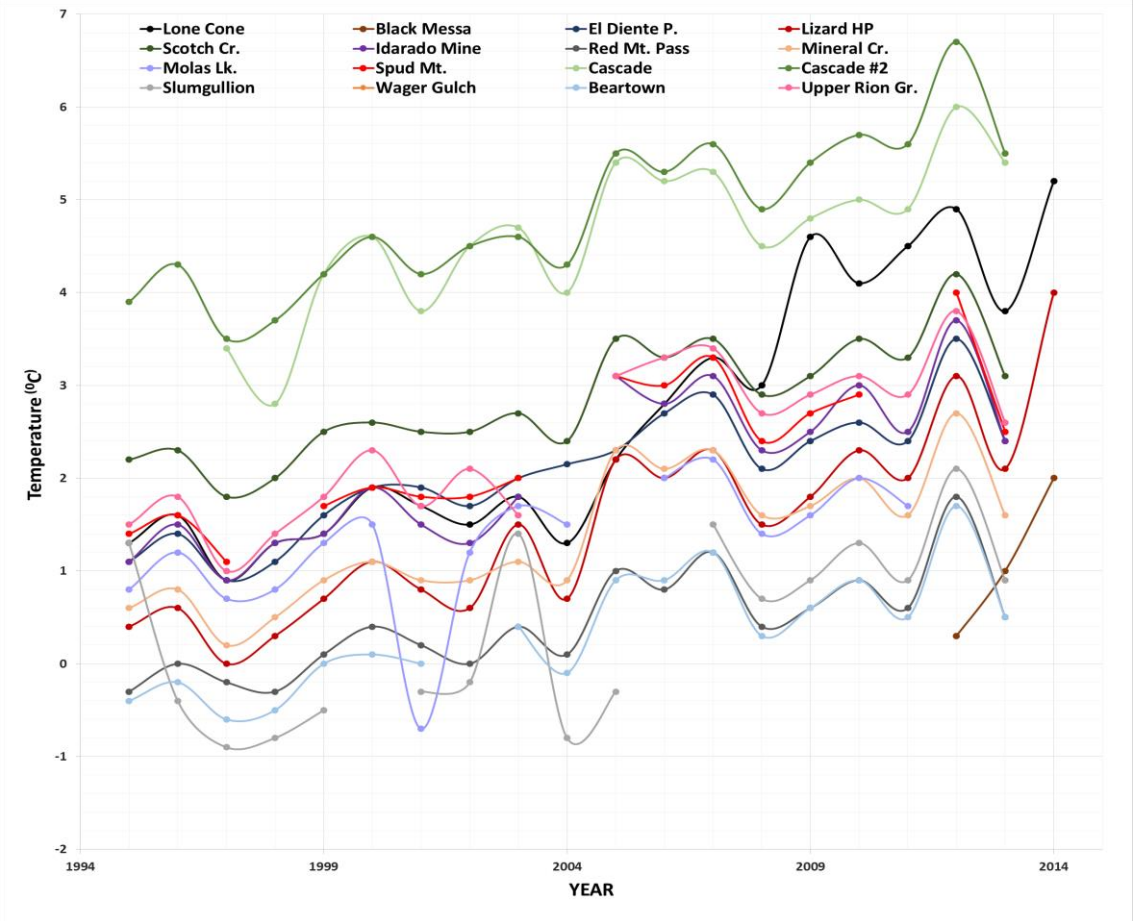

Figure 5.4. Temperature data from the SNOTEL climate division of the San Juan Mountains mean-annual air temperature (MAAT). The profiles show the increasing MAAT in the study area after the period 1995 to 2013.

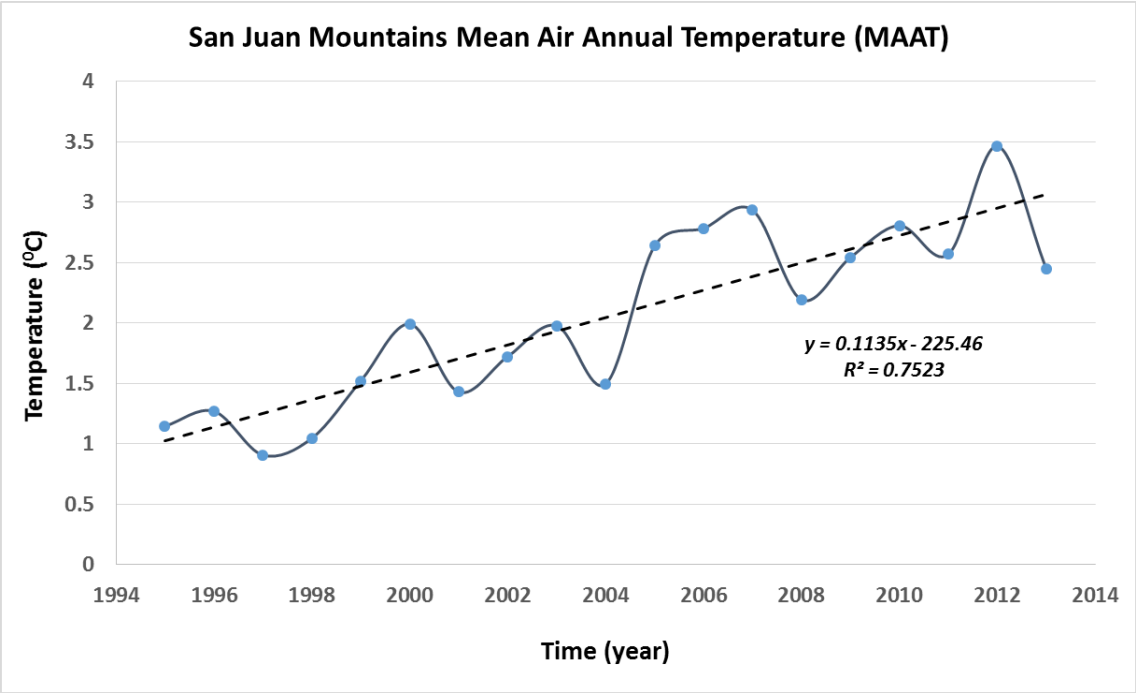

Figure 5.5. Profile of mean air temperature from SNOTEL sites in the San Juan Mountains that shows increasing on MAAT by ~0.11^{0}C annually with R(18) = 0.88, p<0.00000056

The rate of winter warming in the San Juan Mountains has been more than twice the rate of warming during the spring, summer and fall in last decade. This warming influences winter precipitation and snow cover in the study area. Figure 5.7 shows the trend of snow cover in the study area that steadily decreased as a result of increasing temperatures during that period. Throop et al. (2012) found a strong relationship between snow cover and increasing temperatures using a model for the duration of snow cover. Other studies have also shown that increasing temperatures will decrease the snow cover particularly at more marginal and low elevation sites (Karunaratne and Burn, 2004). This phenomena will trigger the snow albedo feedback mechanism because

warmer temperatures melt snow, thus decreasing albedo (i.e., surface reflectivity) and allowing more solar radiation to be absorbed. Warming during the winter season may also result in rainfall instead of snow fall and force unusual melting (i.e., early spring melt) during a normally cold season that will trigger and amplify warming at the surface of Earth.

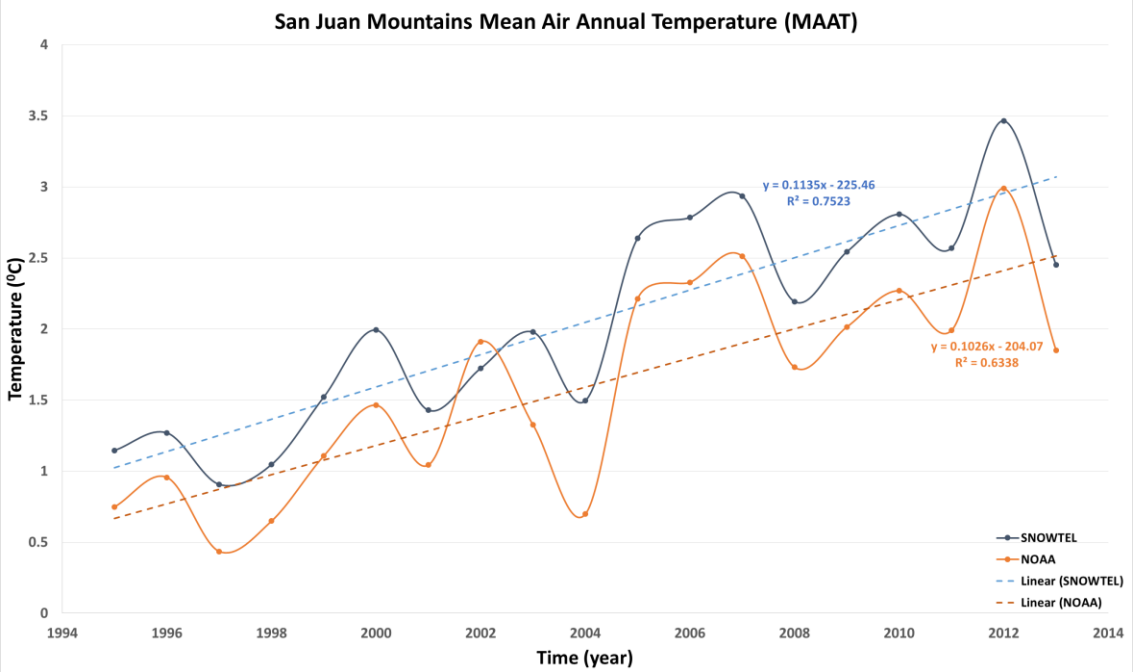

Figure 5.6. Average winter temperature (December to March) profiles of the San Juan Mountains. Both profiles display ~0.1^{0}C temperature increase yearly from 1995 to 2013.

Analysis of MAAT (Figure 5.6) and trend in snow cover and precipitation (Figure 5.7) for four months between 2005 to 2013, show a large rate of warming. These observed trends suggest a shift such that warming occurs in early spring and late fall in

this region. This phenomena may cause significant changes in the availability and quality of surface water and ground water in the region because of an expansion of the growing season. Therefore, greater transpiration and demand for soil moisture may occur.

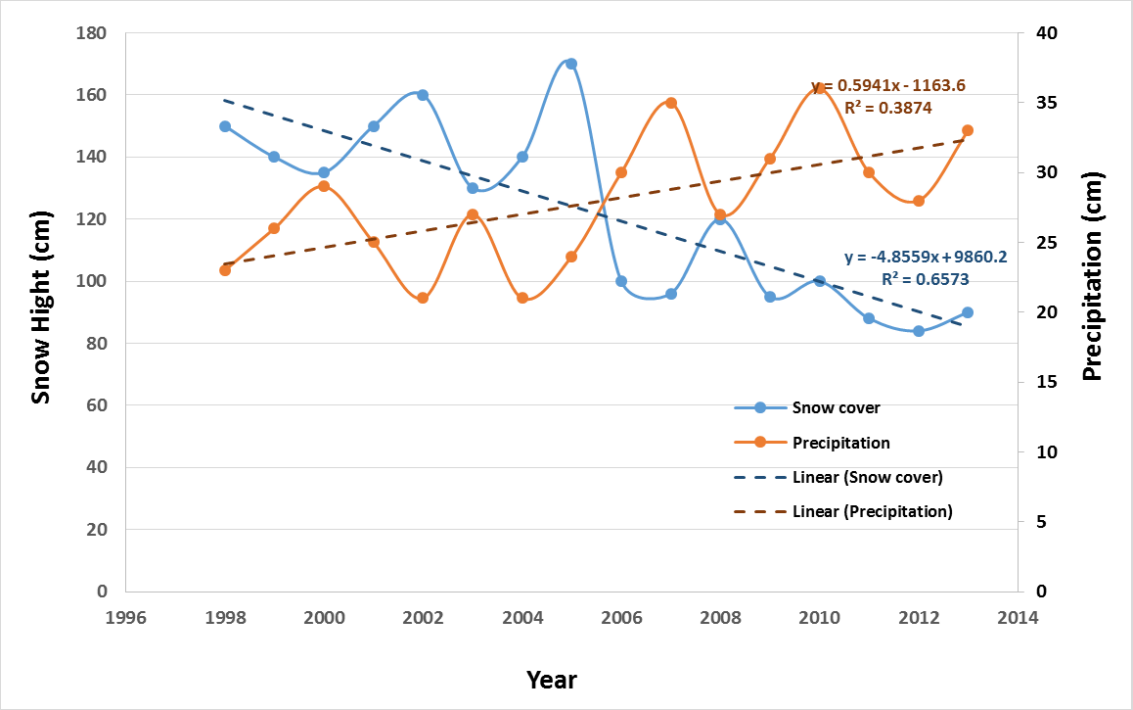

Figure 5.7. Profiles showing a decreasing snow cover by ~5 cm (A) and increasing precipitation by ~0.6 cm (B) annually during winter time (December to March) in the San Juan Mountains because of an increase in temperature of ~0.1^0C during winter season.

Increased temperatures in this region may also significantly affect hydrological and ecological systems. Therefore, these changes can alter the hydrological cycle

resulting in intense precipitation and evaporation (Solomon et al., 2007) resulting in droughts and flooding (Stern, 2006) in this region.

Spatial Distribution of Potential Permafrost

The SNOTEL temperatures data can be seen in Table 4 below. Soil temperatures ranged from a maximum temperature of 16.5^0C to a minimum temperature of -2.5 ^{0}C from January 2011 to December 2014. For the same time period air temperatures ranged from a maximum of 30.0^0C to a minimum of -28.0^0C. The mean-annual soil temperature (MAST) is 4.2^0C, and the mean-annual air temperature is -0.2^0C for all SNOTEL sites in the San Juan Mountains. From Table 4, one can see that minimum and maximum temperatures are greater at the surface (i.e., air temperature) compared to ground temperatures. Maximum temperatures occur in mid-July to early August, whereas minimum temperatures occur at the end of January to early February.

The frost number (F) and temperature at top of the permafrost layer (TTOPL), from seven SNOTEL sites (Table 4), were used to model the probability of the potential permafrost in the study area using a linear interpolation method. Elevation, slope, area, and aspect were used as a secondary variables during the interpolation. The model was adjusted spatially using a lapse rate weighting procedure.

The result of the frost number (F) and temperature at the top of the permafrost layer (TTOP) derived from SNOTEL data can be seen in Table 5. Based on the formula given in eq. 1, the frost number ranges from 0.2 to 0.4, with a mean value of 0.3. For this result, about one third (i.e., an average of 124 days) of the soil is frozen. The calculation

of TTOP by using eq. 3 produces the positive number, which suggests no possibility of permafrost at the SNOTEL sites.

Table 4. Air and soil temperatures in ºC from SNOTEL sites in the San Juan Mountains (See Figure 5.1 for locations of the SNOWTEL sites)

Black Messa (West of Study Area)		**2011-2012**	**2012-2013**	**2013-2014**
Air Temperature (^{0}C)	Average	-0.50	-0.69	-0.17
	Standard Deviation	6.83	8.27	7.39
	Minimum	-19.30	-24.50	-19.60
	Maximum	10.70	14.30	11.90
Soil Temperature (^{0}C)	Average	1.64	2.28	2.33
	Standard Deviation	3.13	3.38	2.69
	Minimum	-1.30	-0.80	0.15
	Maximum	8.53	9.37	7.90
Cascade #2 (in the Study Area)		**2011-2012**	**2012-2013**	**2013-2014**
Air Temperature (^{0}C)	Average		1.67	2.58
	Standard Deviation		7.82	6.46
	Minimum		-23.30	-15.90
	Maximum		15.80	15.70
Soil Temperature (^{0}C)	Average	6.53	6.53	6.61
	Standard Deviation	5.64	5.64	5.22
	Minimum	0.70	0.70	0.60
	Maximum	16.50	16.50	16.93
Lizard Head Pass (in the Study Area)		**2011-2012**	**2012-2013**	**2013-2014**
Air Temperature (^{0}C)	Average	-1.15	-1.77	-0.89
	Standard Deviation	7.08	8.17	6.99
	Minimum	-20.80	-28.00	-21.70
	Maximum	11.90	12.20	12.80
Soil Temperature (^{0}C)	Average	4.96	4.57	4.45
	Standard Deviation	4.77	4.72	4.38
	Minimum	-0.10	-0.13	0.33
	Maximum	13.20	13.03	12.67
Lone Cone (West of Study Area)		**2011-2012**	**2012-2013**	**2013-2014**
Air Temperature (^{0}C)	Average	1.01	0.16	0.25
	Standard Deviation	8.18	9.81	7.68
	Minimum	-23.10	-27.40	-22.20
	Maximum	32.60	40.50	20.20
Soil Temperature (^{0}C)	Average	6.20	5.85	5.37
	Standard Deviation	5.45	5.45	4.90
	Minimum	0.47	0.63	0.60
	Maximum	15.50	15.40	14.37

Table 4. Air and soil temperatures in ºC from SNOTEL sites in the San Juan Mountains (See Figure 5.1 for locations of the SNOWTEL sites) (contiune)

Sharktooth (Southwest of Study Area)		**2011-2012**	**2012-2013**	**2013-2014**
Air Temperature (^{0}C)	Average	2.26	1.06	1.70
	Standard Deviation	7.38	8.00	7.18
	Minimum	-16.70	-22.20	-16.90
	Maximum	15.10	15.70	14.30
Soil Temperature (^{0}C)	Average	4.20	3.68	3.87
	Standard Deviation	4.10	4.11	3.79
	Minimum	0.27	0.13	0.47
	Maximum	11.30	11.33	11.00
Slumgullion (Northeast of Study Area)		**2011-2012**	**2012-2013**	**2013-2014**
Air Temperature (^{0}C)	Average	-0.75	-1.78	-1.22
	Standard Deviation	7.46	8.22	7.37
	Minimum	-20.50	-26.50	-22.60
	Maximum	11.80	12.50	11.30
Soil Temperature (^{0}C)	Average	3.24	2.78	2.84
	Standard Deviation	4.28	4.00	3.63
	Minimum	-1.33	-1.53	-0.37
	Maximum	11.30	10.07	10.77
Upper Rio Grande (East of Study Area)		**2011-2012**	**2012-2013**	**2013-2014**
Air Temperature (^{0}C)	Average	-1.70	-1.19	-2.14
	Standard Deviation	8.96	8.34	9.68
	Minimum	-29.80	-25.60	-29.70
	Maximum	16.50	12.80	13.10
Soil Temperature (^{0}C)	Average	4.71	5.05	5.00
	Standard Deviation	4.94	5.25	5.50
	Minimum	-1.17	-2.23	-2.50
	Maximum	13.33	13.77	13.77

Table 5. The frost number (F) and temperature at the top of the permafrost layer (TTOP) derived from SNOTEL

Site Location	Elevation (meter)	Frost number	TTOP (^{0}C)	Average ground temp. (^{0}C) annually	Average ground temp. (^{0}C) during Winter
Slumgullion	3,846	0.36	0.81	3.01	-1.46
Sharktooth	3,267	0.21	1.12	3.94	0.05
Lone Cone	2,926	0.33	0.74	6.03	0.32
Upper Rio Grande	2,865	0.38	1.47	4.88	-1.99
Black Messa	3,529	0.26	1.24	1.96	-1.15
Cascade #2	2,718	0.34	0.21	6.53	-0.14
Lizard Head Pass	3,108	0.19	1.52	4.45	-0.02

Based on the data for the study area in the San Juan Mountains, it appears that the soil temperatures are affected by the distribution of snow cover (Figure 5.7). The data show that average ground temperature during the winter is -0.4^{0}C. Snow that covers the study sites results in warmer ground temperatures compared to snow-free study sites. Williams and Smith (1989) and Romanovsky et al. (2010) have discussed this phenomenal and concluded that the ground can be warmed by snow cover as thin as 25 to 50 cm. Janke et al. (2012), in his model of permafrost prediction in Rocky Mountain National Park, also concluded that during the winter of each year, ground temperatures of snow-free sites are ~1.8^{0}C colder on average compared to snow-covered sites. In contrast, almost no differences were observed for the averages for ground temperatures of snow-covered and snow-free sites during the spring snowfall season. This factor indicates that during spring (March to May), the ground temperature at snow-free sites warms faster than snow-covered sites. Because the extended period of snowfall during the spring season expanded the cold season, it may be an important factor for the occurrence of potential permafrost. Janke et al. (2012) stated that this extended cold protects underlying ground from summer insolation.

The spatial distribution of the frost number (F), after applying lapse rate and linear interpolating method can be seen in Figure 5.8 below. The figure shows that, in general, high frost numbers occur in the higher elevations and along the north central part of the study area. This suggests that at higher elevations potential permafrost may exist; however, at lower elevations the permafrost may only exist in the north central part of study area. The effect of topography, elevation and direct solar radiation, may

influence the extent of permafrost as has been identified by Cohen and Entekhabi, (1999) and Brenning (2008).

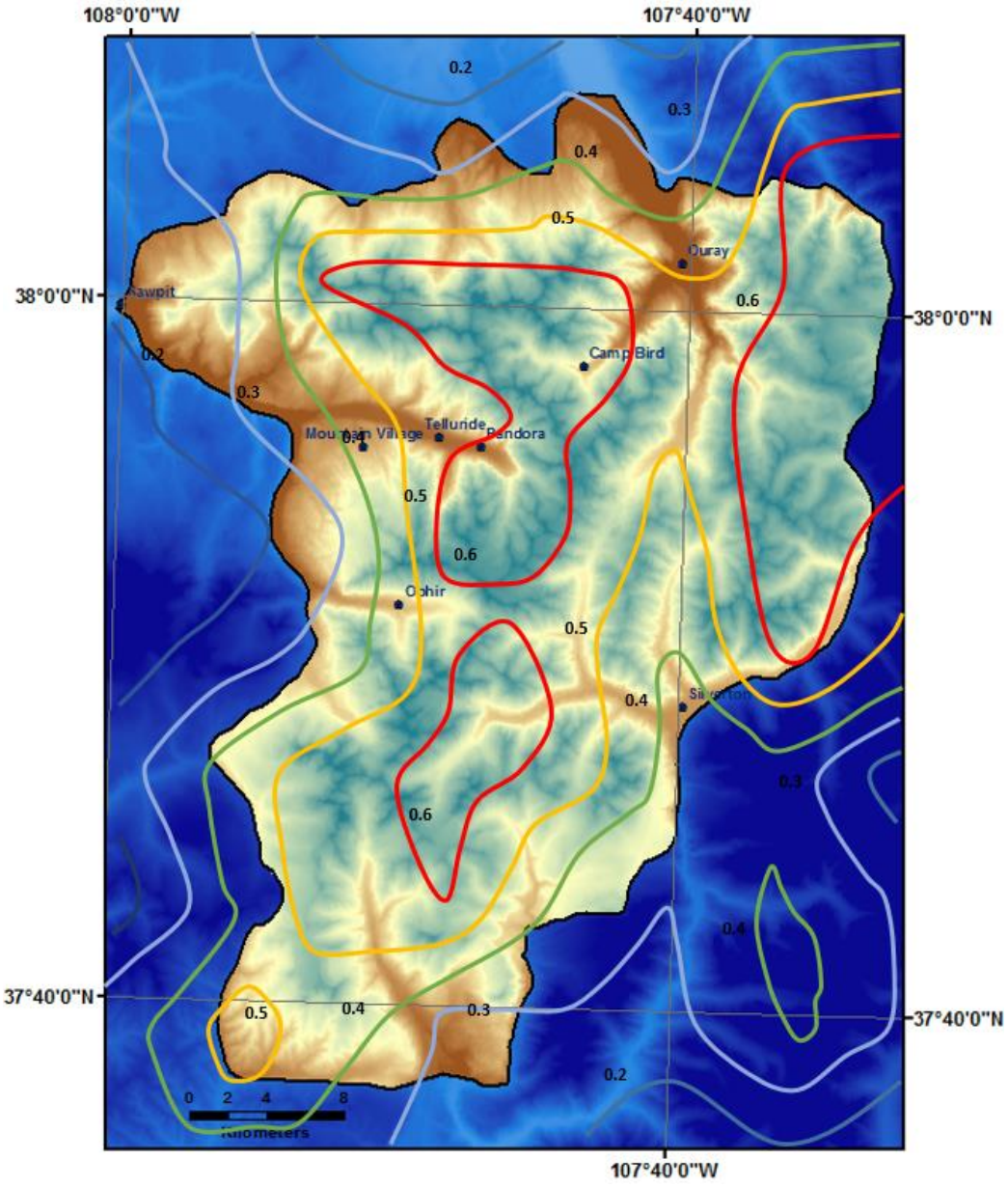

Figure 5.8. Spatial distribution of frost number (F) contour in the San Juan Mountains study area.

Distribution of Potential Permafrost Model

Change in the distribution of the extent of potential permafrost has been observed in many lowland and mountain locations in recent decades (Scherler et al., 2013). Studies have suggested that over the past several decades, temperatures related to permafrost have generally warmed in lowlands and mountain regions. Much of the evidence, however, is indirect and based on changes in forest and tundra vegetation, differential subsidence of the ground surface, and loss of lakes (Clow, 2010; Damm and Langer, 2006; and Knowles et al., 2006). Increases in the thickness of the active-layer have been observed in warm summers especially in the mountainous regions of the southwestern United States, resulting in increased slope failures, ground subsidence in ice-rich terrain, and increased lake drainage (Ernakovich et al., 2014). At regional and global scales, changes in permafrost zonal boundaries are difficult to identify because of geographic irregularities in the distribution of potential permafrost.

The changes in the extent of potential permafrost in this area are a result of changes in the accumulation and melt of seasonal snowpack that may cause substantial reductions in the natural storage of water (Clow, 2010). This phenomena can be seen in Figure 5.7 showing how the proportion of precipitation increases as snow decreases over time. This result suggests that the changes in the San Juan Mountains were the most pronounced in the southwestern part of Colorado where the temperatures are usually not far below freezing.

The relationship between the existence of potential permafrost and topographic and climatic factors has been widely used to predict the distribution of permafrost, using

the temperature profile to construct cooler and warmer model scenarios. In this study it was also be used to calculate the distribution of potential permafrost. The distributions of potential permafrost for cooler and warmer temperature are shown in Figure 5.9 and 5.10, repectively, and the extent of potential permafrost is summarized for each of the scenarios in Table 6. Under a 4^0C warmer climate, ~79% (reducing to 467.37 km^2 from current potential permafrost) of total potential pemafrost decrease in extend occurs. An increase of 0.5^0C temperature in this scenario could reduce the area to 161.97 Km^2 which is an additional reduction of ~28% of the potential permafrost. Alternatively, in a 4^0C cooler climate scenario, 754.41 km^2 (~128%) would be underlain by permafrost. Even in a 0.5^0C cooler climate scenario, the extent of potential permafrost will increase by 214.94 km^2 (~37%).

Based on current data and cooler and warmer models in Figure 5.9 and 5.10, I can predict that if the temperature continues to increase by 4^0C, it would reduce the extent of potential permafrost extent by 79.5% from the current condition by ~2030 to ~467 km^2. This suggests that only ~9.5% of the potential permafrost coverage would remain in the study area. In a 4^0C cooler climate scenario, however, the coverage of potential permafrost in the area would be ~92% or more than 125% increase from current conditions.

Based on the frost number model, the current condition as of June, 2014, of potential permafrost that occurs the study area is ~40% or ~588 km^2. The temperature trend shows an annual average temperatures increase by ~0.12^0C every year (Figure 5.5). If this trend continuous to increase in a linear fashion, based on this climate scenario, it

could decrease the coverage of potential permafrost in the study area to only ~5% left by the year 2100 (see appendix F).

Table 6. The areal coverage for the distribution of potential permafrost change based on scenarios of climates change.

No.	Temperature change ^{0}C	Areal extent (km^2)	Areal extent change (km^2)	Per cent extent change (%)
1	-4.0	1,342.33	754.41	128.32
2	-3.5	1,277.25	689.33	117.25
3	-3.0	1,189.53	601.61	102.33
4	-2.5	1,129.15	541.24	92.06
5	-2.0	1,072.48	484.56	82.42
6	-1.5	1,017.98	430.06	73.15
7	-1.0	897.40	309.48	52.64
8	-0.5	802.86	214.94	36.56
9	0.0	587.92	0.00	0.00
10	0.5	425.95	-161.97	-27.55
10	1.0	371.01	-216.91	-36.89
11	1.5	326.22	-261.70	-44.51
12	2.0	298.70	-289.22	-49.19
13	2.5	252.09	-335.83	-57.12
14	3.0	203.68	-384.24	-65.35
15	3.5	163.27	-424.64	-72.22
16	4.0	120.54	-467.37	-79.50

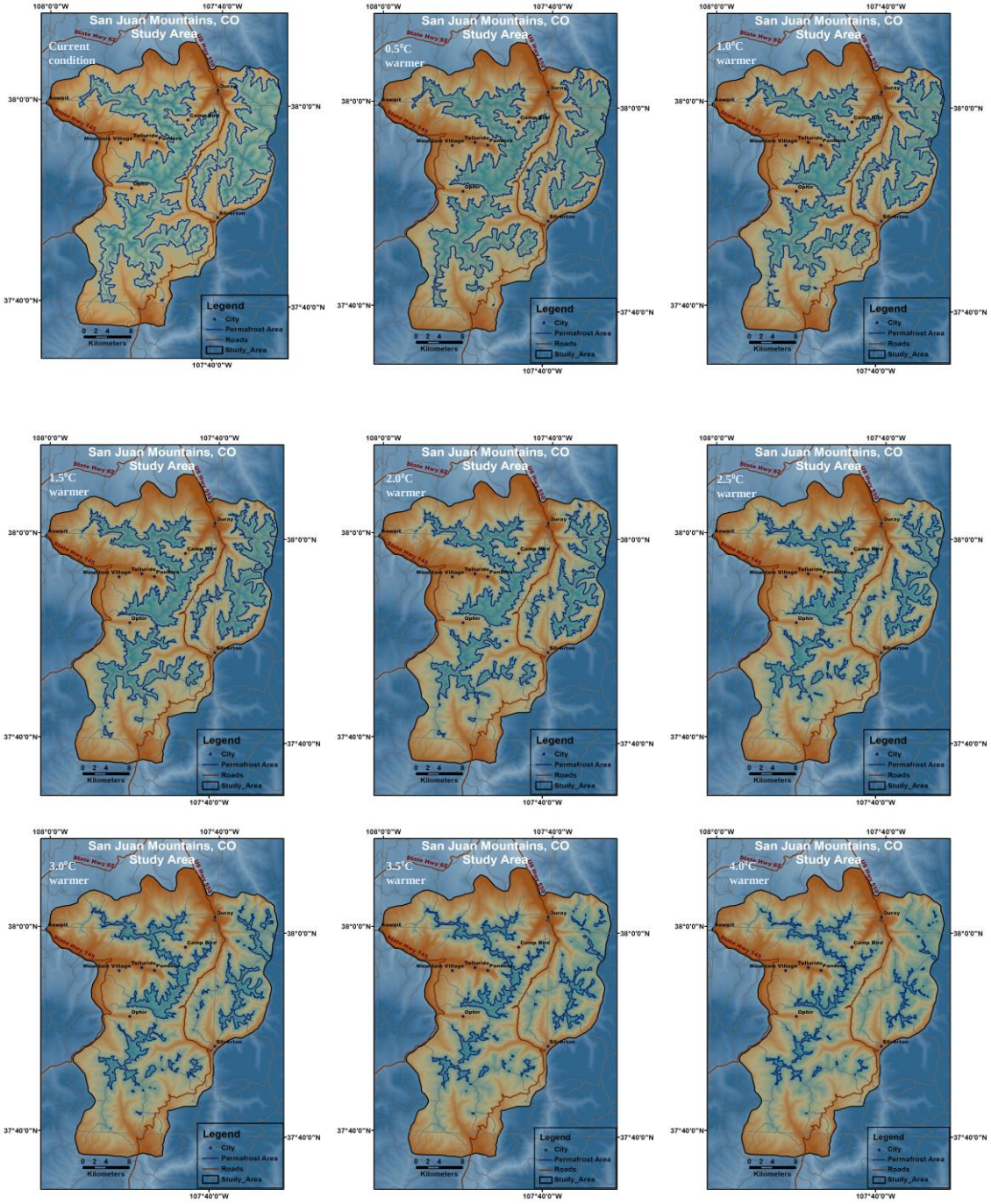

Figure 5.9. The extent of potential permafrost predicted based on warmer climates scenario by using a standard adiabatic rate for mountainous terrain (see APENDIX C for large diagrams at a large scale).

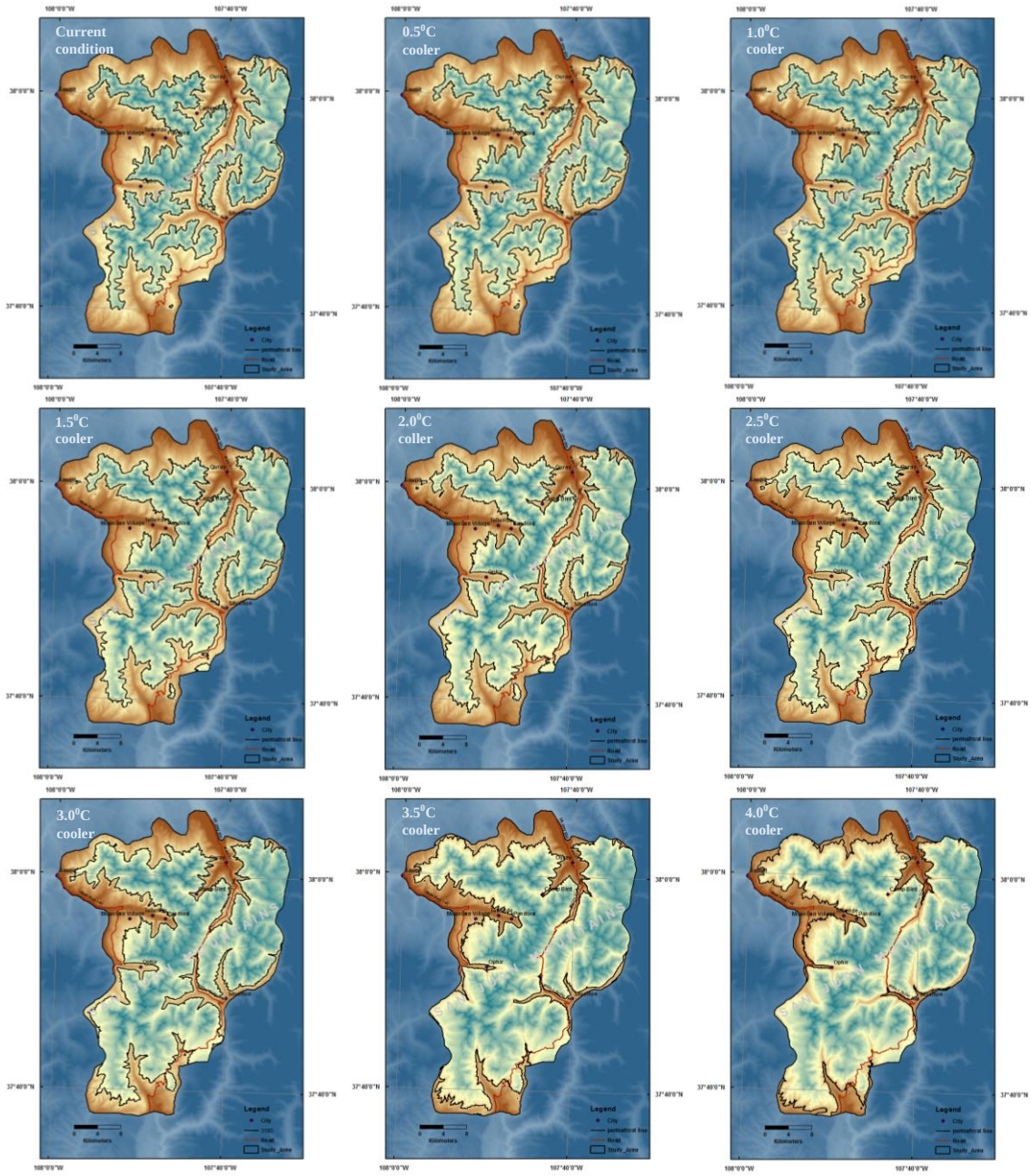

Figure 5.10. The extent of potential permafrost predicted based on cooler climates scenario by using a standard adiabatic rate for mountainous terrain (see APENDIX D for large diagrams at a large scale).

The extent of potential permafrost in the study area also can be seen in Figure 5.11. The profile of the spatial extent of potential permafrost in this Figure is calculated based on the elevation of the toes of rock glaciers. Figure 5.11 shows that almost no difference exists between the extent of potential permafrost for both methods (Table 7). The only difference in outcomes between the two methods occurs at northeastern part of the study area, where no potential permafrost occurs in this area based on tracing the elevation of the toes of rock glaciers. One explaination might be happened the igneous rocks in this area are very resistant to erosion nad thus do not supply sfficient debris which is critical for the development of rock glaciers. Without a sufficient rock supply from cirque highwalls, the rock glaciers do not form.

The estimation of spatial extent of potential permafrost based on the permafrost number (F) and the elevation of the toes of rock glaciers is ilustrated in Table 7 and Figure 5.12. The table shows the areal coverage of potential permafrost in three regions within study area. The northwestern area has a large areal coverage of potential permafrost compared to other areas, whereas the eastern region shows a significant difference between the two models. The elevation of the toe of rock glaciers display a small areal coverage in the northeastern site because rock glaciers exist only on the southern site of this area as a result of lack of a sufficient debris to facilitate rock glacier formation. In the other hand, no rock glaciers exist on the northern part because of steep slopes and insufficient of rock supply.

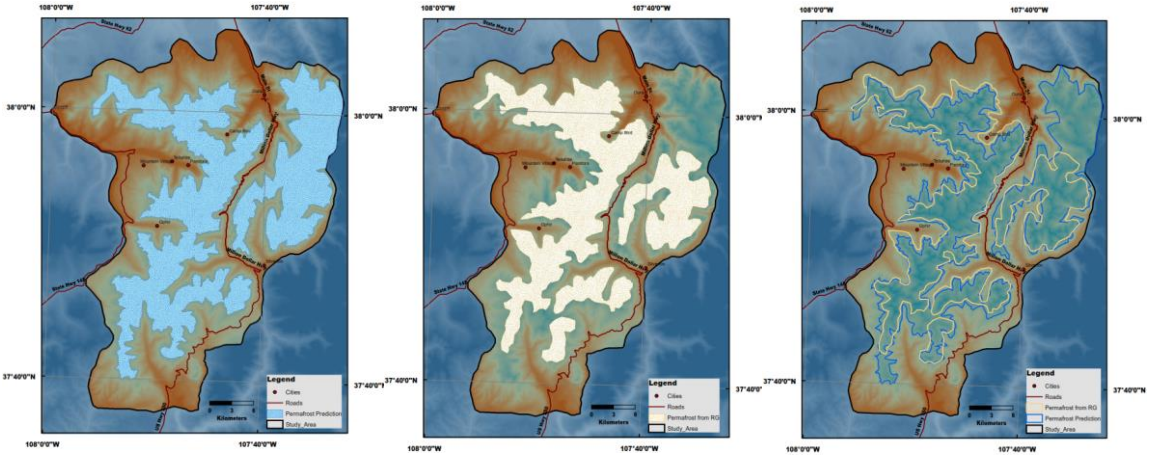

A **B** **C**

Figure 5.11. Potential permafrost profile based on frost-number prediction and tracing the elevation of the toes of rock glaciers. A). Profile of potential permafrost current condition based on calculated frost-number as shown in Figure 5.9a and 5.10b. B). Profile of potential permafrost based on the manually tracing of the elevation of the toes of rock glaciers. C). Comparison of potential permafrost profile between prediction and tracing the toe of rock glaciers (see APENDIX E diagrams for at a large scale).

Table 7. Comparison between the spatial extent of potential permafrost calculated from the permafrost number (F) and the elevation of the toes of rock glaciers.

Model	Areal Coverage (km^2)			Total areal coverage (km^2)
	Northwestern Section	Eastern Section	Southern Section	
Permafrost number (F) model	222.82	166.79	198.31	587.92
Toe of rock glaciers tracing	236.66	74.17	164.65	475.48
(Frost # - Toe of RG)	(13.84)	92.62	33.66	112.44

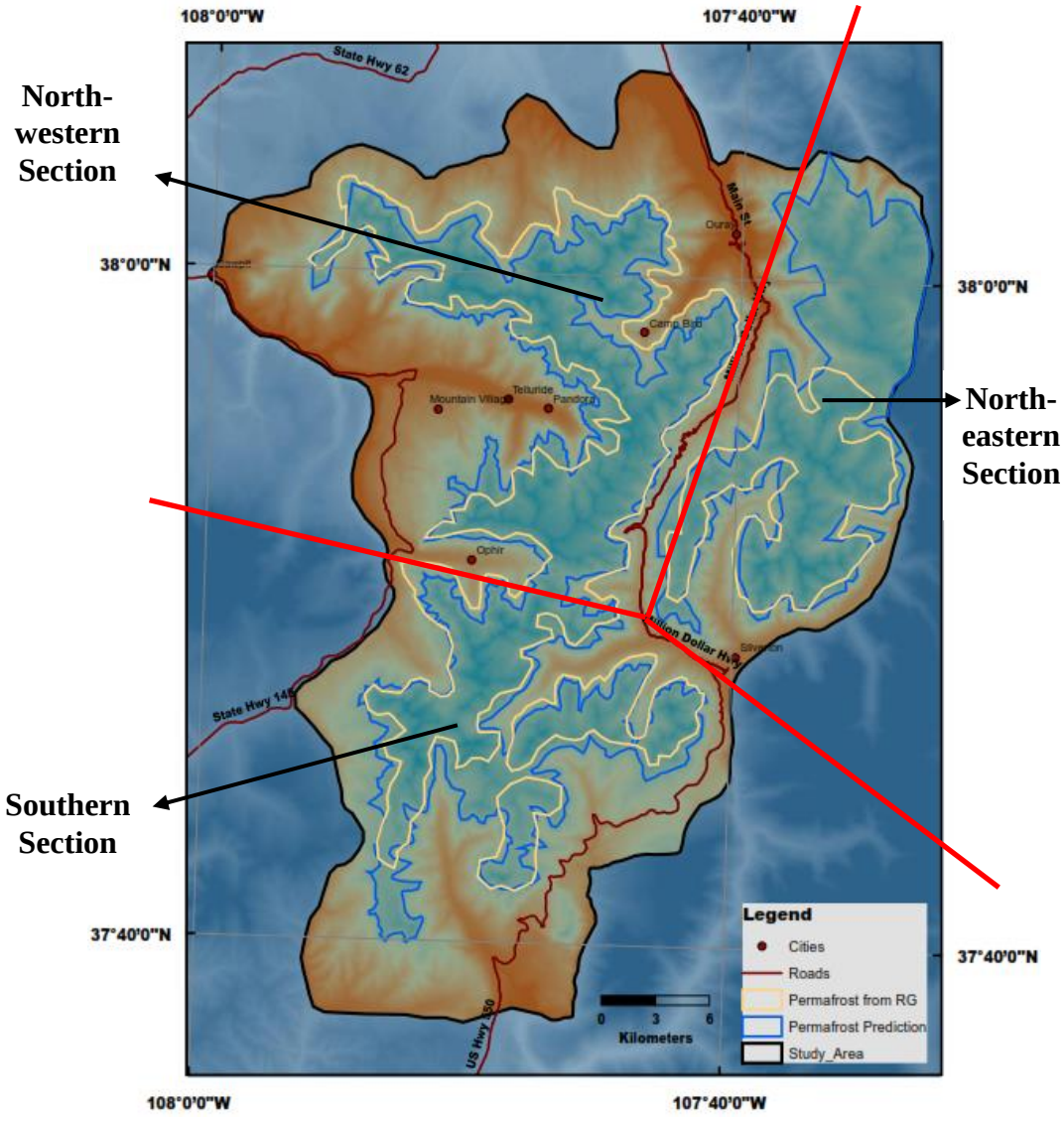

Figure 5.12. The spatial extent of potential permafrost based on the permafrost number (F) and the elevation of the toes of rock glaciers. The trhee division of the study area are shown as: Northwestern section, Northeastrn section, and Southern section.

Figure 5.13 shows the elevation differences of the extent of potential permafrost between the frost-number model and the method of tracing the elevation of the toe of rock glaciers. In this figure, potential permafrost associated with location rock glacier acts as an elevation-based profile that can be compared to potential permafrost derived from the frost-number model. The differences between the two models range from positive to negative numbers. The positive numbers indicate that the elevation of potential permafrost derived from tracing the elevation of the toe of rock glacier is lower than from the frost-number model. The negative numbers indicates that the elevation of potential permafrost derived from tracing the elevation of the toe of rock glacier is higher than from the frost-number model. The figure also demonstrates that in the northern part of study area, the extent of potential permafrost occurs at a lower elevation than the frost number model because of the existence of rock glaciers.

Potential permafrost in the study area mostly underlies by rock glaciers, where the internal structure of ice is protected from solar radiation by a matrix of coarse surface debris, which serves as thermal blanket (Janke, 2005; Haeberli, 1985). The internal ice in the rock glacier is maintained by Balch ventilation. Therefore, the warming response will likely not occur.

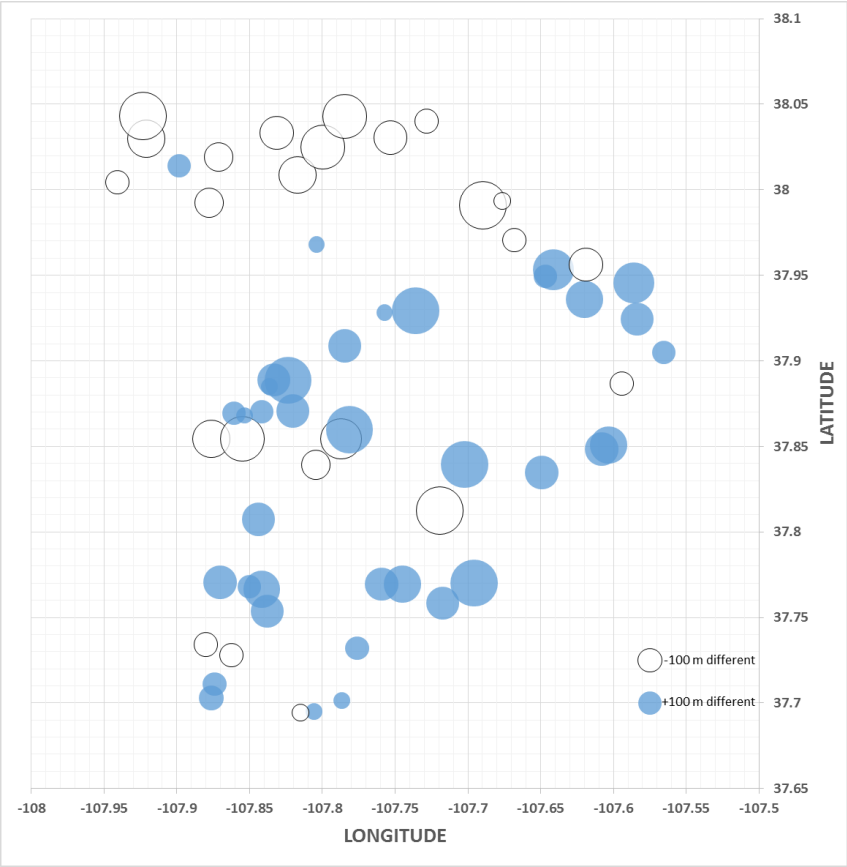

Figure 5.13. Elevation differences of permafrost based on tracing the elevation of the toes of rock glaciers compared with the frost-number of the permafrost model.

In the study area, the existence of potential permafrost is controlled by change in seasonal temperatures and also by elevation, aspect, and surface conditions. There some conditions have been described by Salzmann et al., (2007) and Hasler et al., (2014) for other location. Unusual forms, such as south-facing slope of permafrost can sometimes be found in areas that have a MAAT several degrees above freezing (Gruber and Haeberli, 2007). Temperature does not simply increase with depth, but becomes a complex subsurface-temperature boundary condition governed by lateral heat flux,

which is controled by topography and variable surface conditions. Therefore, types of surface covers and materials, which influence ground temperature, play an important role in the extent of potential permafrost. Haeberli et al. (2006) stated that rock glaciers and other creep phenomena indicate the presence of permafrost in mountainous areas. This complex landform according to Hasler et al. (2014), can result in permafrost being induced under warm sun-exposed slope from cold and slope nearby. This can be seen in Figure 5.14 which shows the presence of rock glaciers on south facing-slopes indicated and indicate that potential permafrost could exist because of the presence of cold air drainage from north-facing slope nearby.

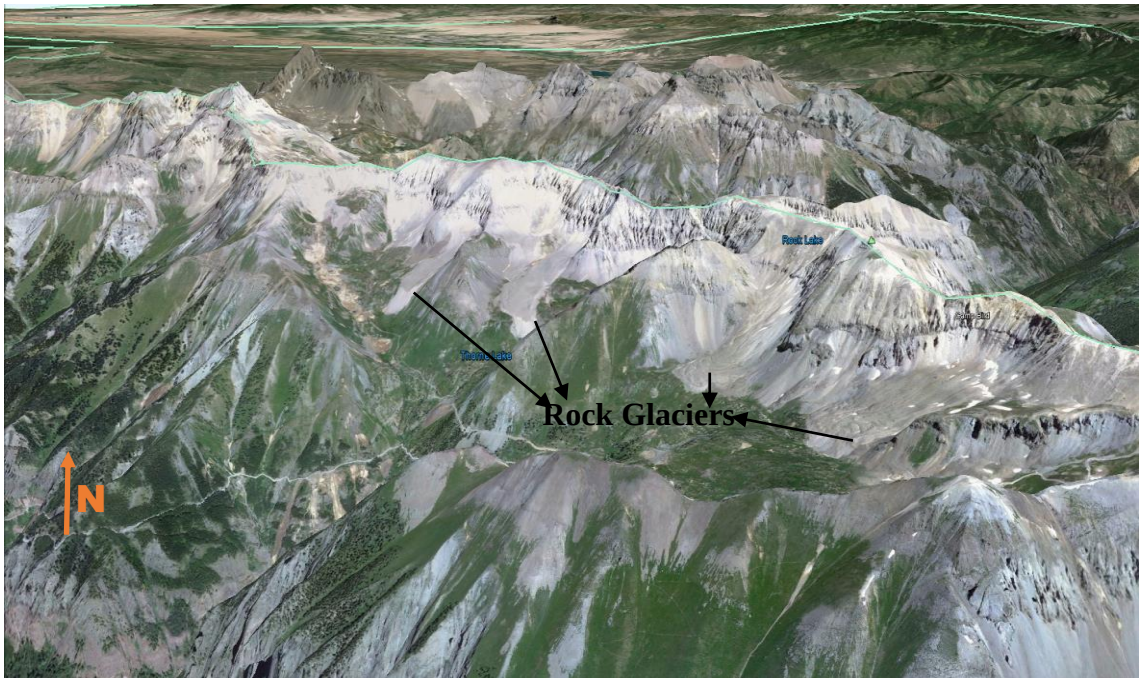

Figure 5.14. The existence of rock glaciers where possible permafrost exists on south facing slopes in the study area of the San Juan Mountains, Colorado (plotted on a Google Earth image).

The Impact of Aspect and Orientation on the Distribution of Potential Permafrost

A total of 98 rock glaciers were identified in the study area and all of there of rock glaciers occur above 3,000 m, mean sea level (MSL). Less than 1% rock glaciers exist between 3,000 m to 3,300 m elevation. About 66% of the rock glaciers are present above 3,500 m as shown in Figure 5.15. Most of the rock glaciers are on north facing slopes. In the lower elevations below 3,500 m, most rock glaciers have a north to north-east aspect. Only rock glaciers that occur above 3,500 m in elevation, which is about 26% of rock glaciers, have a southern aspect. At the elevation above 3,500 m, however, north to northeastern-facing slope have 75% more rock glaciers than south to southwest facing rock glaciers.

The total area of coverage by rock glaciers is ~18 km^2 of total 588 km^2 potential permafrost area in the study area. The areal coverage of rock glaciers predominantly occurs on north-easterly aspects and can be seen in Figure 5.16. The figure also shows that 44% of rock glaciers exist in 0.1 km^2 areal coverage and are spread in all aspects. The trend of the areal coverage of rock glaciers, however, shows that a small areal coverage occurs in south-westerly aspects compared to large areal coverages found in northwesterly to north-easterly aspects. This distribution suggest that north-facing slopes are colder and wetter than slopes with other aspect. Thus, they create more ideal condition for rock glacier formation.

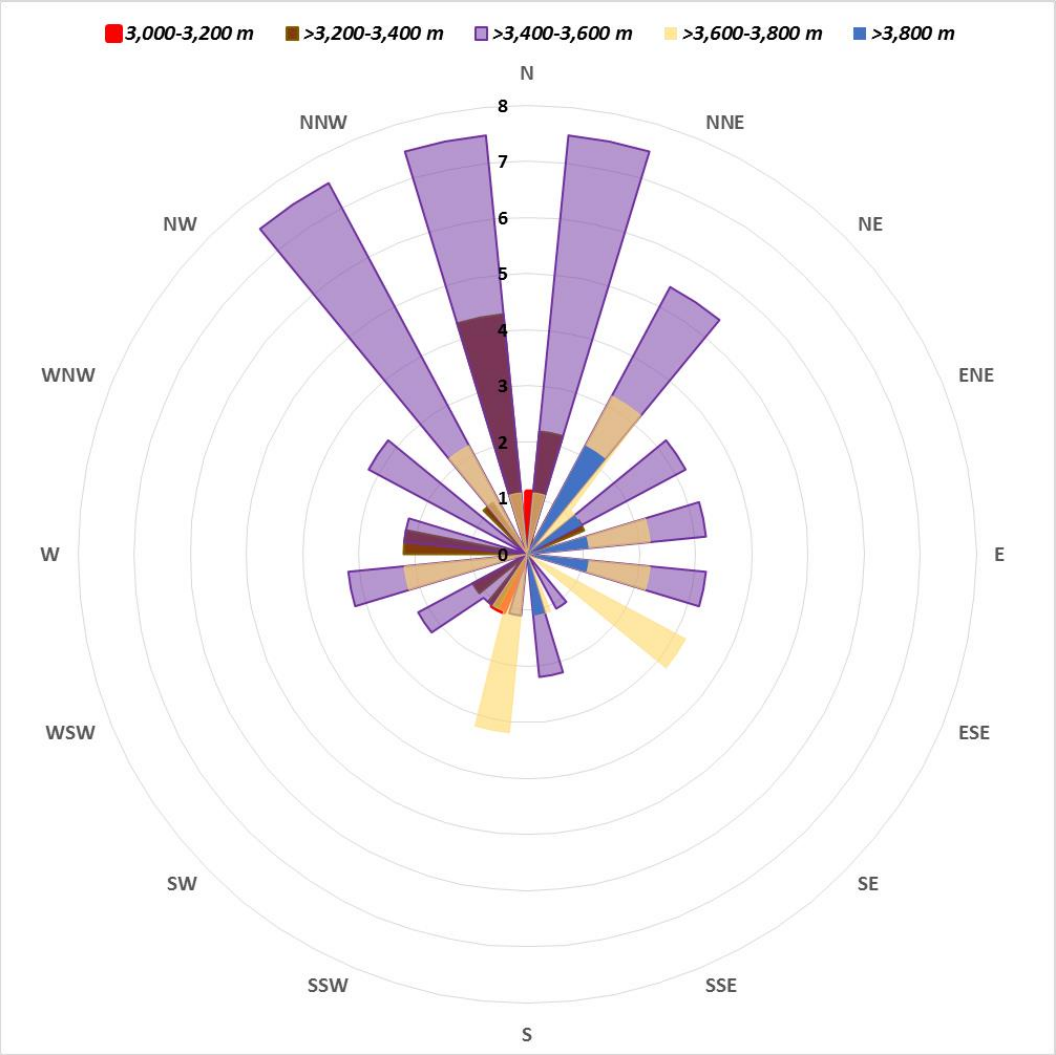

Figure 5.15. The rose diagram of elevation versus orientation of rock glaciers in San Juan Mountains study area.

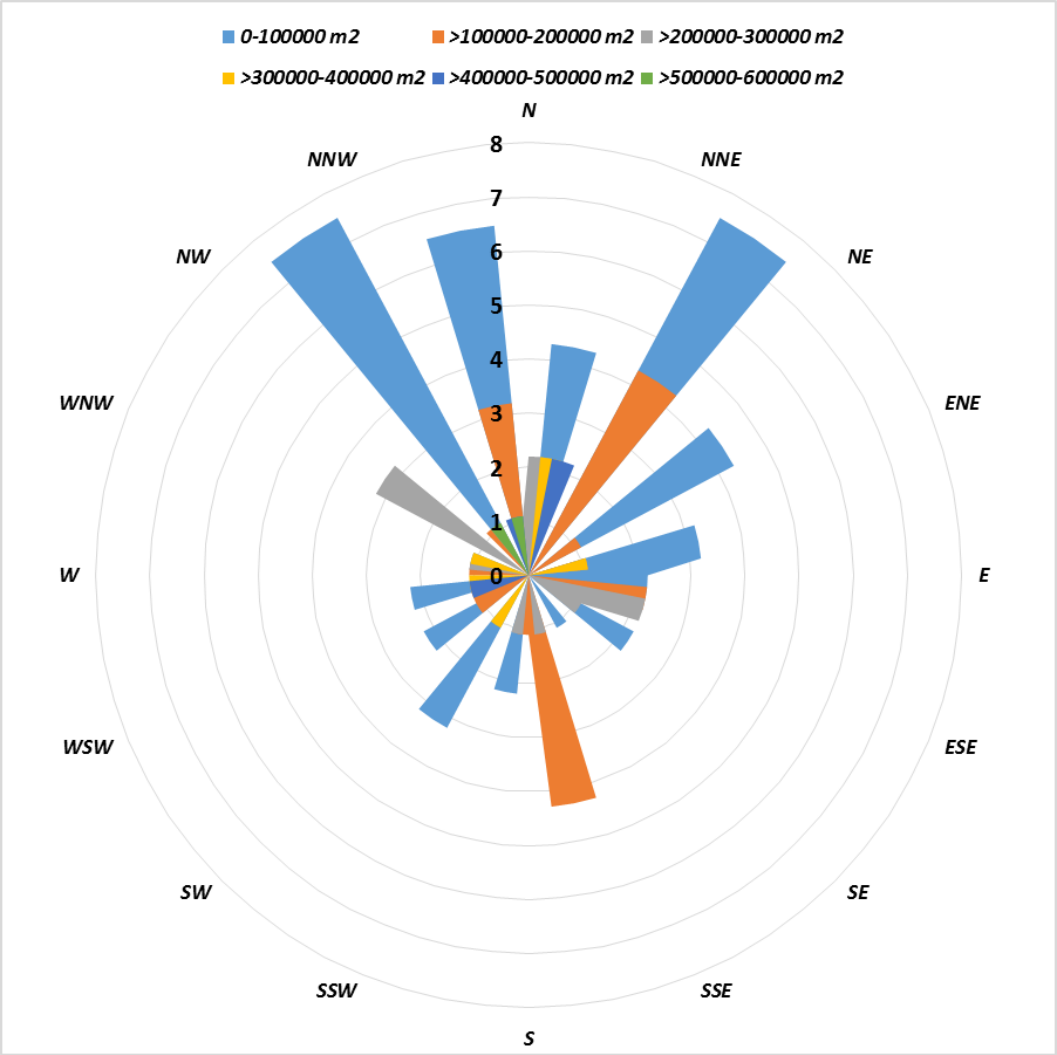

Figure 5.16. The rose diagram of areal coverage versus orientation of rock glaciers in San Juan Mountains study area. The trend line is 3rd order best-of-fit polynomials.

The sloped angel with orientation and number of rock glaciers is shown in Figure 5.17. The rose diagram shows that rock glaciers mostly occur between 10^0 to 35^0 slopes and the dominate orientation is northwest to southeast facing slope. It suggest that no visual differences seem to exist for rock glaciers on these slopes either north or south facing slope. Only a few of rock glaciers, however, occur on slop less than 10^0 and on

slope greater than 35^0, and are on the north facing slopes. Only a few of rock glaciers, however, occur below 10^0 and above 35^0 slopes and all of them are in the north facing slope.

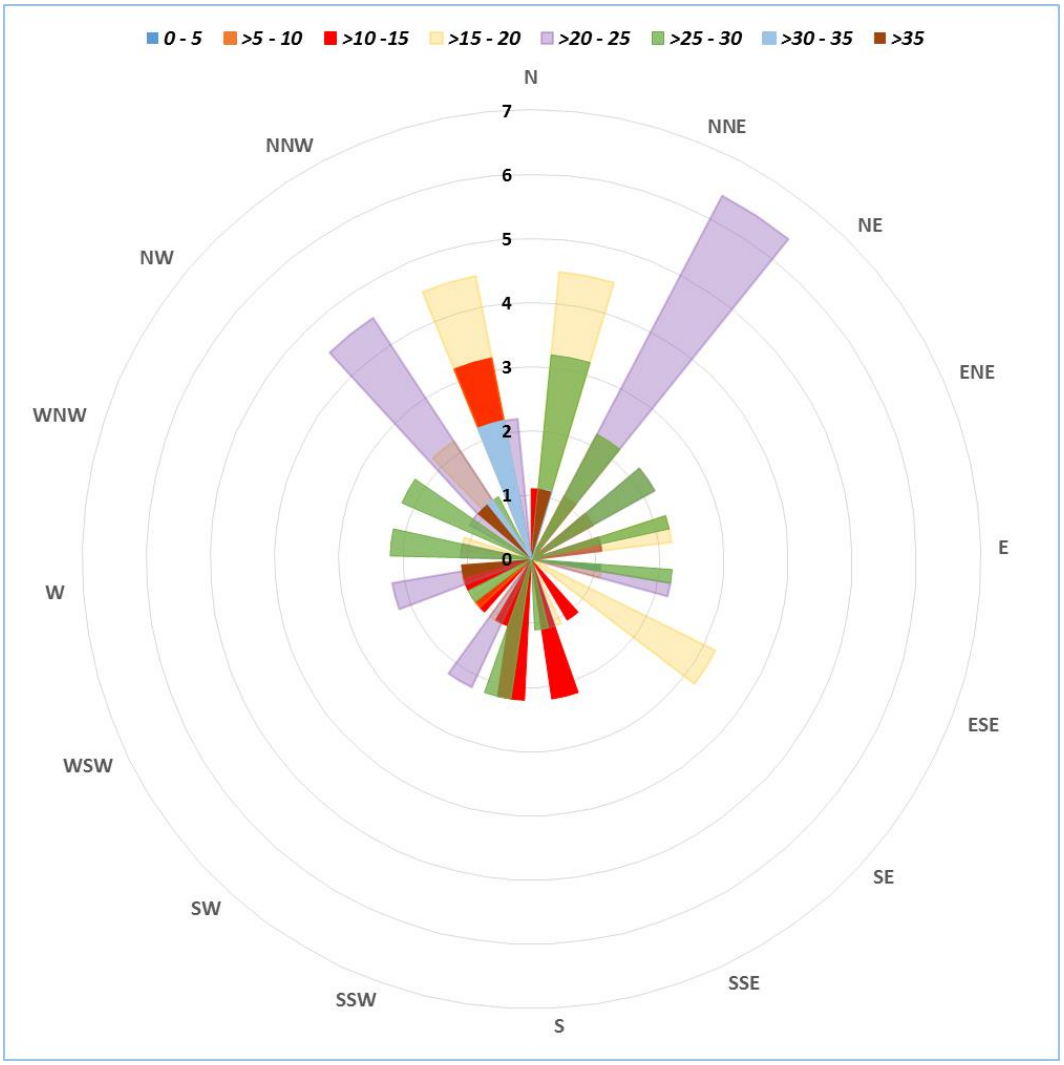

Figure 5.17. The rose diagram of slope versus orientation of rock glaciers in San Juan Mountains study area. The trend line is 3rd order best-of-fit polynomials.

Rock glaciers are found in the study area at decreasing elevations along a latitudinal transect from south to north (Figure 4.12). When considering aspect, rock glaciers have been shown to exist mainly on slopes facing northeast. Janke (2005), in his study on the rock glaciers in the Colorado Front Range, found that rock glaciers existed on slopes facing north which is similar to the finding in this present study. On the eastern slopes north of study area, rock glaciers occur in lower elevations whereas in the southern region rock glaciers exist at higher elevations at above 3,500 m.

CHAPTER VI

SUMMARY

The temperature of the study area of the southwestern San Juan Mountains has warmed by 2.7^0C between 1890 and 2013, and almost all this warming occurred between 1980 and 2013 by ~2.2^0C. The general warming pattern in the study area during the time period observed is similar to the pattern observed in Colorado. The late twentieth-century global warming trend which has been observed to begin around 1990, it began much earlier than began later in the study area. The warming trend which began in the San Juan Mountains around 1995. However, the warming trend in the San Juan Mountains appear to be more rapid than the global areal. It is because study area has a small areal courage where local atmospheric zone differs from the surrounding area. Meanwhile, the global climate is resulted from the average climate over the entire planet that has a lot of modifications.

The warming trend in San Juan Mountains is increasing at a greater rate than global average and faster than state of Colorado. This warming trend may be associated in part with regional circulation and precipitation changes (on a small area).

Over the past several decades the extent of potential permafrost in San Juan Mountains appear to have decreased. This conclusion is supported by frost model, which is based on observed temperature trend for over a hundred years. Even though the decline in the extent of potential permafrost in San Juan Mountains is mostly from a

warming trend, topography, ground condition, and surface conditions, and aspect also impact the extent of potential permafrost.

Future changes in the extent of potential permafrost will be driven by changes in climate primarily by changes in temperature and precipitation changes. Even though no climate models take into account all of these driving forces (Romanovsky et al., 2010), future climate scenarios model should be applied and specified to predict future extent of potential permafrost. From the estimation of the distribution of potential permafrost for a 2.0^0C warmer-model scenario, a dramatic reduction in the extent of permafrost by ~49 % of the total is probably occurred in study area. If this scenario occurs, the frequency of debris flow, rockfalls, and other large events would increase and create and impact in this area.

The spatial pattern of potential permafrost change in relation to the location of the toe of rock glaciers varies across the study area. The northeast region is orientation-dependent whereas the southwest region displays elevation- and slope-dependent response. Through detailed analysis of topographic profiles and elevational location of the toes of rock glaciers, it was determined that most of the rock glaciers are found at higher elevation above 3,000 m. In term of orientation, more than 60% of rock glaciers form on north or north-east facing slopes. Rock glaciers are larger if located on north or north-east facing slope.

Global temperature changes have influenced potential permafrost in the study area of San Juan Mountains. Higher summer and winter temperature in the last decade since 1980 with less precipitation might be the reasons for the decreasing extent of

permafrost. Beside the warming trend, the elevation, slope, and aspect have a combined influence on the rate of change in the distribution of permafrost in this area.

TTOP model can be used to predict the potential permafrost loss under different scenarios of MAAT increase. The model reveals the change in distribution of potential permafrost in complex topography of study area is a key factor in examining large geomorphic events associated with permafrost degradation, especially on slopes. Further research is required, however, to understand the casual mechanism and to determine what is the relative contribution of natural variability and responses to increases in temperature and decreases in permafrost.

REFERENCES

Admunson, R., Richter, D. D., Humphreys, G. S., Jobbagy, E. G., and Gaillardet, J. (2007). Coupling between biota and earth material in the critical zone: *Element*, 3, 327-332.

Anderson, S. P., von Blanckenburg, F., and White, A. (2007). Physical and chemical controls on the critical zone: *Elements*, 3, 315-319.

Anderson, S. P., Bales, R. C., and Duffy, C. J. (2008). Critical zone observatories: Building a network to advance interdisciplinary study of Earth surface processes: *Mineral Magazine*, 72, 7-10.

Anisimov, O. A. and Nelson, F. E. (1996). Permafrost distribution in the Northern Hemisphere under scenarios of climate change: *Global and Planetary Change*, 14, p. 59-72.

Atwood, W.A., and Mather, K.F. (1932). Physiography and Quaternary geology of the San Juan Mountains, Colorado: *U.S. Geological Survey Professional Paper*, 166.

Atwood, W. W. (1915). Eocene glacial deposits in southwestern Colorado: *U.S. Geological Survey Professional Paper*, 95, p. 13-26.

Baars, D. L. (1992). The American Alps, the San Juan Mountains of southwest Colorado: Albuquerque, NM: *University of New Mexico Press*, Albuquerque.

Baars, D. l. (2000). The Colorado Plateau: Geologic History: *The University of New Mexico Press*, Albuquerque.

Baroni, C., Armiraglio, S., Gentili, R., Carton, A. (2007) Landform-vegetation units for investigating the dynamics and geomorphologic evolution of alpine composite debris cones (Valle dell'Avio, Adamello Group, Italy): *Geomorphology*, 84, p.59–79

Barsch, D. (1977). Nature and importance of mass-wasting by rock glaciers in alpine permafrost environments: *Earth Surface Processes*, 2: 231-245.

Barsch, D. (1996). Rock glacer: Indicator for the present former geomorphology: *John Waley*, New York, 69-90.

Bales, R.C., Hopmans, J.W., O'Geen, A.T., Meadows, M., Hartsough, P.C., Kirchner, P., Hunsaker, C.T., and Beaude D. (2011). Soil moisture response to snowmelt and rainfall in a Sierra Nevada mixed-conifer forest: *Vadose Zone J*. 10:786–799.

Blair, R. (1996). Western San Juan Mountain: their geology, ecology and human history. Niwot, CO: *University Press of Colorado*, 1st ed, Colorado.

Brenning, A. (2008). The impact of mining on rock glaciers and glaciers: example from central Chile; in Darkening Peaks: *Glacier Retreat, Science, and Society* edited by Benjamin S. Orlove, Ellen Wiegandt, Brian H. Luckman. University of California.

Briggs, M. A., Walvoord, M. A., McKenzie, J. M., Voss, C. I., Day-Lewis, F. D., and Lane, J. W. (2014). New permafrost is forming around shrinking Arctic lakes, but will it last?: *Geophysical Research Letter*, 41, p. 1585–1592.

Bronniman, S., Andrade, M., and Diaz, HF. (2014). Mountain and climate change. A global concern: *Sustainable Mountain Development Series*. Austraian Development Cooperation and the Swiss Agency for Development and Cooperation.

Burger, K. C., Degenhardt J. J, and Giardino, J. R. (1999). Engineering geomorphology of rock glaciers: *Journal of Geomorphology*. 31: 93-132.

Burke, E. J., Hartley, I. P., and Jones, C. D. (2012). Uncertainties in the global temperature change caused by carbon release from permafrost thawing: *The Cryosphere*, 6, p. 1063-1076.

Burn, C. (2013). Recent advance in mountain permafrost research. Transaction of the International Permafrost Association: *Permafrost and Periglacial Processes*, 24, 2, 99-107.

Caine, N. (2010). Recent hydrology change in a Colorado alpine basin: an indicator of permafrost thaw?: *Annals of Geology*, 51, v. 56, p. 130-134.

Carrara, P. E. (2011). Deglaciation and postglacial timberline fluctuation in the San Juan Mountains, Colorado: *US Department of the Interior and USGS Professional Paper*, 1782, p. 1-58.

Carrara, P.E., and Andrews, J.T. (1975). Holocene glacial/periglacial record—Northern San Juan Mountains, southwestern Colorado: *Zeitschrift fûr Gletscherkunde und Glazialgeologie*, v. 11, p. 155–174.

Chadburn, S. E., Burke, E. J., Essery, R. L. H., Boike, J., Langer, M., Heikenfeld, M., Cox, P. M., and Friedlingstein, P. (2015). Impact of model developments on present and future simulations of permafrost in a global land-surface model: *The Cryosphere*, 9, 1505-1521.

Chin, K., Lento, J., Culp, J., Lacelle, D. and Kokelj, S. (2016). Permafrost thaw and intense thermokarst activity decreases abundance of stream benthic macroinvertebrates: *Glob Change Biol*. Accepted Author Manuscript.

Christensen, T. R. (2004). Thawing sub-arctic permafrost: Effects on vegetation and methane emissions: *Geophycal Research Letter*, 31, L04501.

Clow, D. W. (2010). Changes in the timing of snowmelt and stream flow in Colorado: A response to recent warning: *American Meteorological Society*, 23, p. 2293 – 2306.

Cohen, J. and Entekhabi, D. (1999). Eurasian sbow cover variability and Nortern Hemisphere climate predictability: *Geophysical Research letter*, 26 (3), p. 345 – 348.

Damm, B. and Langer, M. (2006). Mapping and regionalisation of permafrost phenomena as a basis for natural hazard analyses in south Tyrol (Italy): *Mitt. Der Osterreichischen Geog. Ges*, 148, p. 295–314.

Degenhardt, J.J. (2009). Development of tongue-shaped and multilobate rock glaciers in alpine environments — interpretations from ground penetrating radar surveys: *Geomorphology*, 109, p. 94–107.

Degenhardt Jr, J. J. and Giardino, J. R., Junck, M. B. (2003). GPR survey of a lobate rock glacier in Yankee Boy Basin, Colorado, USA. In: Bristow, C.S., Jol, H.M. (Eds.), Ground Penetrating Radar in Sediments: *Geological Society of London, Special Publications*, 21, p. 167–179.

Desyatkin, R., Fedorove, A., Desyatkin, A., and Kostantinove, P. (2015). Air temperature changes and their impact on permafrost ecosystems in eastern Siberia: *Thermal Science,* 19 (2), 351-360.

Escobedo, D., 2008. Rock glacier response to climate change. Rocky Mountain National Park, Continental Divide Research Learning Center: *National Park Service*, U. S. Dept. of Interior.

Ernakovich, J., Hopping, K., Berdanier, A., Simpson, R., Kachergis, E., Steltzer, H., and Wallenstein, M. (2014). Predicted responses of artic and alpine ecosystems to altered seasonality under climate change: *Global Change Biology*, 20, p. 3256-3269.

Etzelmüller, B., Farbrot, H., Guðmundsson, Á., Humlum, O., Tveito, O.E. and Björnsson, H. (2007): The regional distribution of mountain permafrost in Iceland: *Permafrost and Periglacial Processes*, v. 18, p. 185-199.

Fischer, L., Huggel, C., Kaab, A., and Haeberli, W. (2013). Slope failure and erosion rates on a glacierized high-mountain face under climate change: *Earth Surface and Landforms*, 38, 8, 836-846.

Gaillardet, J., Dupré, B., Louvat, P., and Allègre C. J. (2004). Global silicate weathering and CO consumption rates deduced from the chemistry of large rivers: *Chemical Geology*, 159: 3-30.

Gamache, G. (2014): The Impact of Geologic and Geomorphic Characteristics on Drainage Efficiency and Discharge; Uncompahgre, San Miguel, and Animas River Watersheds, Colorado, USA. Geology and Geophysics, Texas A&M University, Texas: *Ph.D Dissertation*.

Genxu, W., Yuansour, L., Yibo, W., and Oingbo, W. 2008. Effects of permafrost thawing on vegetation and soil carbon pool losses on the Qinghai–Tibet Plateau, China: *Geoserma*, 143, 1-5, 143-152.

Giardino, J. R. (1979). Rock glacier mechanics and chronologies: Mount Mestas, Colorado: *University of Nebraska*, 244.

Giardino, J. R. (1983). Movement of ice-cemented rock glacier by hydrostatic pressure: an example from Mount Mesta, Colorado USA: *Artic and Alpine research*, 16, p. 299-309.

Giardino, J. R., and Vitek, J. D. (1988). The significant of rock glaciers in the glacial-periglacial landscape continuum: *Journal of Quaternary Science*, 3, p. 97-103.

Gonzales, D. A. and Karlstrom, K. E. (2011). The eastern San Juan Mountains: A Legacy of Mountains Past and Present in the San Juan Region: *University Press of Colorado*, Colorado.

Grosse, G., Schirrmeister, L., Kunitsky, V. V., Hubberten H. W. (2005). The use of CORONA images in remote sensing of periglacial geomorphology: an illustration from the NE Siberian coast: *Permafrost & Periglacial Processes*, 16, p. 163-172.

Gruber, S. and Haeberli, W. (2007). Permafrost in steep bedrock slopes and its temperature-related destabilization following climate change: *Journal of Geophysical Research*, vol 112.

Guvorushko, S. M. (2011). Natural processes and human impact: Interactions between pumanity and the environment: *Springer*.

Haeberli, W. (1985). Creep of mountain permafrost: internal structure and flow of alpine rock glaciers: *Mitteilungen der Versuchsanstalt fur Wasserbau, Hydrologie und Glaziologie Nr*. 77, Zurich, 183.

Haeberli W., Hallet B., Arenson L., Elconin R., Humlum O., Kääb A. and Vonder Mühll D. (2006). Permafrost Creep and Rock Glacier Dynamics: *Permafrost and Periglacial Processes*, 17, p. 189–214.

Haeberli, W., 2013. Mountain permafrost – research frontiers and a special long-term challenge: *Cold Region Science and Technology*, Vol. 96, p. 71 - 76.

Hasler, A., Geertsema, M., Foord, V., and Noetzli, J. (2014). The influence of surface characteristics, topography and continentality on mountain permafrost in British Columbia: *The Cryosphere*, 9, p. 1025 -1038

Hoffman, M. J., Fountain, A. G., and Achuff, J. M. (2007). 20th-century variations in area of cirque glaciers and glacierets, Rocky Mountain National Park, Rocky Mountains, Colorado, USA: *Annals of Glaciology*, 46, p. 349 –354.

Howe, E. (1909): Landslides of the San Juan Mountains, Colorado: *U.S. Geological Survey Professional Paper*, 67.

Humlum, O., (2000). The climatic significance of rock glaciers: *Permafrost and Periglacier Processes*, 9: 375-395.

Janke, J. R., William, M. W., and Evan Jr, A. (2012). A comparison of permafrost prediction models along a section of Trail Ridge Road, Rocky Mountain National Park, Colorado, USA: *Journal of Geomorphology*.

Janke, J. R. (2005): Modeling past and future alpine permafrost distribution in the Colorado Front Range. Earth Surface Processes and Landforms, 30, p. 1495 – 1508.

Jansen, F. and Hergarten S. (2006). Rock Glacier dynamic: Stick-slip motion couple to hydrology: *Geophysical Research Letters*, Vol. 33, L10502.

Johnson, K. D., Harden, J., McGuire, A. D., Bliss, N. B., Bockheim, J. G., Clark, M., Nettleton-Hollingsworth, T., Jorgenson, M. T., Kane, E. S., Mack, M., O'Donnell, J., Ping, C. L., Schuur, E. A. G., Turetsky, M.R., and Valentine, D. W. (2011). Soil carbon distribution in Alaska in relation to soilforming factors: *Geoderma*, 167–168: 71–84.

Jorgenson, M. T., Racine, C. H., Walters, J. C., and Osterkamp, T. E. (2001), Permafrost degradation and ecological changes associated with a warming climate in central Alaska: *Climate Change*, 48, p. 551–579.

Jorgenson, M. T, Romanovsky, V. E., Harden, J., Shur, Y. L., O'Donnell, J., Schuur, T., and Kanevskiy, M. (2010): Resilience and vulnerability of permafrost to climate change: *Canadian Journal of Forest Research*, 40, p. 1219–1236.

Kanevskiy, M., Daniel, F., Yuri, S., Matthew, B., and Torre, J. (2008). Detailed cryostratigraphic studies of syngenetic permafrost in the winze of the CRREL permafrost tunnel, Fox, Alaska: *Proceedings of the Ninth International Conference on Permafrost,* Vol 1, June 29–July 3, 2008, ed. D.L. Kane and K.M. Hinkel, 889–894. Fairbanks, AK: Institute of Northern Engineering.

Karunaratne, K. C. and Burn, C. R. (2004). Relation between air and surface temperature in discontinuous permafrost terrain near Mayo Yukon Territory: *Canadian Journal of Earth Science*, 41, p. 1438 – 1451.

Konrad, S. K., and Humphrey, N. F. (2000). Staedy-state flow model of debris-covered glaciers (rock glaciers): *IAHS Publ*, No. 264.

Lemke, P., Ren, J., Alley, R. B., Allison, I., Carrasco, J., Flato, G., Fujii, Y., Kaser, G., Mote, P., Thomas, R. H., and Zhang, T. (2007). Observations: Changes in Snow, Ice and

Frozen Ground, Climate Change: The Physical Science Basis. Contribution of Working Group I to the Fourth Assessment Report of the Intergovernmental Panel on Climate Change: *Cambridge University Press*, S Solomon, D Qin, M Manning, Z Chen, M Marquis, KB Averyt, M Tignor and HL Miller (ed), Cambridge, UK, p. 337-383.

Knowles, N., Dettinger, M. D., and Cayan, D. R. (2006). Trends in snowfall versus rainfall in the western United States: *J. Climate*, 19, p. 4545–4559.

Leopold, M., Völkel, J., Dethier, D. P., and William, M. W. (2014). Changing mountain permafrost from the 1970s to today – comparing two examples from Niwot Ridge, Colorado Front Range, USA: *Zeitschrift fur Geomorphologie*, Supplemenatry Issue, 58, 1, 137-157.

Leopold, M., Voelkel, J., Dethier, D., William, M., and Caine, N. (2010). Mountain Permafrost - a valid archive to study climate change? Examples from the Rocky Mountains Front Range of Colorado, USA: *Nova Acta Leopoldina*, v. 112, p. 281-289.

Lin, H. S. (2009). Earth's critical zone and hydropedology: concepts, characteristics, and advances: *Hydrology and Earth System Sciences Discussion*, 6, 3417-3481.

Lipman, P.W., Steven, T.A., and Mehnert, H.H. (1970). Volcanic history of the San Juan Mountains, Colorado, as indicated by potassium-argon dating: *Geological Society of America Bulletin*, v. 81, p. 2327–2352.

Liu, L., Zhang, T., and Wahr, J. (2010). InSAR measurements of surface deformation over permafrost on the North Slope of Alaska: *J. Geophys. Res.*, 115.

Martin, L., and Whaley, W. B. (1987). Rock glacier: a review. Part I: *Progress in Physical Geography*, 11: 260-282.

Millar, Cl. L., and Westfall, W. B. (2010). Distribution and climatic relationships of the American Pika (Ochotona princeps) in Siera Nevada and Western Great Basin, USA. Periglacial Landforms as Refugia in warming climates: *Artic Antarctic and Alpine Research*, 11, 260-282.

Nelson, F. E. and Outcalt, S. I. (1987). A computational method for prediction and regionalization of permafrost: *Arctic and Alpine Research*, Vol. 19, No. 3, p. 279-288.

Nyenhuis, M., Bonn, M., Hoelzie, Z., and Bonn, R. D. (2005). Rock glacier mapping and permafrost distribution modeling in the Turtmanntal, Valais, Switzerland. *Z*: *Geomorph. N. F*, 49, 3, p. 275-292.

Park, H., Kim, Y., and Kimball, J. (2016). Widespread permafrost vulnerability and soil active layer increases over the high northern latitudes inferred from satellite remote sensing and process model assessments: *Remote Sensing of Environment*, 175: 349–358.

Pauli, H., Gottfried, M., and Graherr, G. (2003). Effect of climate change on the alpine and nival vegetation of the Alps: *Journal of Mountain Ecology*, 7, p. 9-12.

Pirkle, E. C., and Yoho, W. H. (1985). Natural landscapes. Dubuque, IA: *Kendal/Hunt*, 416.

Quinton, W. and Baltzer, J. (2013). Changing surface water systems in the discontinues permafrost zone; Implication for streamflow: *IAHS-AISH Publication*, 360, 85-92.

Rangwala, I and Miller, R, M. (2011). Long-term temperature trends in the San Juan Mountains.

http://marine.rutgers.edu/~rangwala/pubs/other/Rangwala&Miller_2011_BookChapter.pdf

Romanovsky, V.E., Smith, S.L., and Christiansen, H.H. (2010). Permafrost thermal state in the polar Northern Hemisphere during the International Polar Year 2007–2009: a synthesis: *Permafrost and Periglacial Processes*, 21(2), p. 106–116.

Salzmann, N., Noetzli, J., Hauck, C., Gruber, S., Hoelzle, M., and Haeberli, W. (2007). Ground surface temperature scenarios in complex high-mountain topography based on regional climate model results: *Journal of Geophysical Research-Earth Surface*, 112.

Scherler, M., Hauck, C., Hoelzle, M., and Salzmann, N. (2013). Modeled sensitivity of two alpine permafrost sites to RCM-based climate scenarios: *Journal of Geophysical Research: Earth Surface*, 118, 780-974.

Smith, S. L., Romanovsky, V. E., Lewkowicz, A. G., Burn, C. R., Allard, M., Clow, G. D., Yoshikawa, K., and Throop, J. (2010). Thermal state of permafrost in North America – A contribution to the International Polar Year: *Permafrost and Periglacial Processes*, 21, p. 117-135.

Smith, M. W., and Riseborough, D. W. (2002). Climate and the limits of permafrost: a zonal analysis: *Permafrost and Periglacial Processes,* Vol 13, p. 1-15.

Smith, S. L., Romanovsky, V. E., Lewkowicz, A. G., Burn, C. R., Allard, M., Clow, G. D., Yoshikawa, K., and Throop, J. (2010). Thermal state of permafrost in North America – A contribution to the International Polar Year: *Permafrost and Periglacial Processes*, 21, p. 117-135.

Solomon, S., Qin, D., Manning, M., Chen, Z., Marquis, M., Averyt, K. B., Tignor, M., and Miller, H. L. (2007). Climate Change 2007: The Physical Science Basis. Contribution of Working Group I to the Fourth Assessment Report of the Intergovernmental Panel on Climate Change. Cambridge: *Cambridge University Press*.

Steven, T. A., and Lipman, P. W. (1976). Calderas of the San Juan volcanic field, southwestern Colorado: *U.S. Geological Survey, Professional Paper*, 958.

Stoffel, M. and Huggel, C. (2012). Effects of climate change on mass movements in mountain environments: *Progress in Physical Geography*, 3, p. 421-439.

Stoffel, M., Mendlik, T., Bollschweiler, M. S., and Gobiet, A. (2014). Possible impacts of climate change on debris-flow activity in the Swiss Alps: *Climate Change*, 122, p. 141-155.

Throop, J., Lewkowica, A. G., and Smith, S. L. (2012). Climate and ground temperature relations at site across the continuous and discountinous permafrost zone, nothrn Canada: *Canadian Journal of Earth Science*, 49, p. 865 – 876.

van Everdingen, R. (2005). Multi-language glossary of permafrost and related ground-ice terms. Boulder, CO: *National Snow and Ice Data Center/World Data Center for Glaciology*.

Wahrhaftig, C., and Cox, A. (1959). Rock glaciers in the Alaska Range: *Bulletin of the Geological Society of America*, 70, 4: 383-436.

Wellman, T. P., Voss, C. I., and Walvoord, M. A. (2013). Impactsofclimate, lake size, and supra- and sub-permafrost groundwater flow on lake-talik evolution, Yukon Flats, Alaska (USA): *Hydrogeol. J.*, 21(1), 281–298.

Whiting, K., Al Kahili, K., and Carmona, L. G. (2014). Alteraciones a los Entornos de Permafrost Inducidas por el Cambio Climático: *Ambiente y Sostenibilidad*, 4, 31-38.

Williams, P. J., and Smith, M. W. (1989). The Frozen Earth: Fundamentals of Geocryology: *Cambridge University Press*, New York, N.Y.

William, M. W., Kanuf, M., Caine, N., Liu, F., and Verplanck, P. I. (2006). Geochemistry and source of water of rock glacier outflow, Colorado Front Range: *Permafrost and Periglacial Processes*, 17, p. 13-33.

Woo, M.-K., and T. C. Winter (1993). The role of permafrost and seasonal frost in the hydrology of northern wetlands in North America: *Journal of Hydrology*, 141, p. 5–31.

APPENDIX A

SNOTEL AND NOOA MEAN ANNUAL TEMPERATURE

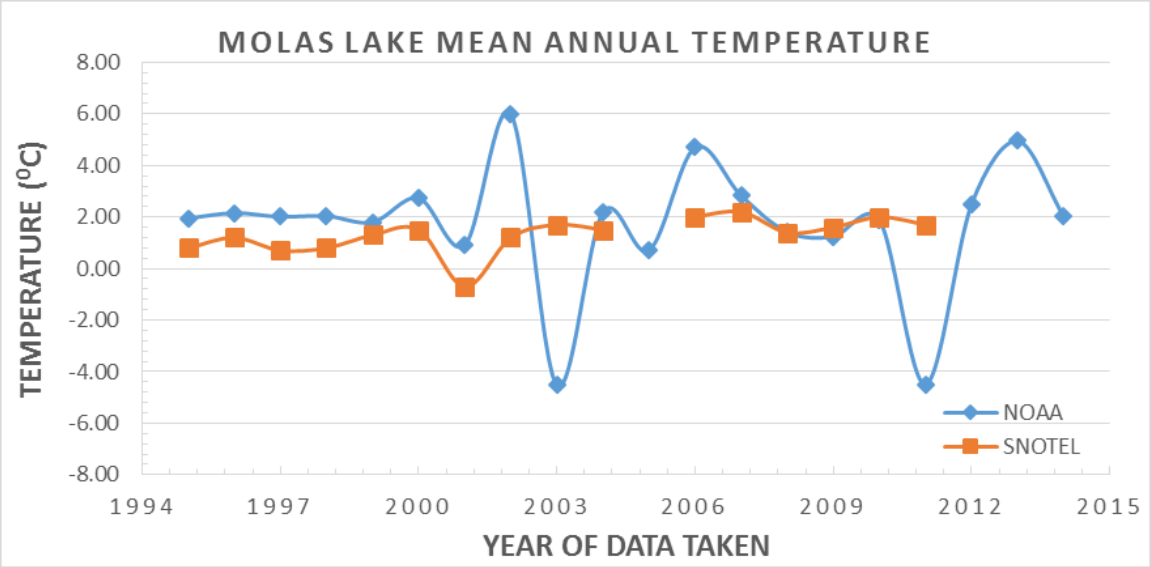

Figure A1. NOAA and SNOTEL mean annual temperature data at Molas Lake Station at an elevation of 3,200.4 meters.

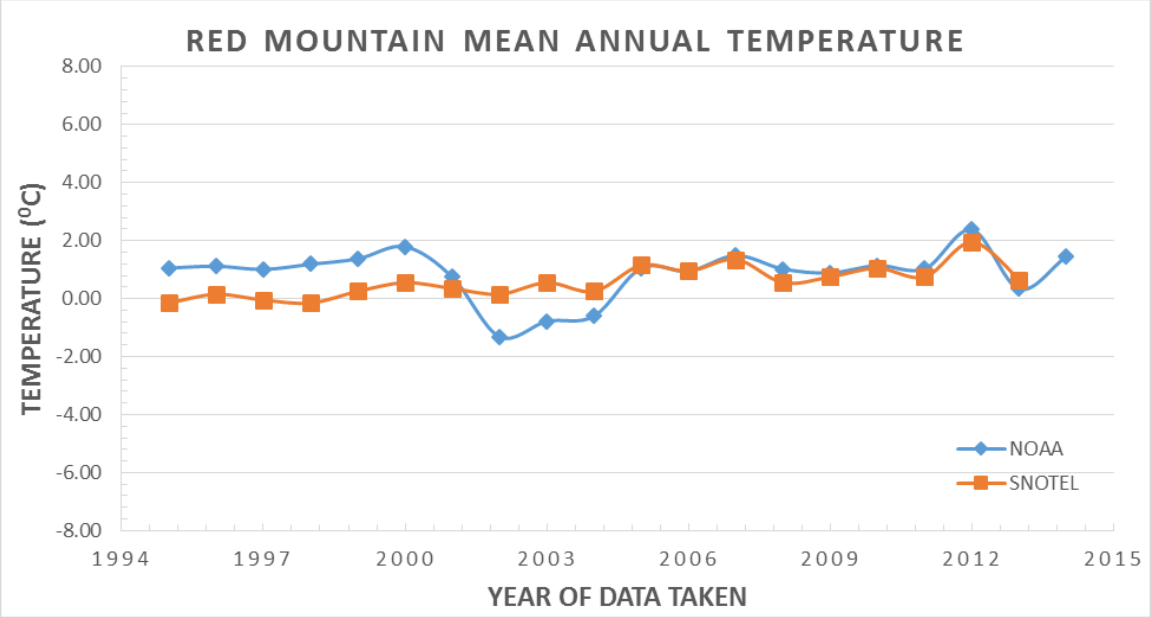

Figure 2. NOAA and SNOTEL mean annual temperature data at Red Mountain Station at an elevation of 3,398.52 meters.

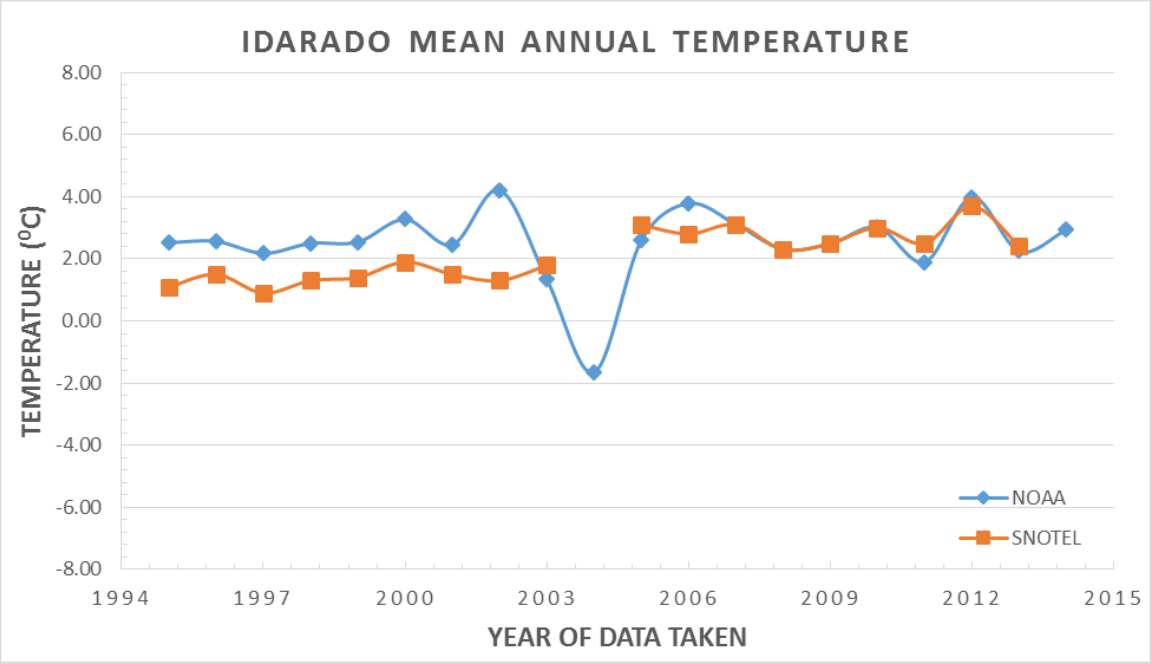

Figure 2. NOAA and SNOTEL mean annual temperature data at Idarado Station at an elevation of 2,987.04 meters.

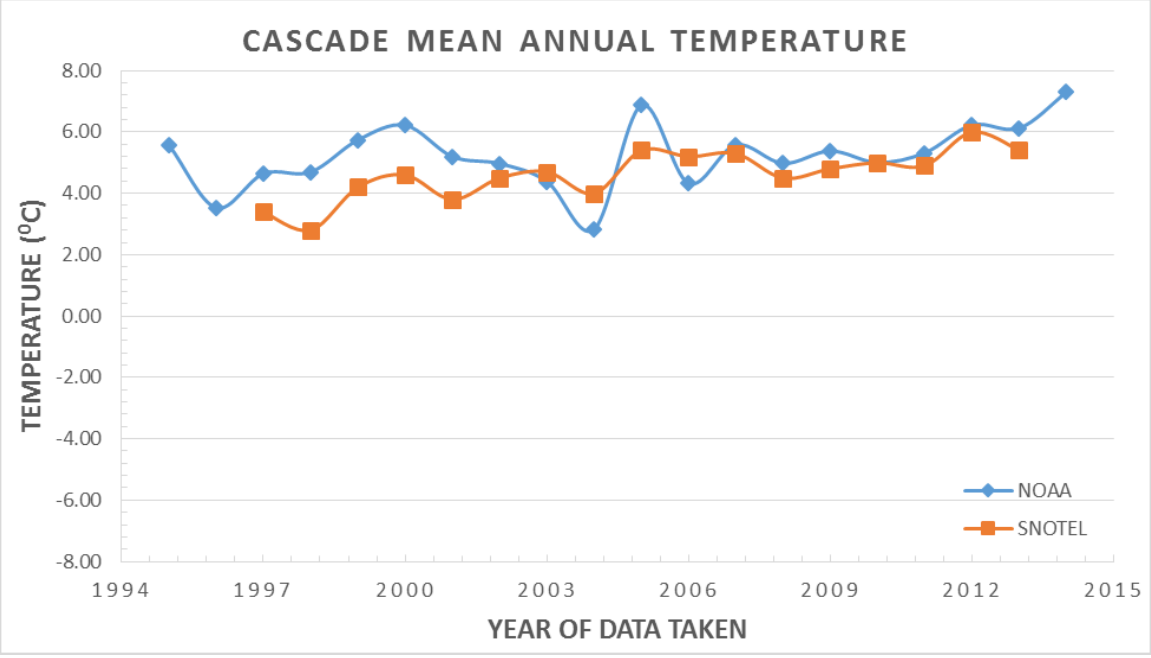

Figure 2. NOAA and SNOTEL mean annual temperature data at Cascade station Station at an elevation of 2,706.62 meters.

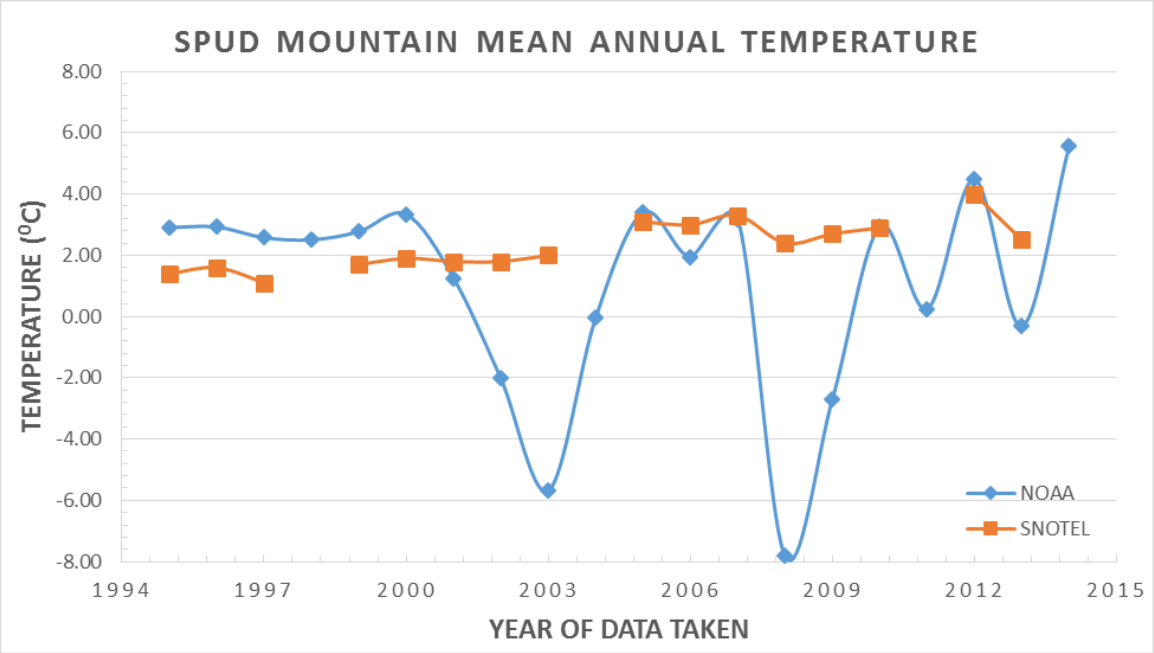

Figure 2. NOAA and SNOTEL mean annual temperature data at Spud Mountain Station at an elevation of 3,249.17 meters.

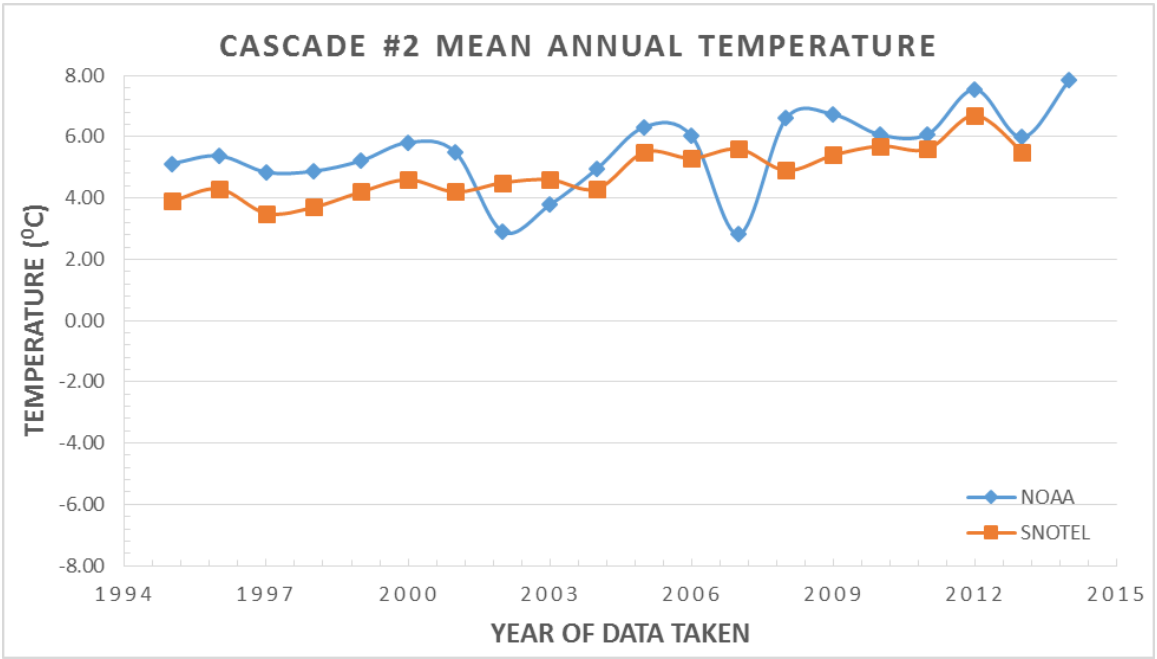

Figure 2. NOAA and SNOTEL mean annual temperature data at Cascade #2 Station at an elevation of 2,718.82 meters.

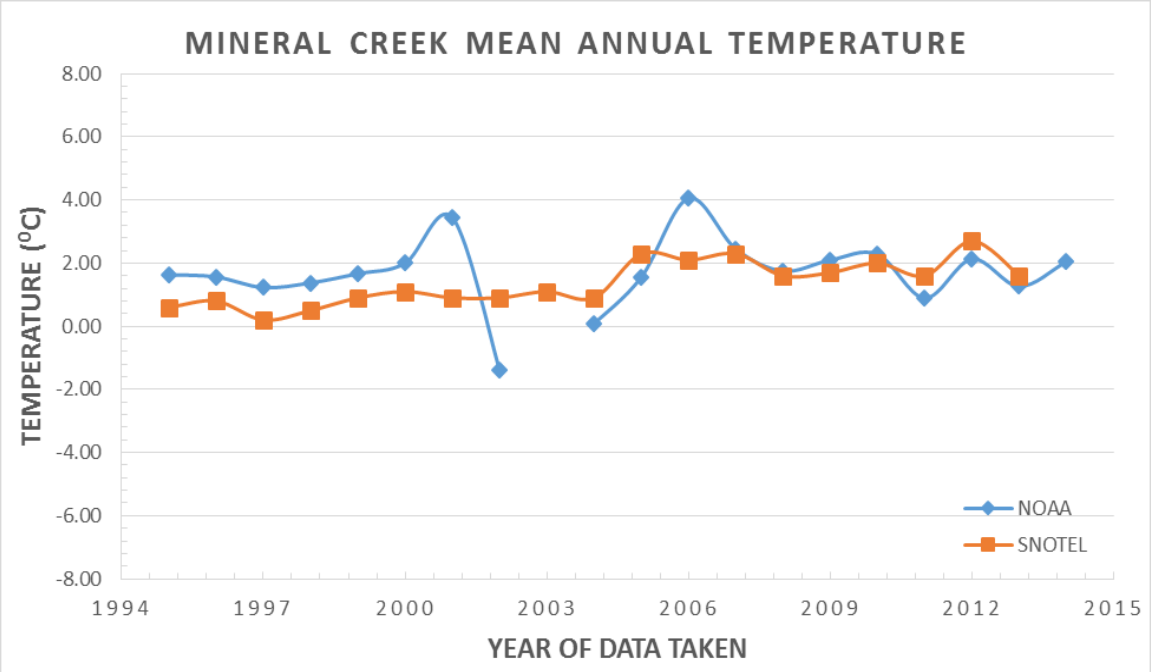

Figure 2. NOAA and SNOTEL mean annual temperature data at Mineral Creek Station at an elevation of 3,060.2 meters.

APPENDIX B

CHANGE OF TEMPERATURE CONTOUR IN THE SAN JUAN MOUNTAINS

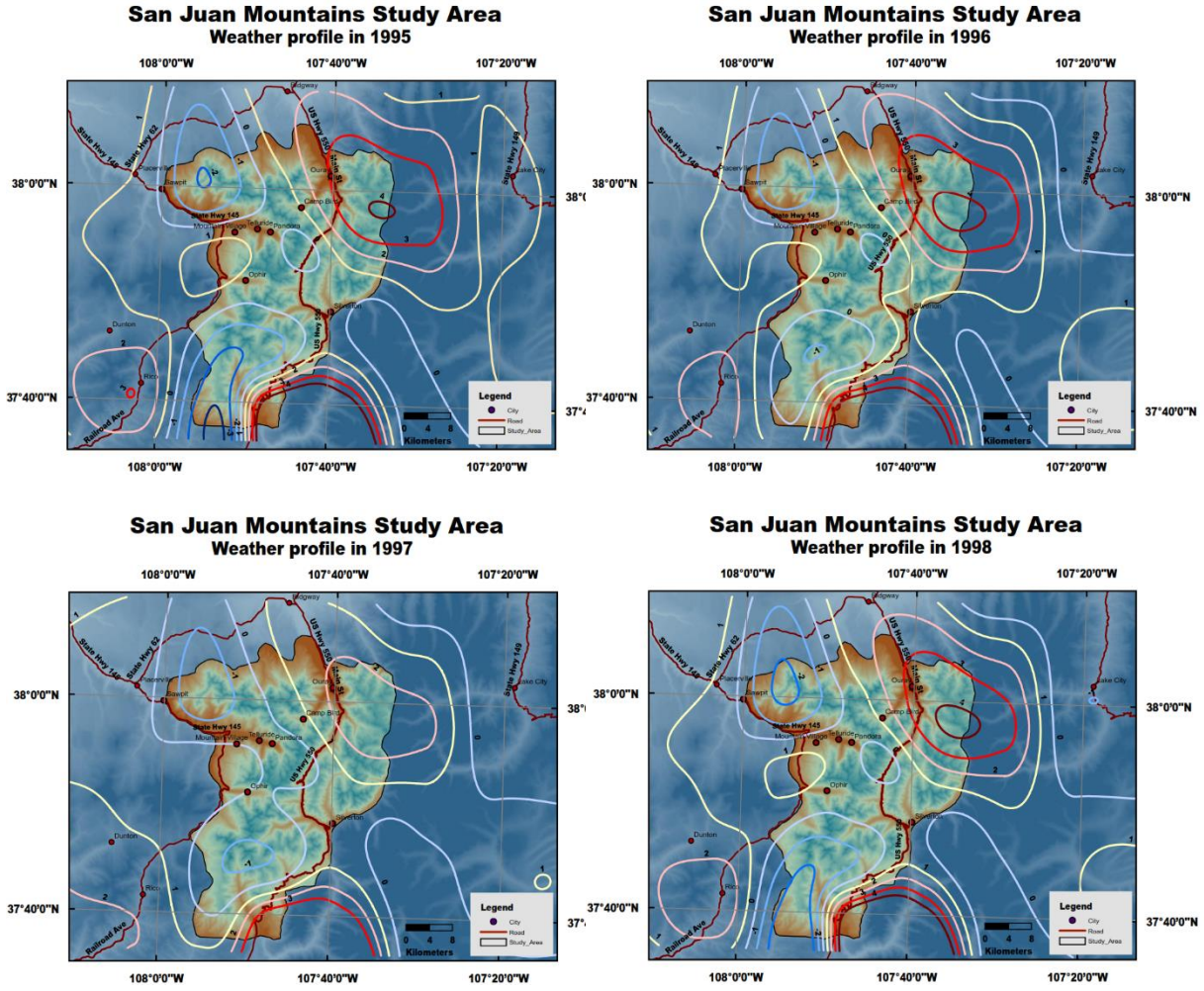

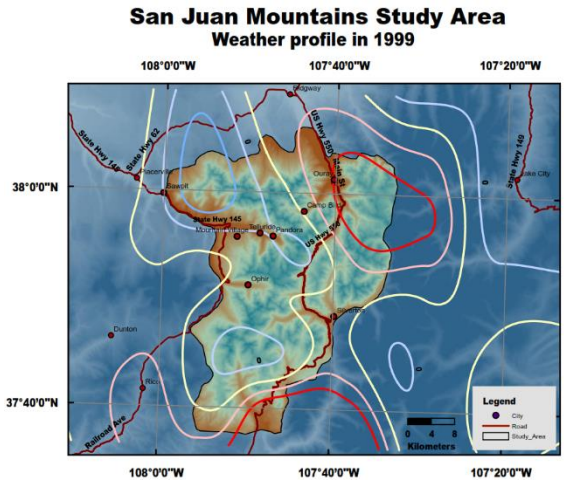
San Juan Mountains Study Area
Weather profile in 1999
108°0'0"W
107°40'0"W
107°20'0"W
38°0'0"N
37°40'0"N
Legend
City
Road
Study_Area
Kilometers

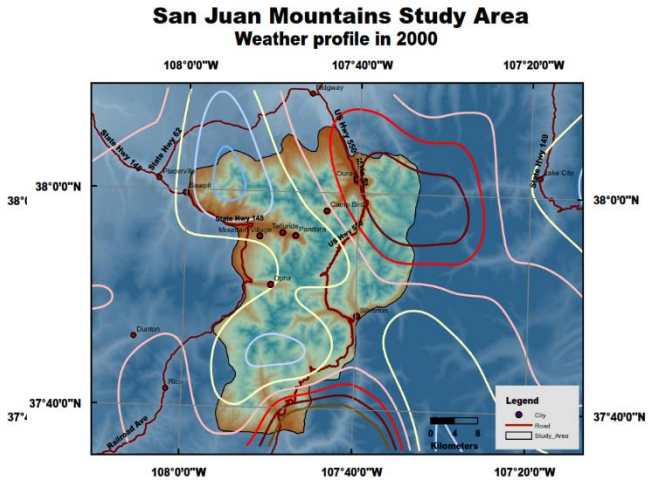
San Juan Mountains Study Area
Weather profile in 2000
108°0'0"W
107°40'0"W
107°20'0"W
38°0'0"N
37°40'0"N
Legend
City
Road
Study_Area
Kilometers

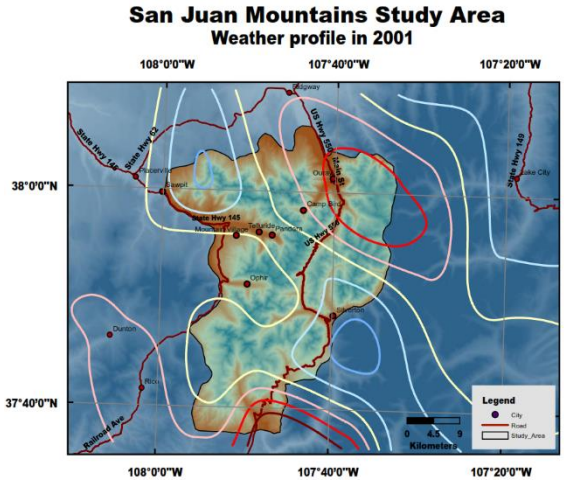
San Juan Mountains Study Area
Weather profile in 2001
108°0'0"W
107°40'0"W
107°20'0"W
38°0'0"N
37°40'0"N
Legend
City
Road
Study_Area
Kilometers

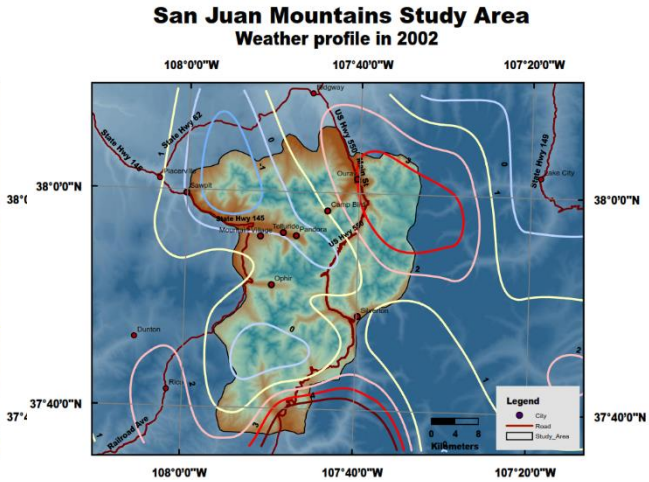
San Juan Mountains Study Area
Weather profile in 2002
108°0'0"W
107°40'0"W
107°20'0"W
38°0'0"N
37°40'0"N
Legend
City
Road
Study_Area
Kilometers

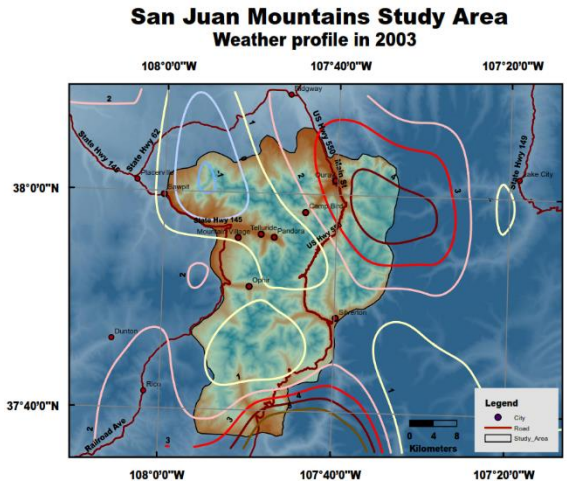
San Juan Mountains Study Area
Weather profile in 2003
108°0'0"W
107°40'0"W
107°20'0"W
38°0'0"N
37°40'0"N
Legend
City
Road
Study_Area
Kilometers

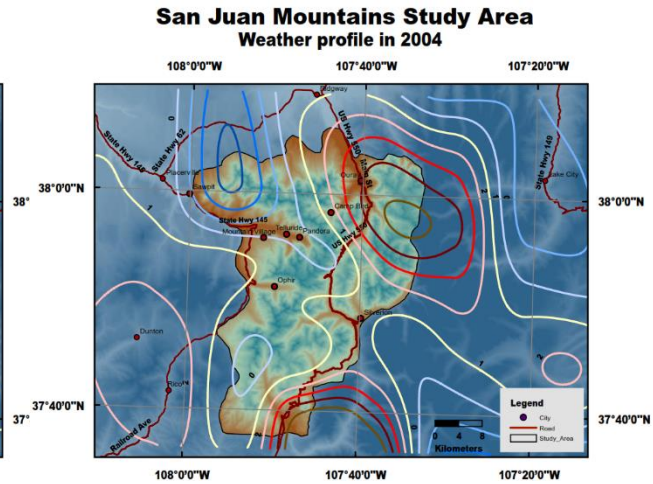
San Juan Mountains Study Area
Weather profile in 2004
108°0'0"W
107°40'0"W
107°20'0"W
38°0'0"N
37°40'0"N
Legend
City
Road
Study_Area
Kilometers

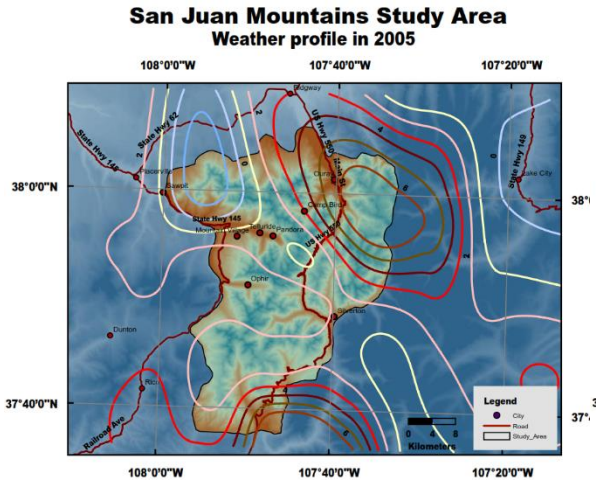
San Juan Mountains Study Area
Weather profile in 2005
108°0'0"W
107°40'0"W
107°20'0"W
38°0'0"N
37°40'0"N
Legend
City
Road
Study_Area
Kilometers

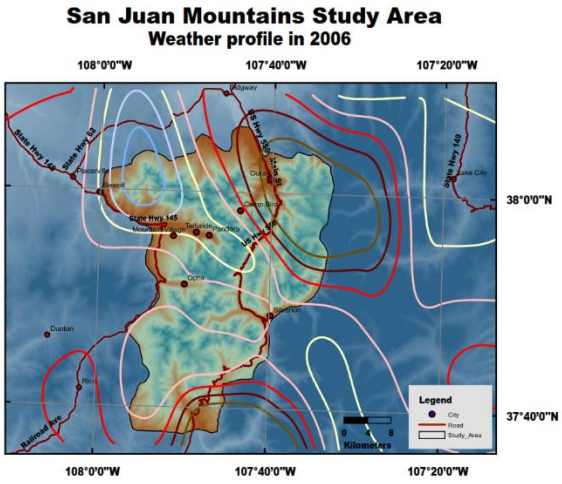
San Juan Mountains Study Area
Weather profile in 2006
108°0'0"W
107°40'0"W
107°20'0"W
38°0'0"N
37°40'0"N
Legend
City
Road
Study_Area
Kilometers

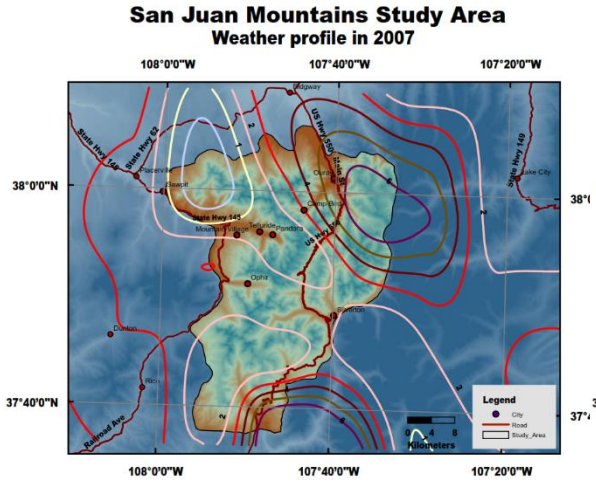
San Juan Mountains Study Area
Weather profile in 2007
108°0'0"W
107°40'0"W
107°20'0"W
38°0'0"N
37°40'0"N
Legend
City
Road
Study_Area
Kilometers

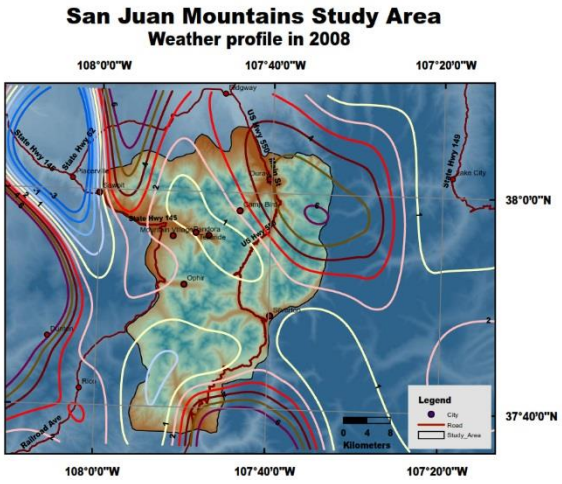
San Juan Mountains Study Area
Weather profile in 2008
108°0'0"W
107°40'0"W
107°20'0"W
38°0'0"N
37°40'0"N
Legend
City
Road
Study_Area
Kilometers

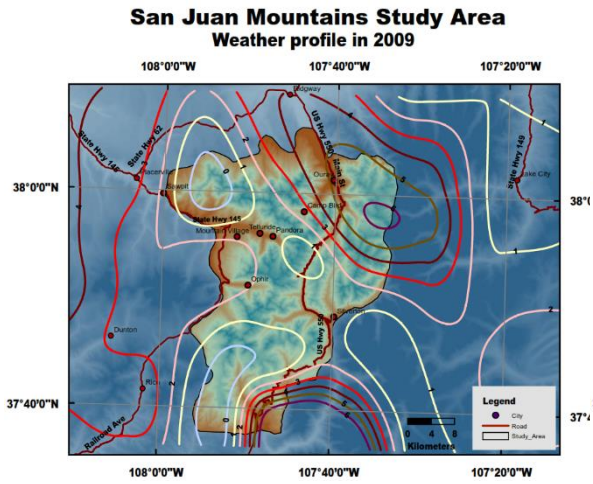
San Juan Mountains Study Area
Weather profile in 2009
108°0'0"W
107°40'0"W
107°20'0"W
38°0'0"N
37°40'0"N
Legend
City
Road
Study_Area
Kilometers

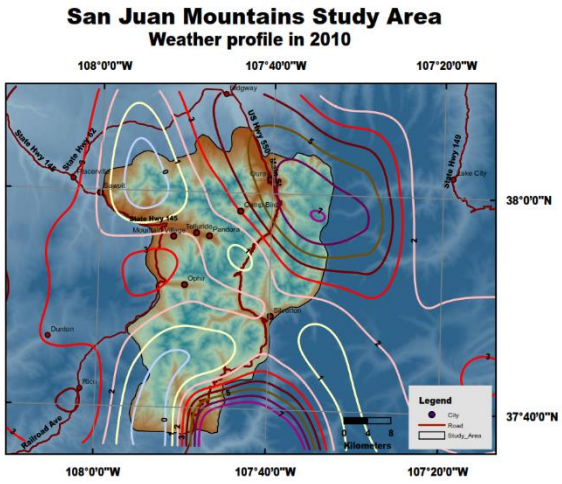
San Juan Mountains Study Area
Weather profile in 2010
108°0'0"W
107°40'0"W
107°20'0"W
38°0'0"N
37°40'0"N
Legend
City
Road
Study_Area
Kilometers

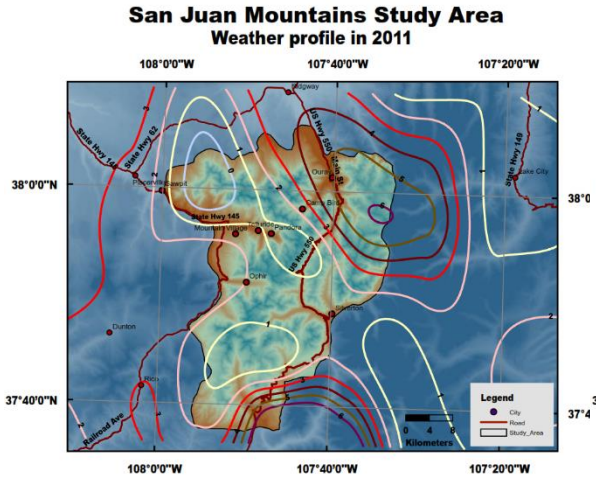
San Juan Mountains Study Area
Weather profile in 2011
108°0'0"W
107°40'0"W
107°20'0"W
38°0'0"N
37°40'0"N
Legend
City
Road
Study_Area
Kilometers

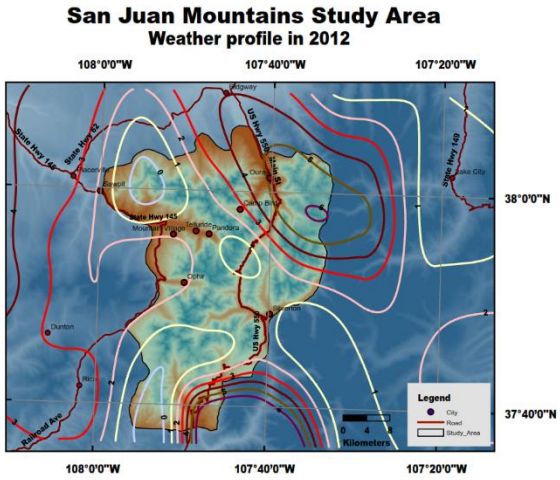
San Juan Mountains Study Area
Weather profile in 2012
108°0'0"W
107°40'0"W
107°20'0"W
38°0'0"N
37°40'0"N
Legend
City
Road
Study_Area
Kilometers

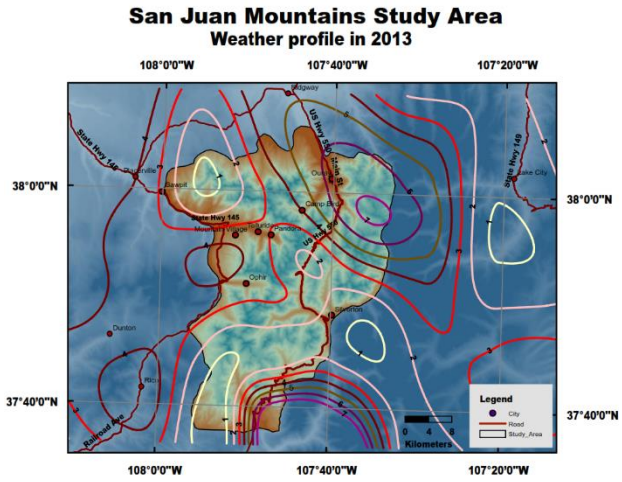
San Juan Mountains Study Area
Weather profile in 2013
108°0'0"W
107°40'0"W
107°20'0"W
38°0'0"N
37°40'0"N
Legend
City
Road
Study_Area
Kilometers

APENDIX C

PERMAFROST EXTENT BASED ON WARMER CLIMATE SCENARIO

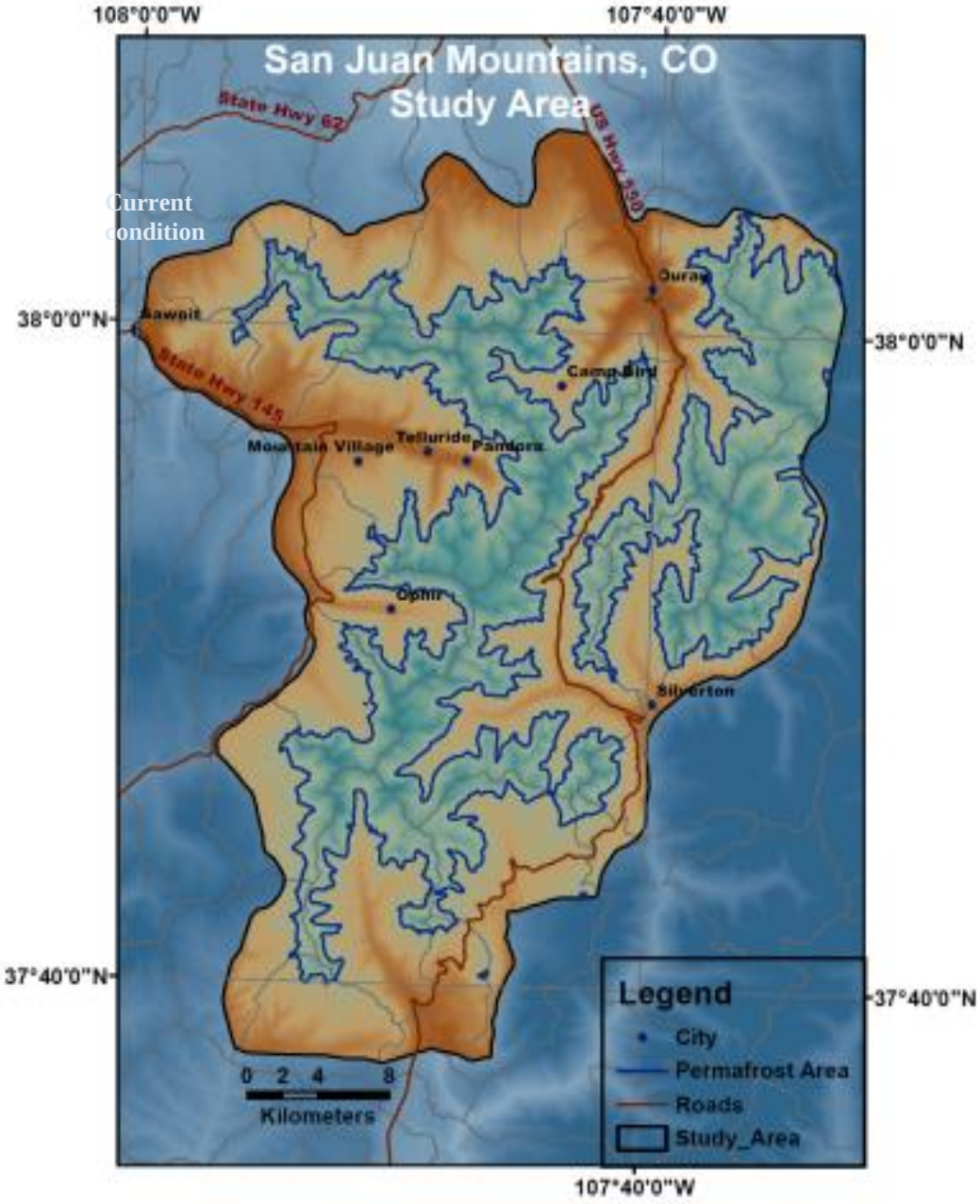

Figure C1. Potential permafrost profile at current condition.

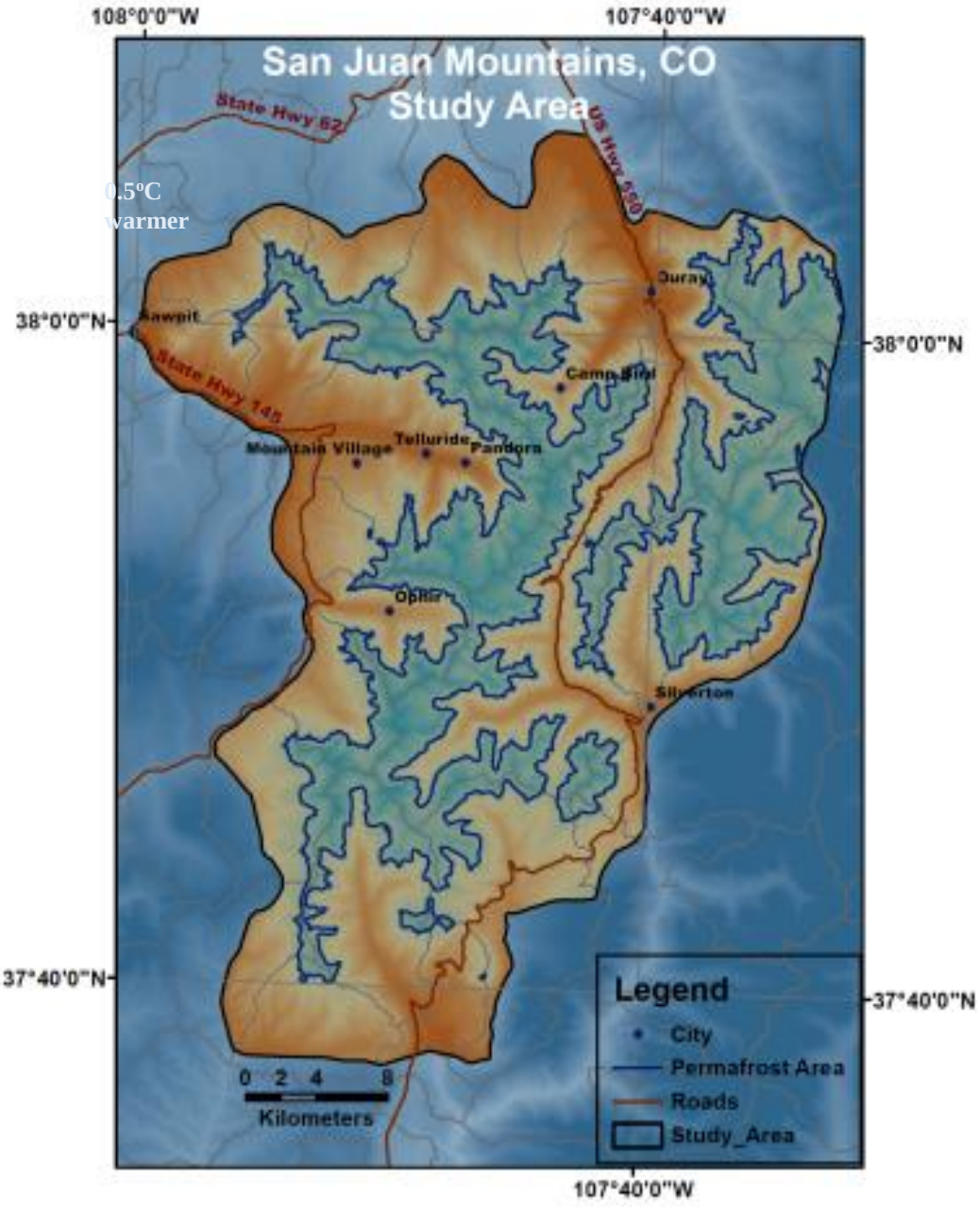

Figure C2. The extent of potential permafrost predicted based on 0.5ºC warmer climate scenario.

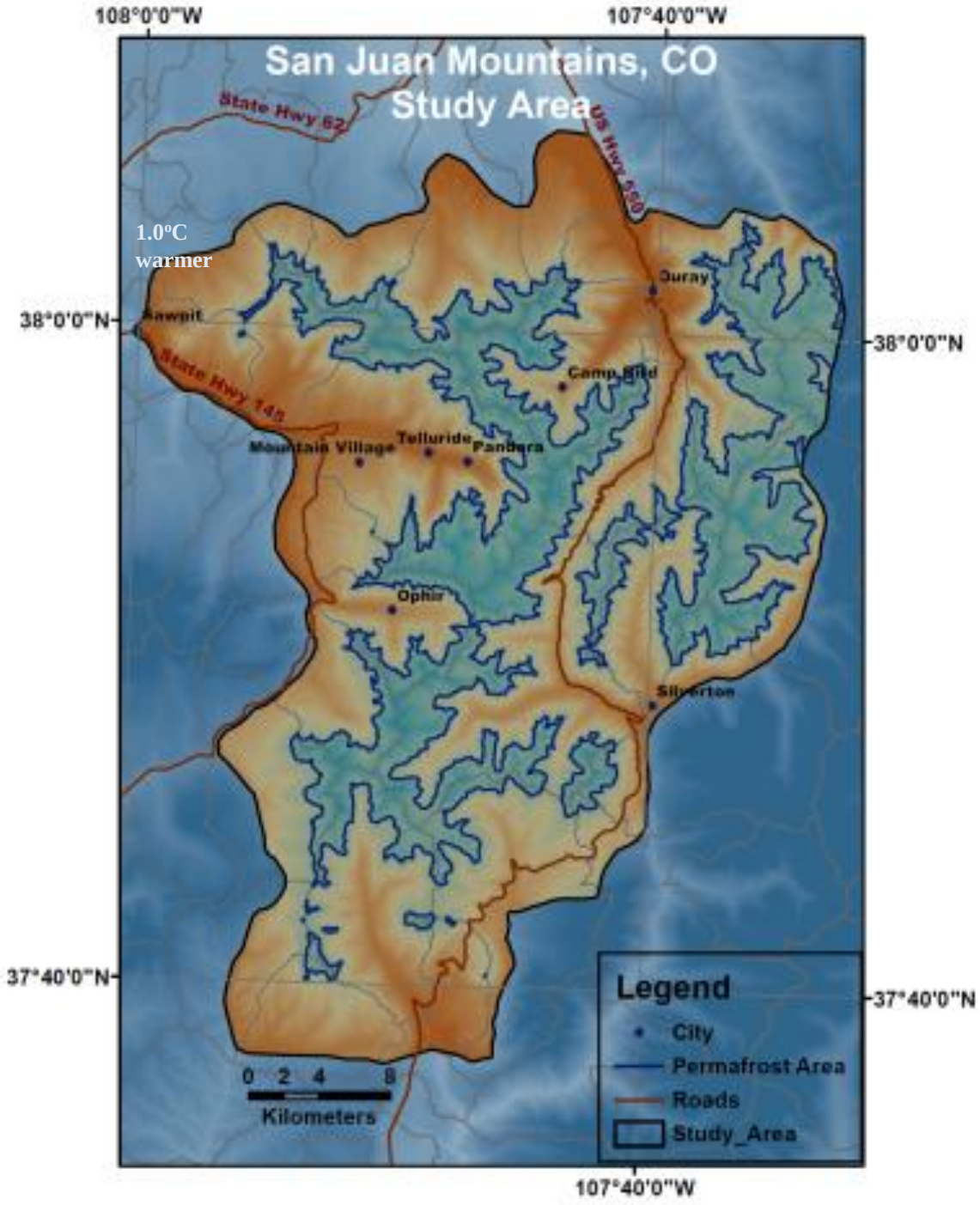

Figure C3. The extent of potential permafrost predicted based on 1.0°C warmer climate scenario.

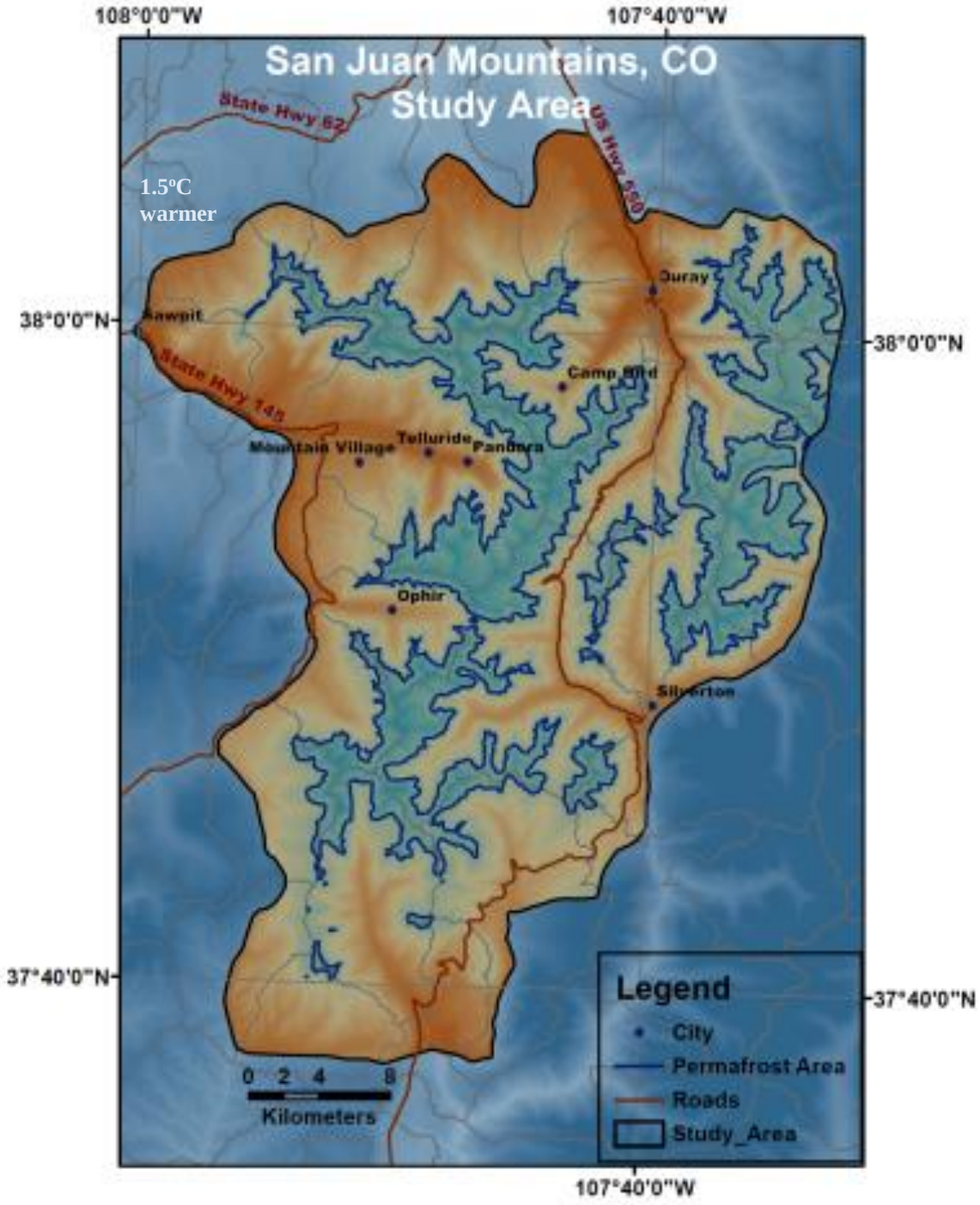

Figure C4. The extent of potential permafrost predicted based on 1.5°C warmer climate scenario.

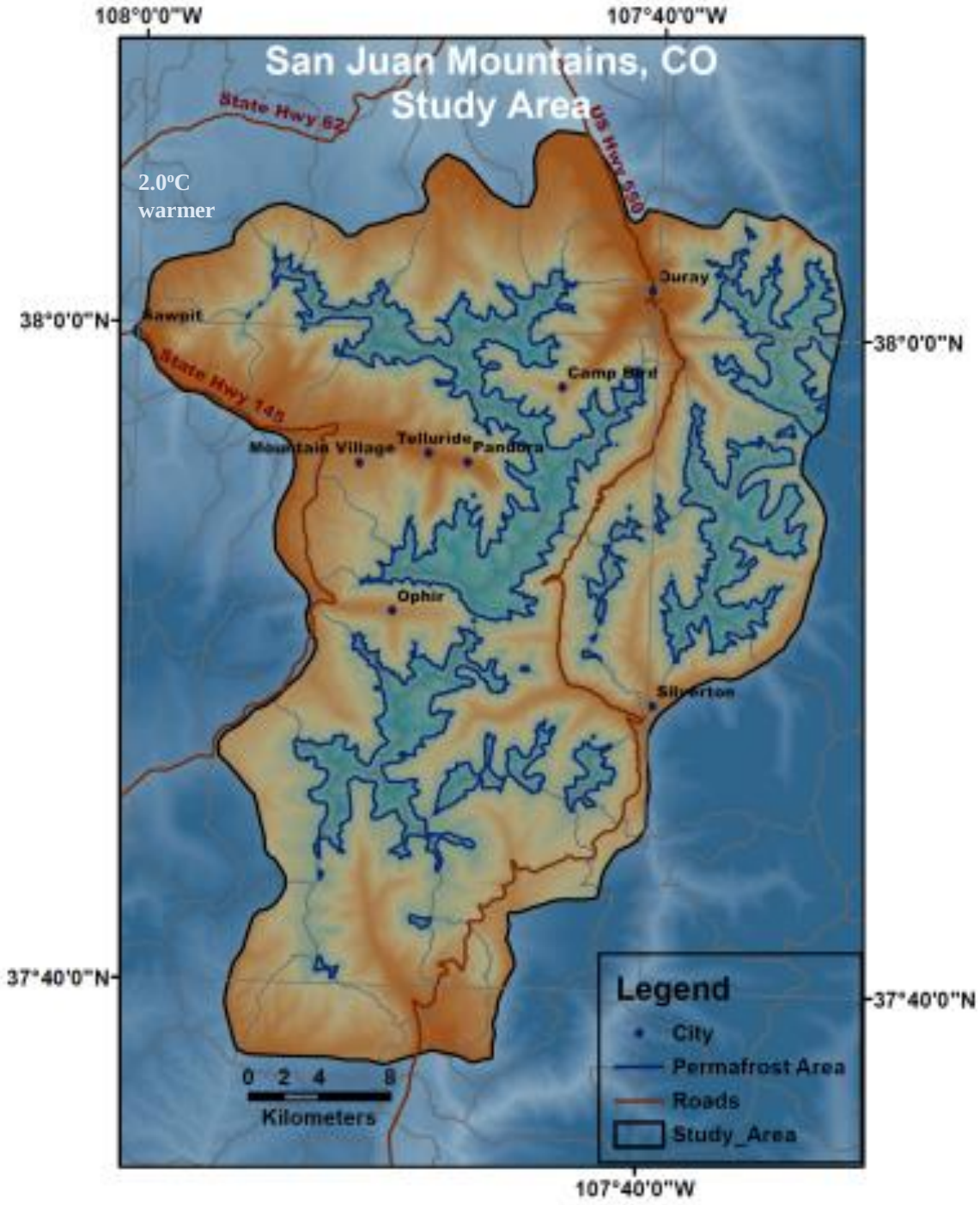

Figure C5. The extent of potential permafrost predicted based on 2.0°C warmer climate scenario.

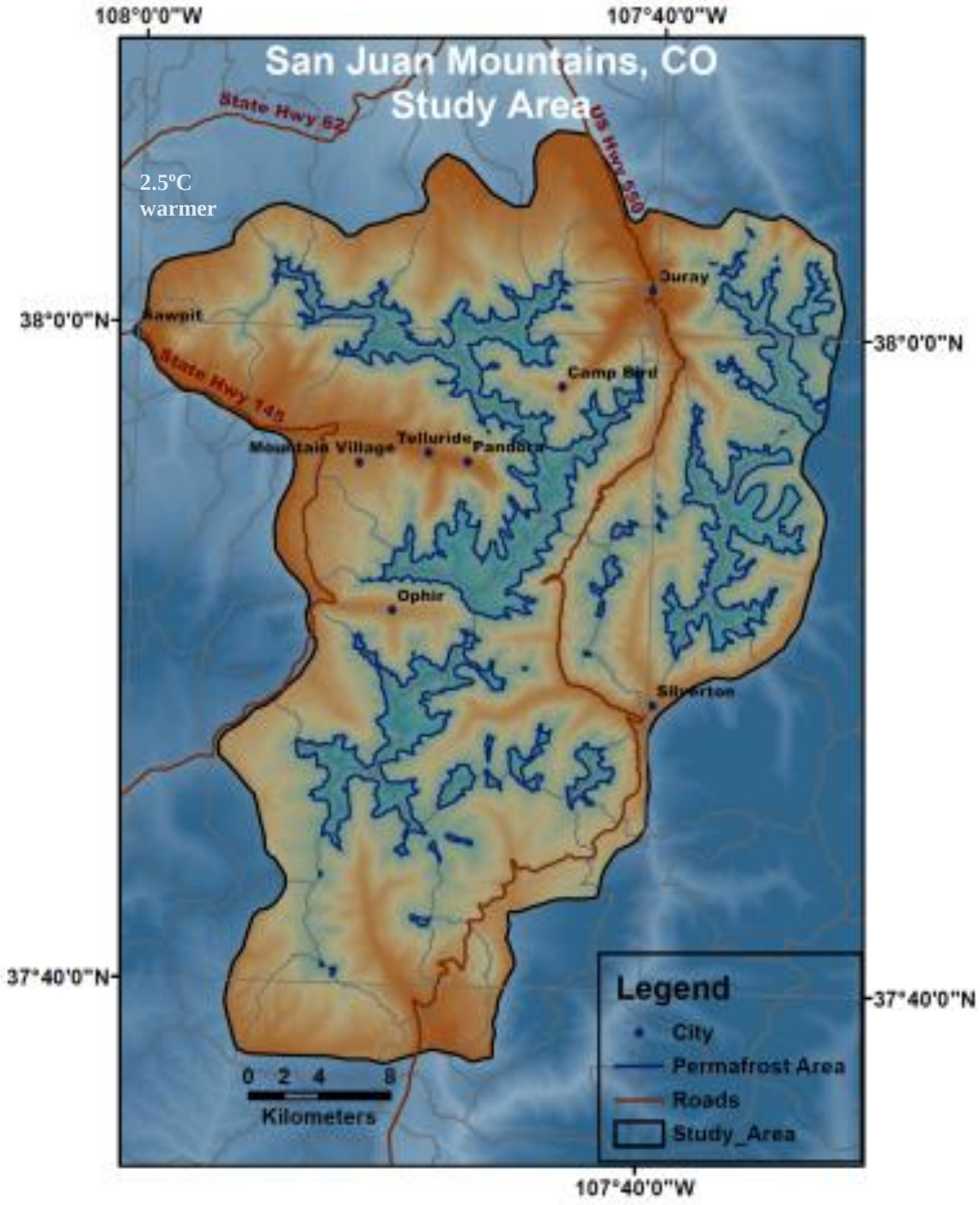

Figure C6. The extent of potential permafrost predicted based on 2.5°C warmer climate scenario.

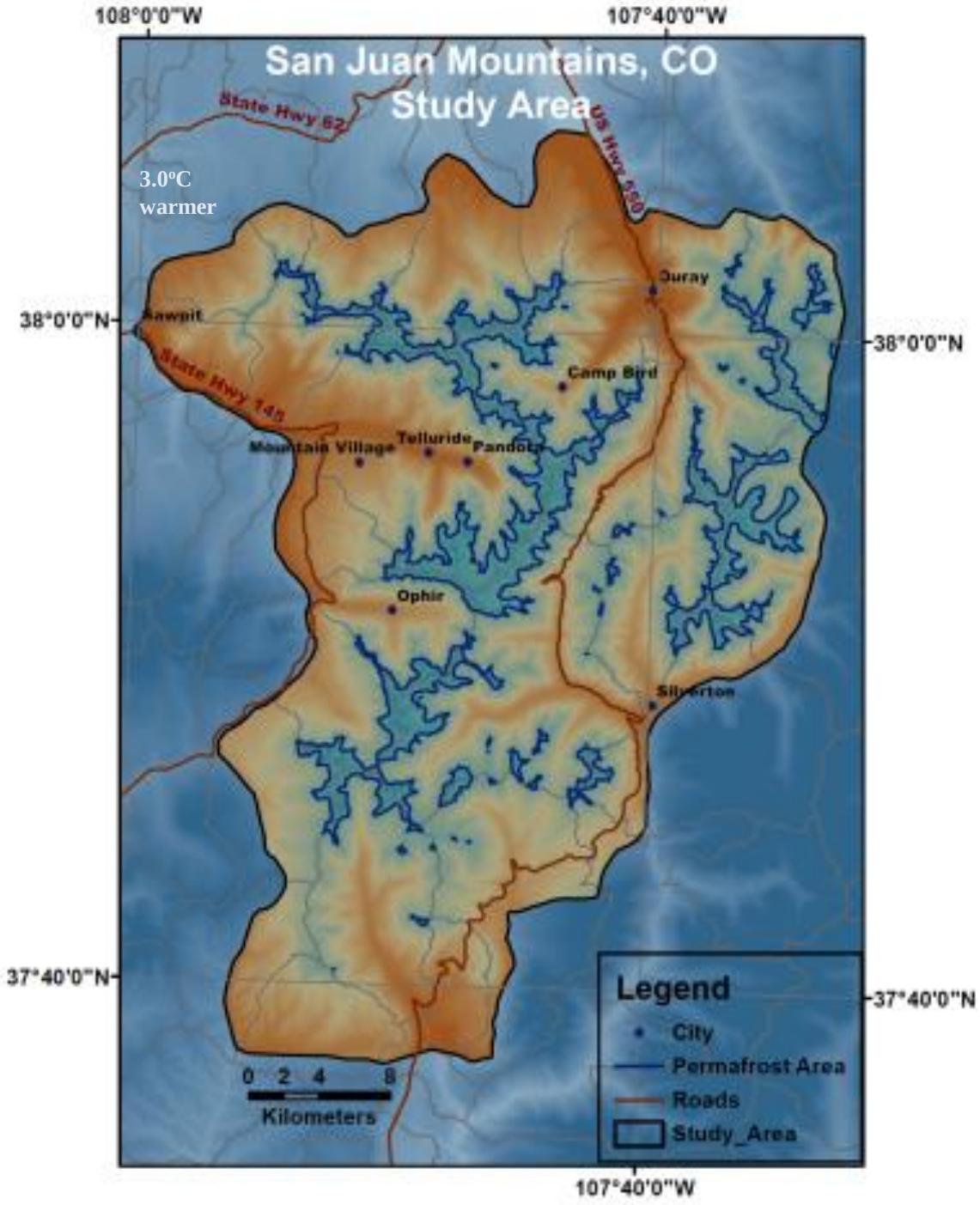

Figure C7. The extent of potential permafrost predicted based on 3.0°C warmer climate scenario.

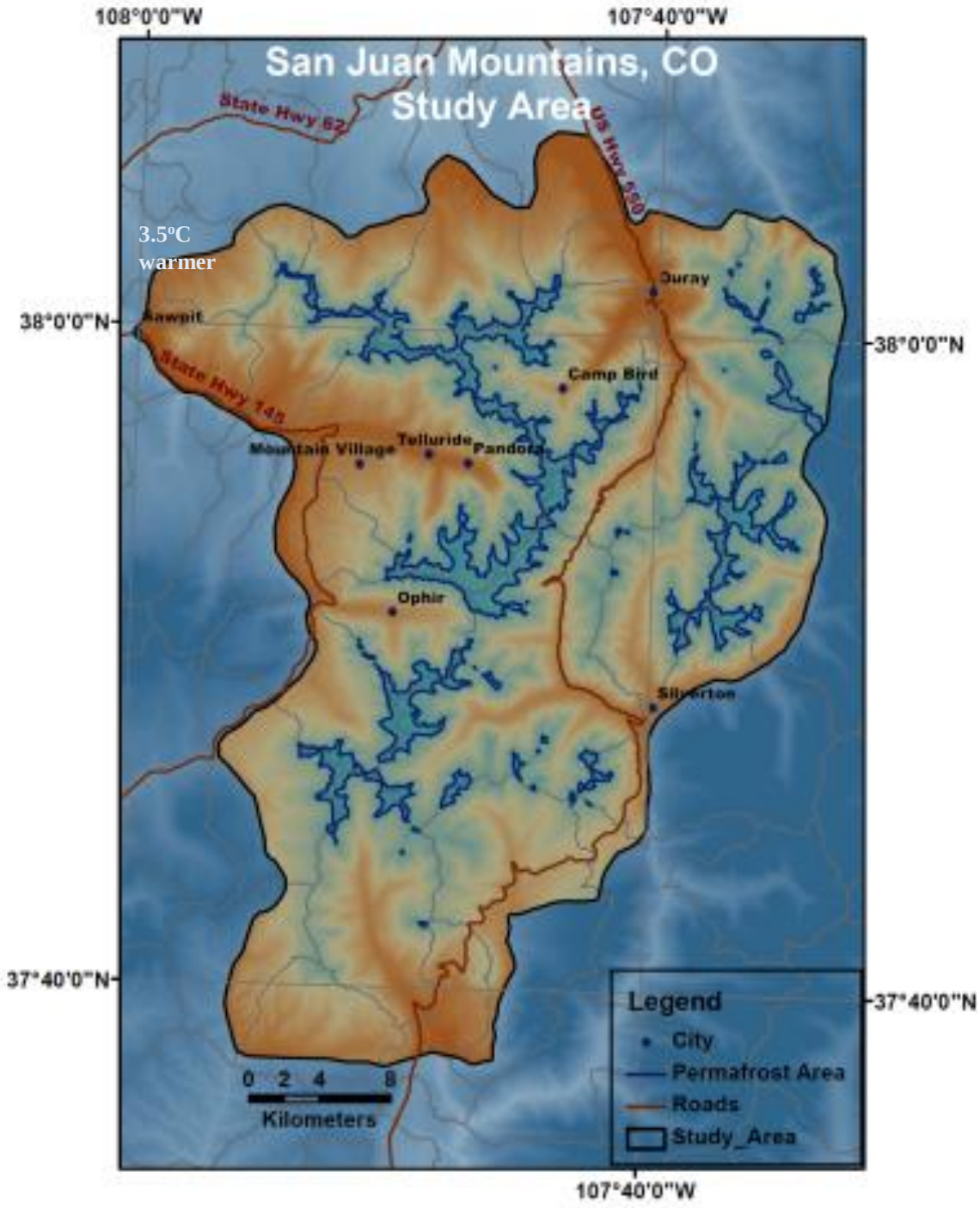

Figure C8. The extent of potential permafrost predicted based on 3.5ºC warmer climate scenario.

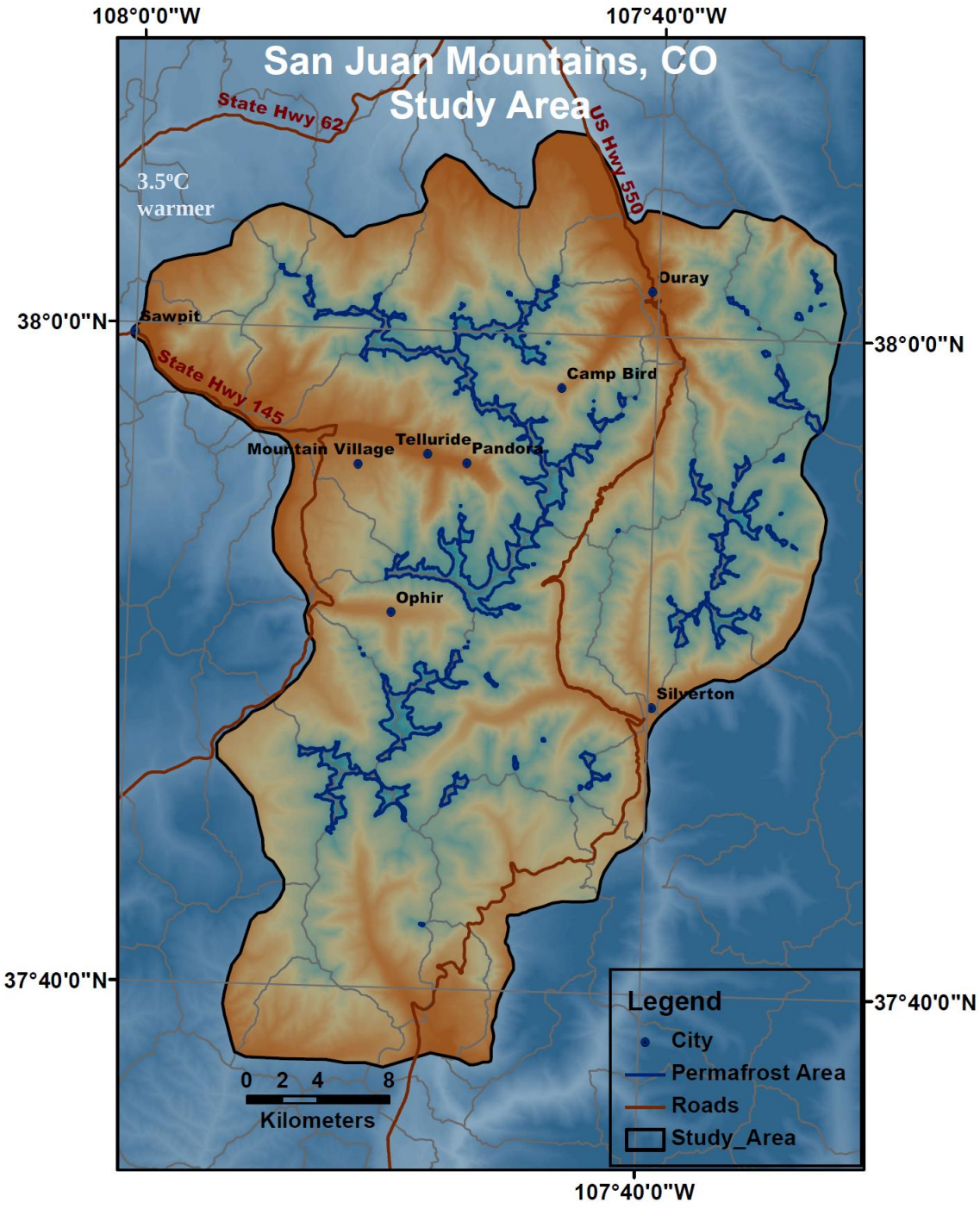

Figure C9. The extent of potential permafrost predicted based on 4.0°C warmer climate scenario.

APENDIX D

PERMAFROST EXTENT BASED ON COOLER CLIMATE SCENARIO

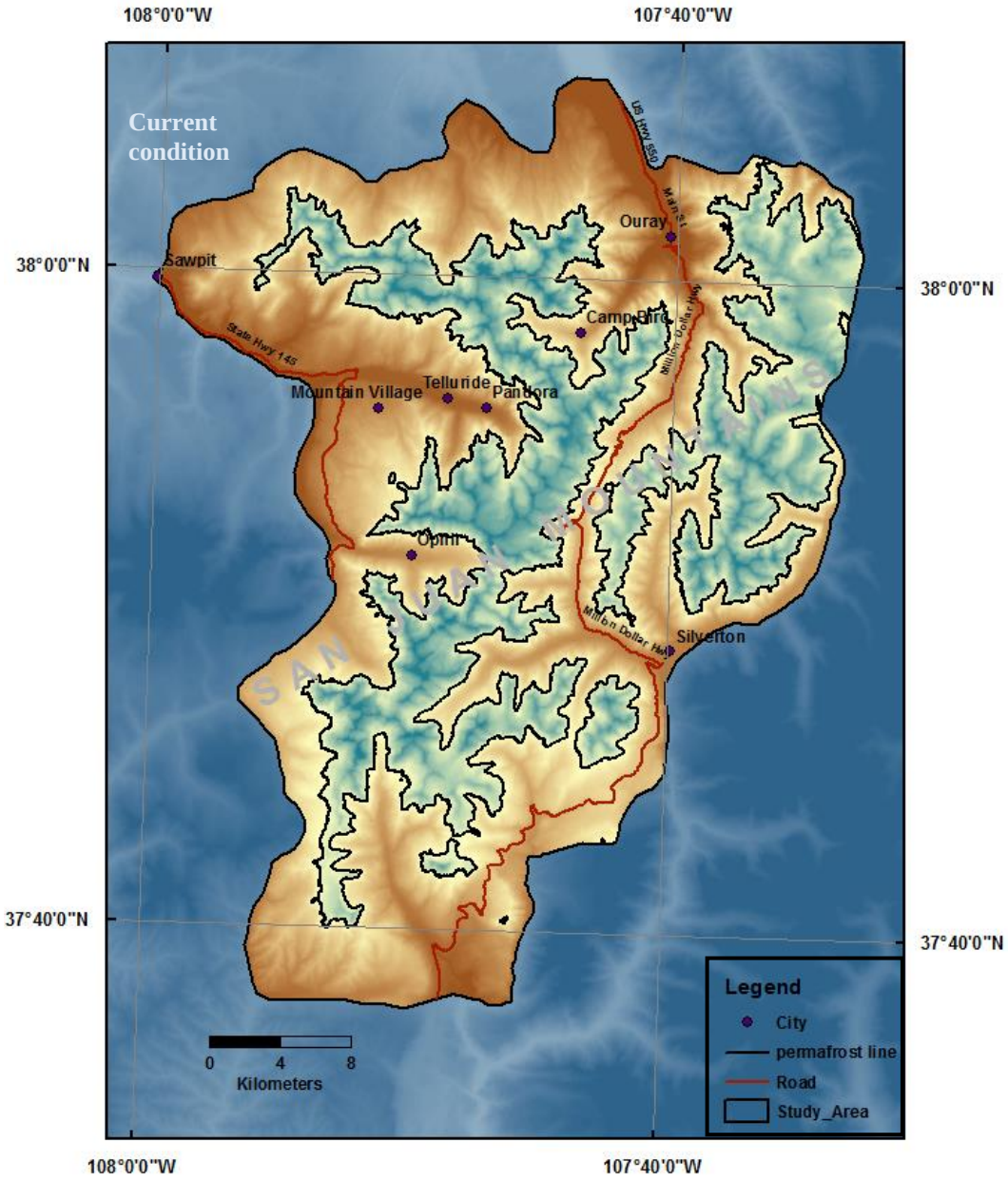

Figure D1. The profile of extent of potential permafrost at current condition.

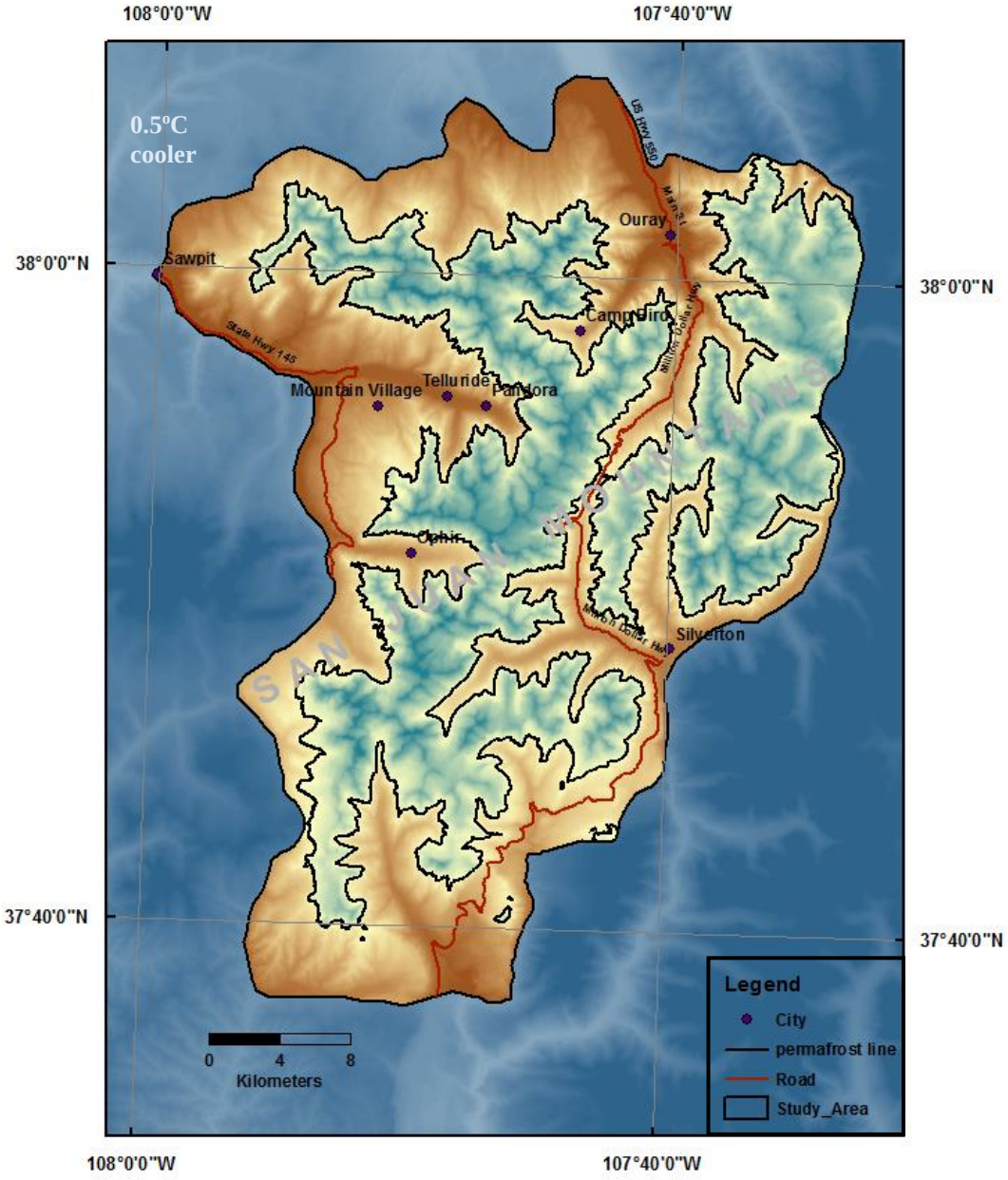

Figure D2. The extent of potential permafrost predicted based on 0.5ºC cooler climate scenario.

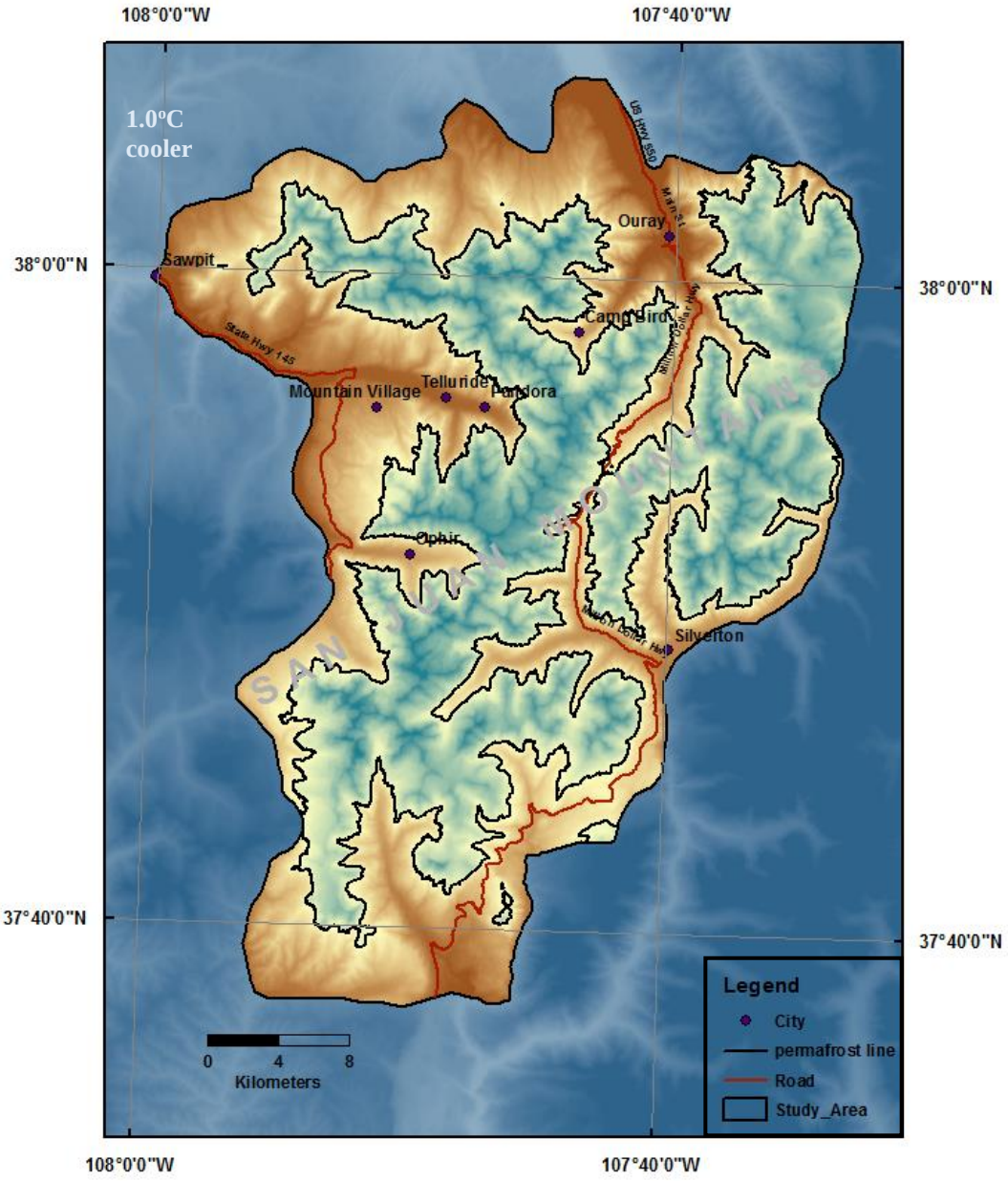

Figure D3. The extent of potential permafrost predicted based on 1.0°C cooler climate scenario.

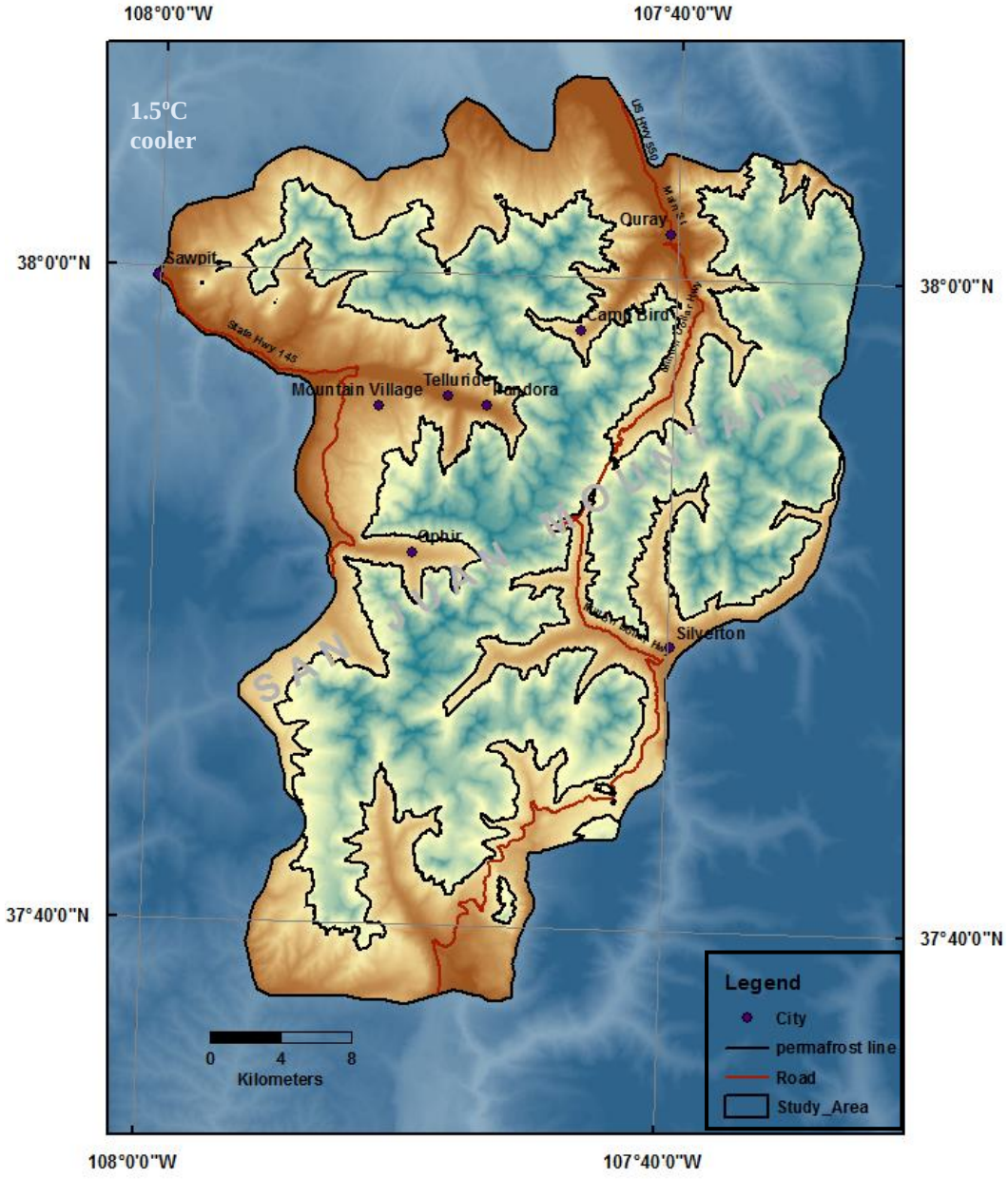

Figure D4. The extent of potential permafrost predicted based on 1.5°C cooler climate scenario.

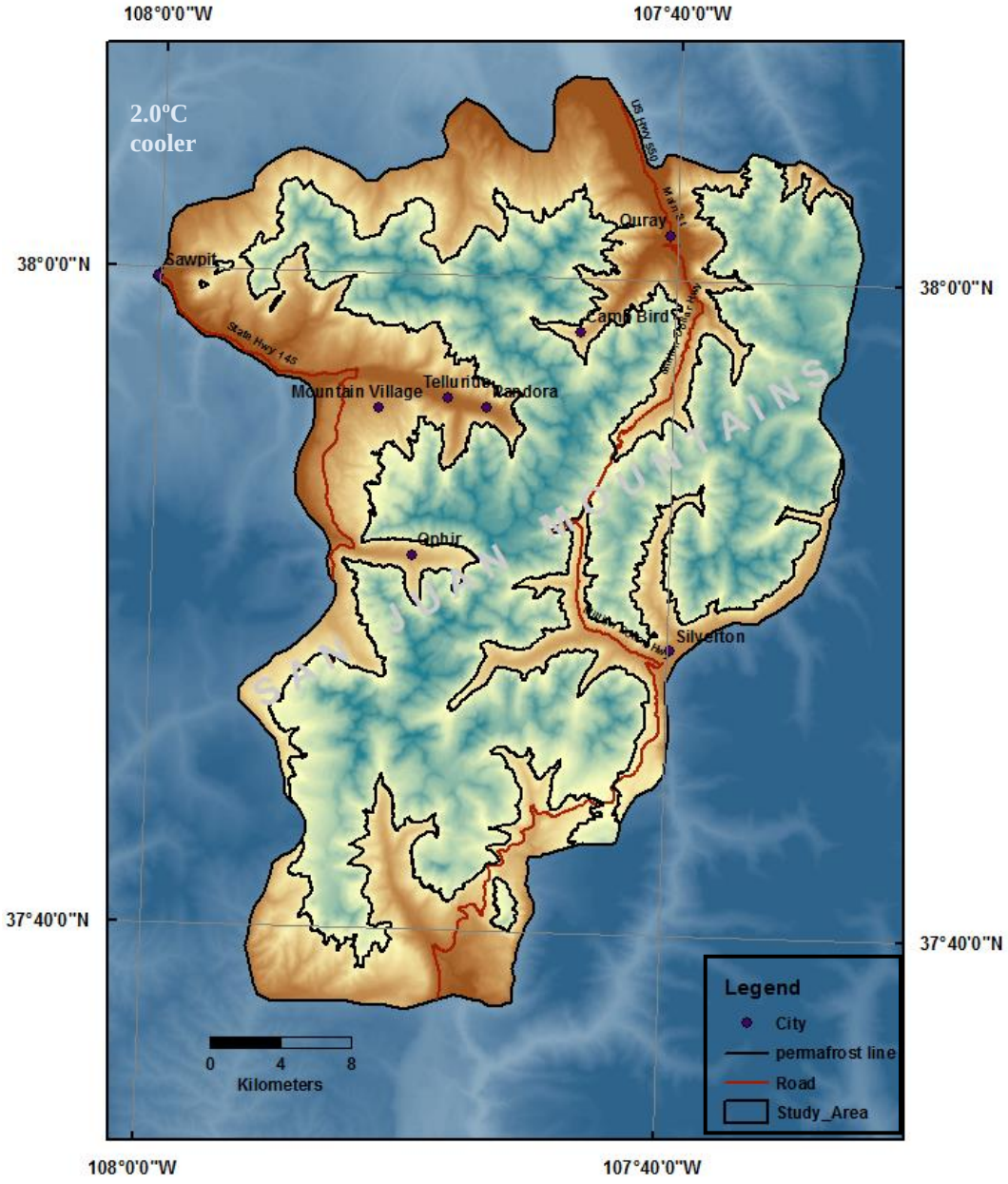

Figure D5. The extent of potential permafrost predicted based on 2.0°C cooler climate scenario.

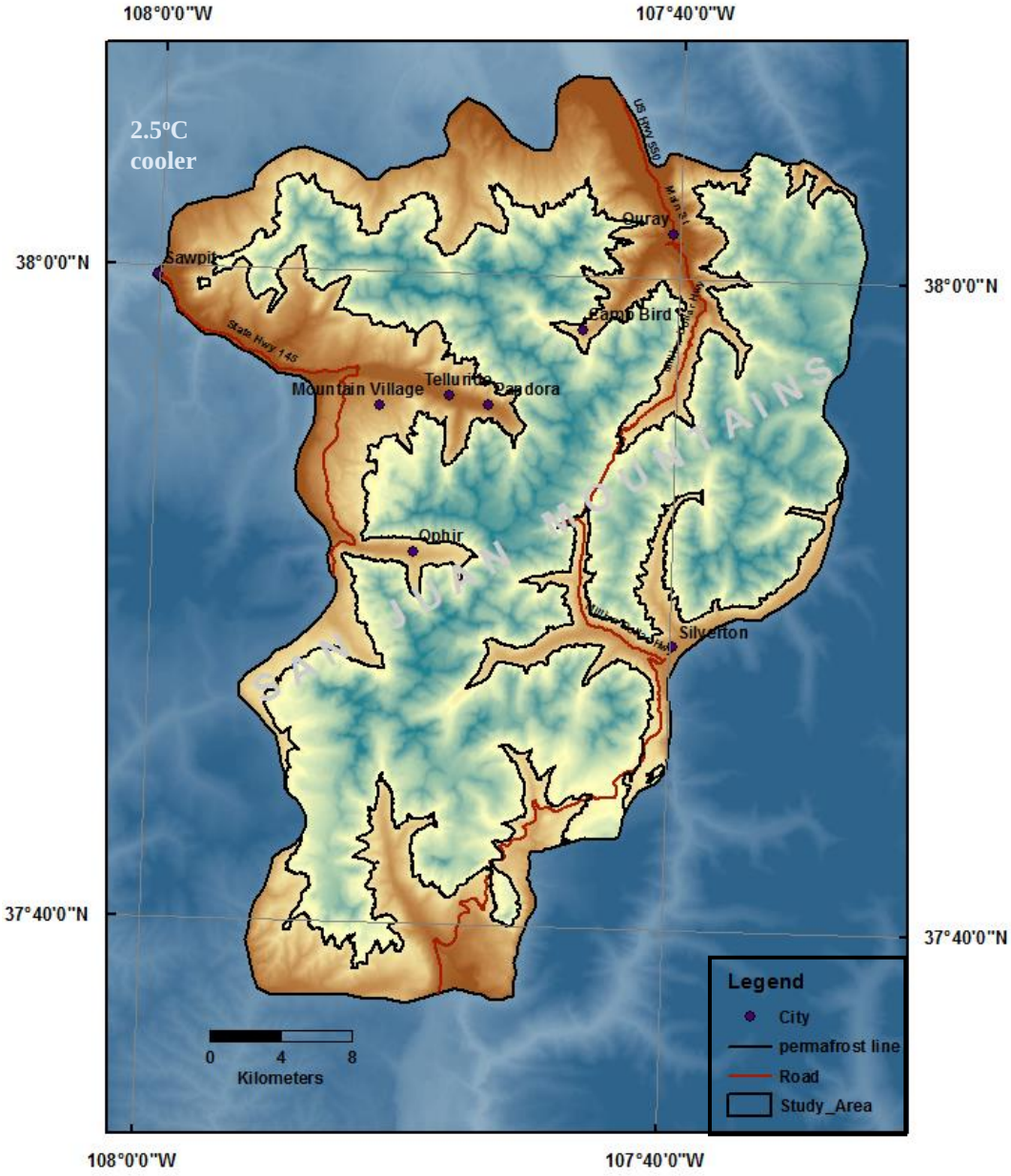

Figure D6. The extent of potential permafrost predicted based on 2.5°C cooler climate scenario.

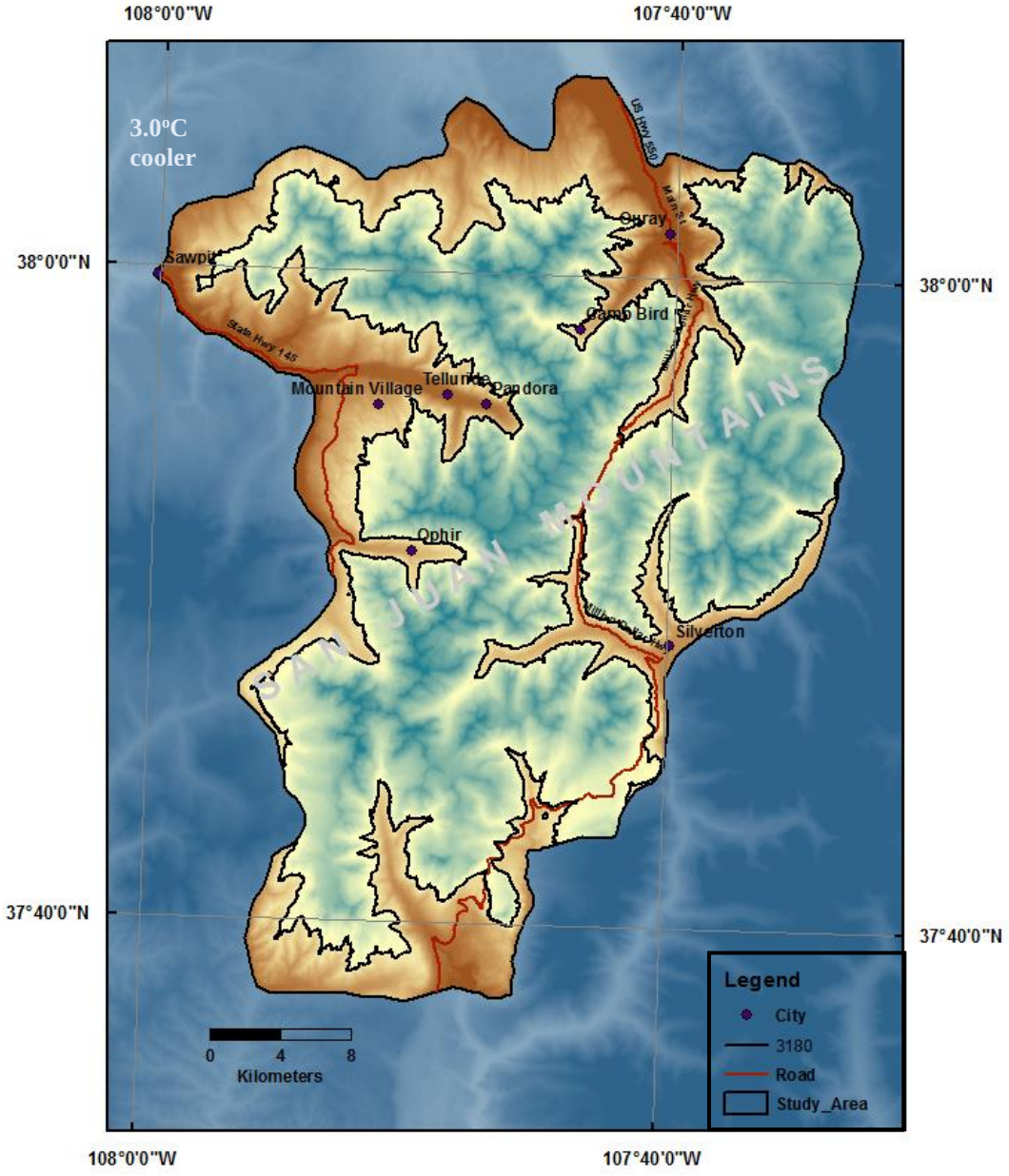

Figure D7. The extent of potential permafrost predicted based on 3.0°C cooler climate scenario.

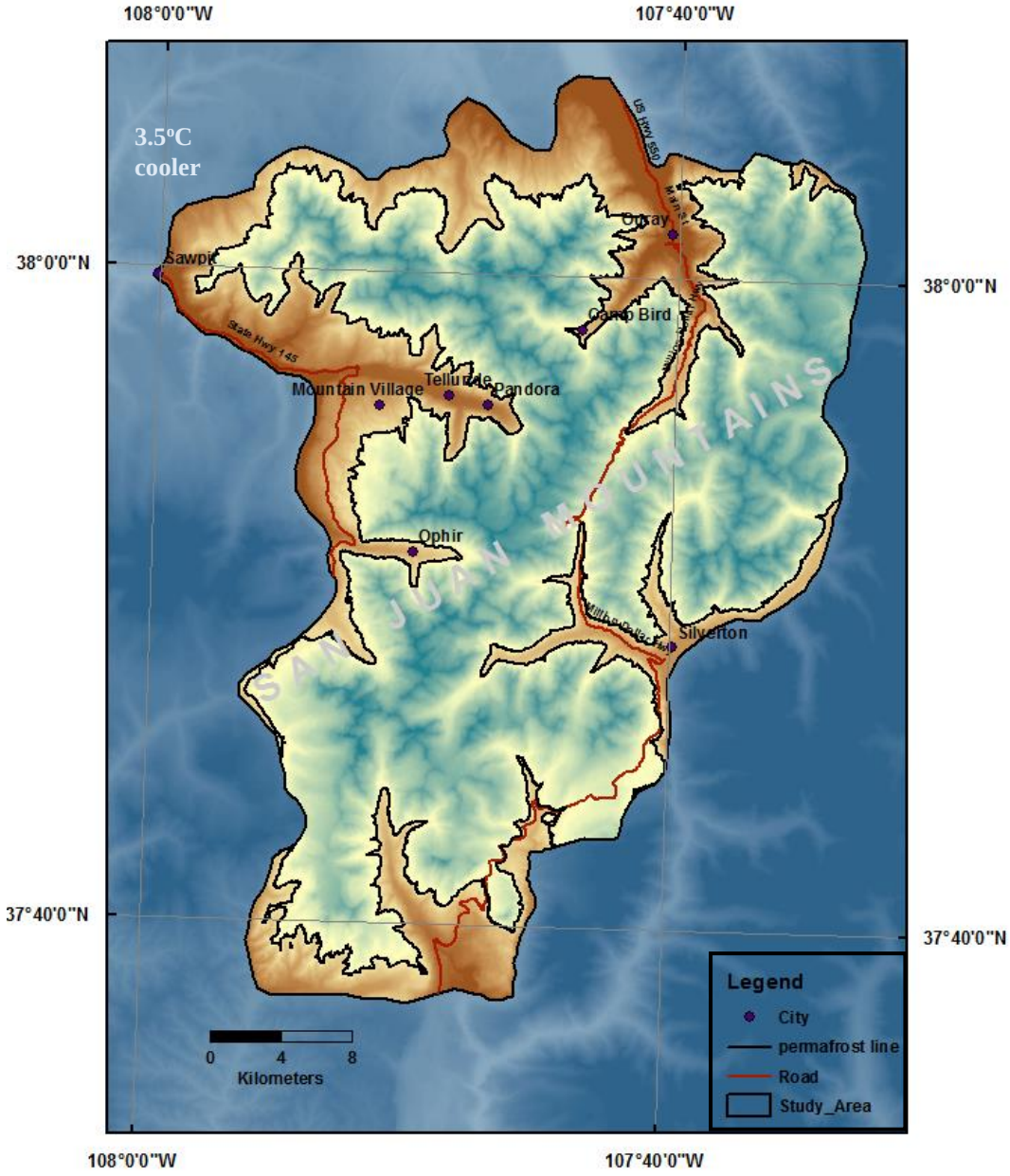

Figure D8. The extent of potential permafrost predicted based on 3.5ºC cooler climate scenario.

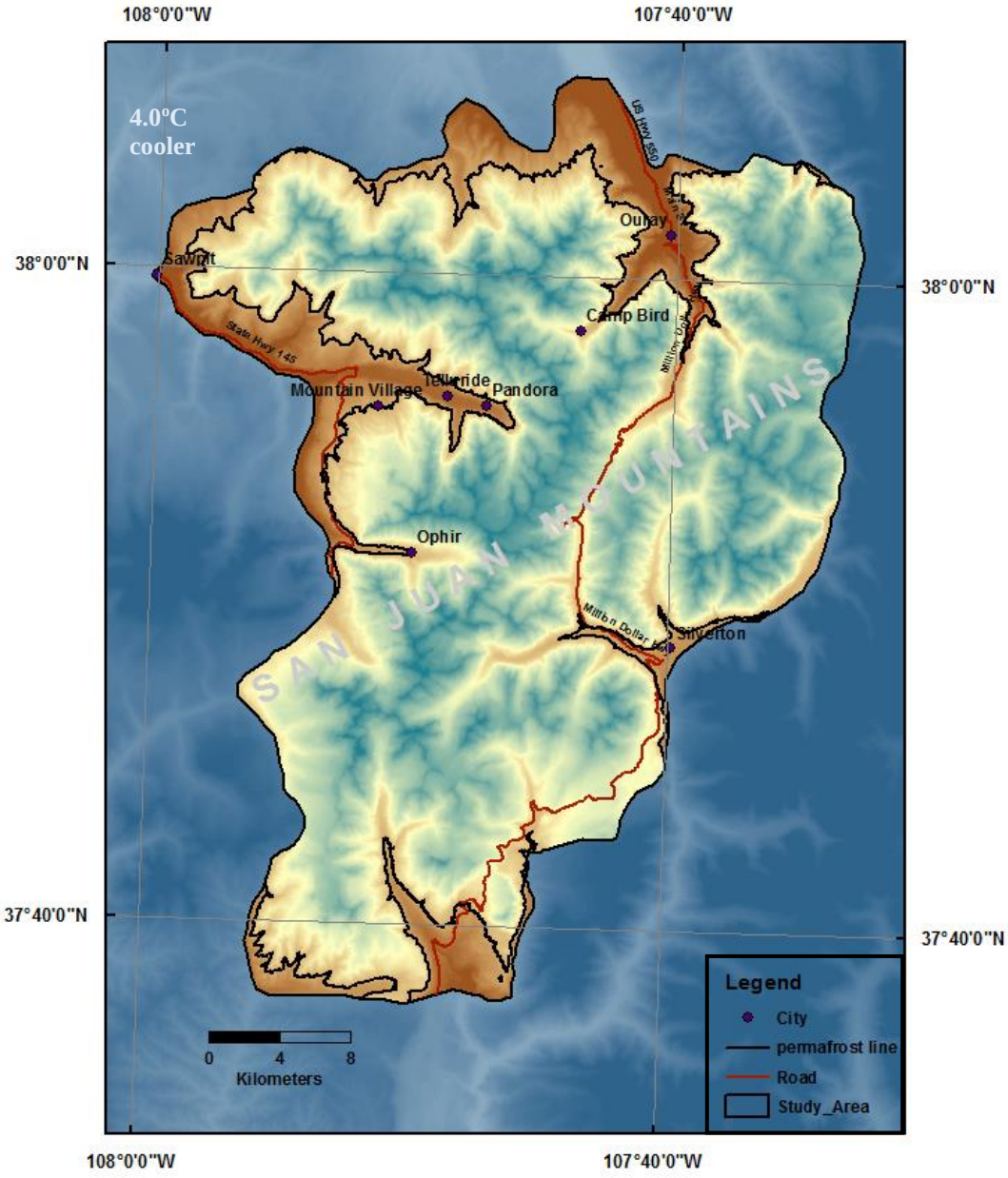

Figure D9. The extent of potential permafrost predicted based on 4.0°C cooler climate scenario.

APPENDIX E

PERMAFROST PROFILE BASED ON FROST NUMBER

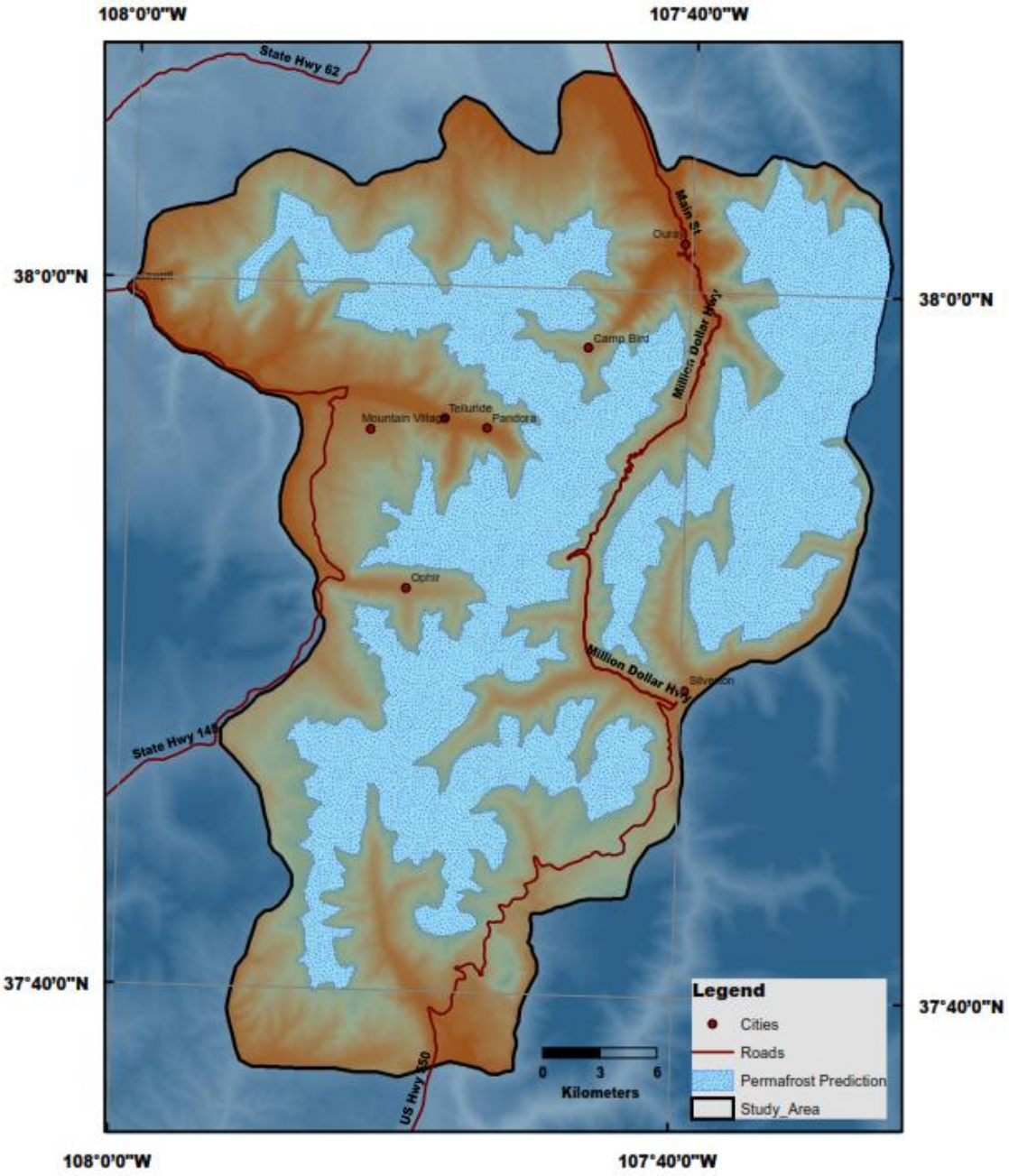

Figure D1. Potential permafrost profile based on frost number prediction as shown in Figure 5.9a and 5.10b.

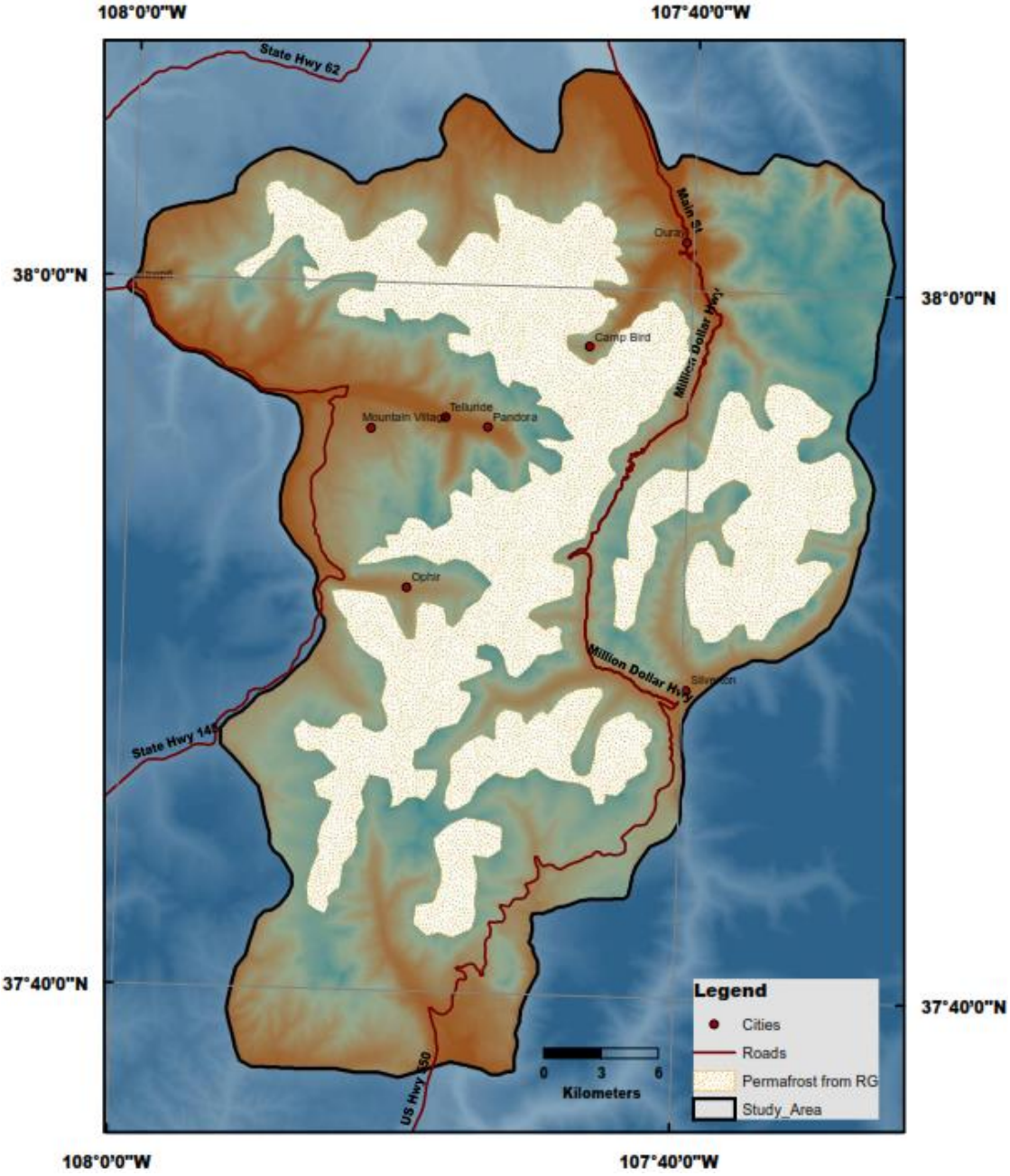

Figure D2. Profile of potential permafrost based on the tracing elevation of the toe of rock glacier.

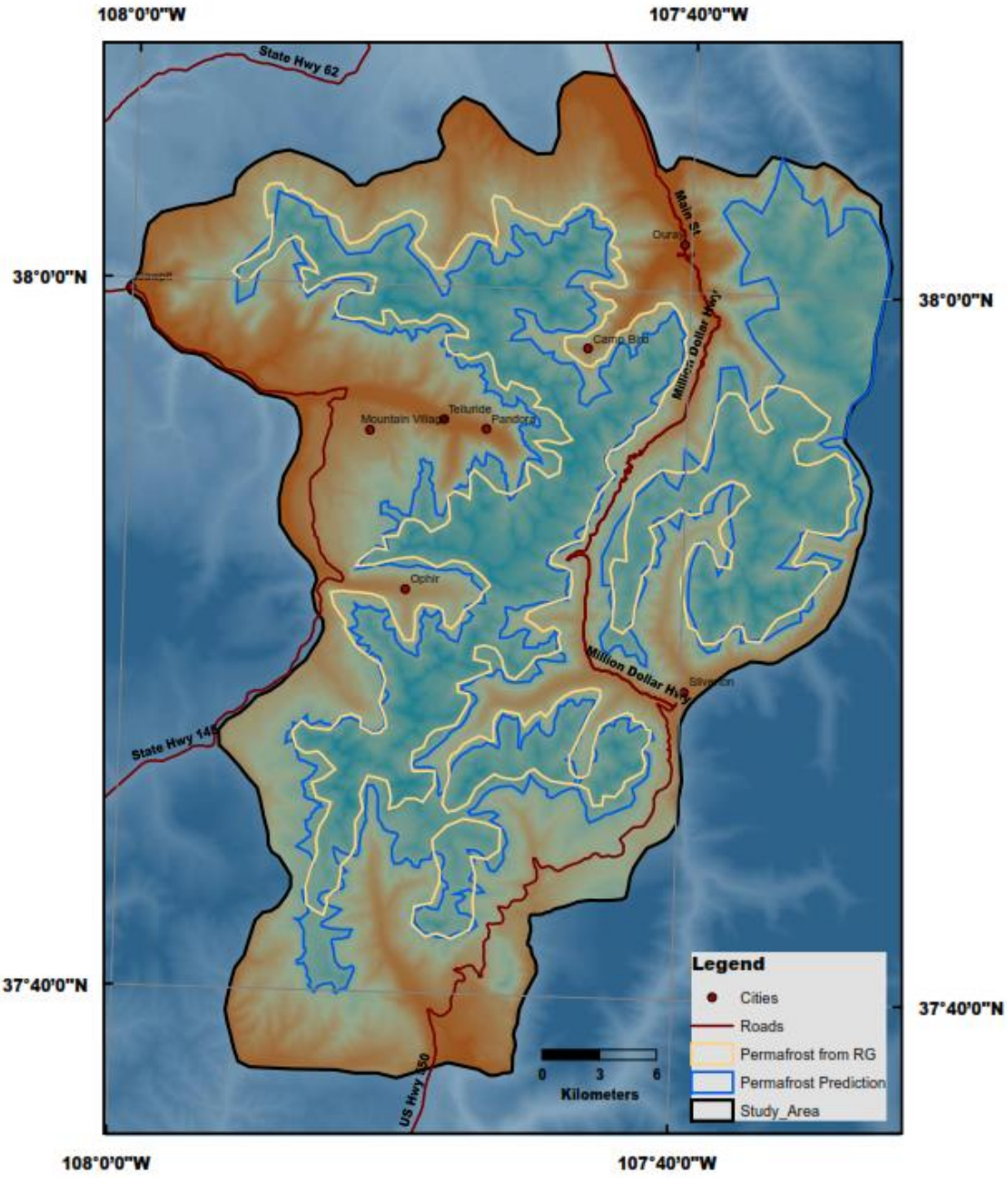

Figure D3. Permafrost profile based on frost number prediction and tracing elevation of the toe of rock glacier. The profile shows comparison of permafrost profile between prediction and toe tracing.